DISSERTATION ZUR ERLANGUNG DES DOKTORGRADES DER
FAKULTÄT FÜR CHEMIE UND PHARMAZIE
DER LUDWIG-MAXIMILIANS-UNIVERSITÄT MÜNCHEN

FKBP10 Inhibition as a Promising Strategy to Interfere with Collagen Synthesis and Maturation in Lung Fibrosis

LARISSA DOROTHEA KNÜPPEL

AUS STARNBERG

2018

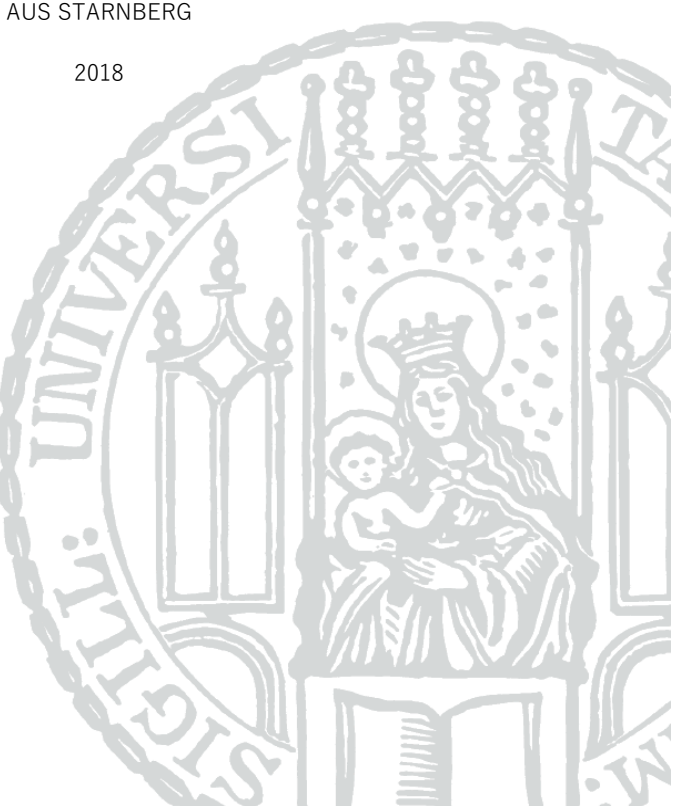

ERKLÄRUNG

Diese Dissertation wurde im Sinne von § 7 der Promotionsordnung vom 28. November 2011 von Herrn Prof. Dr. Karl-Peter Hopfner betreut.

Eidesstattliche Versicherung:

Diese Dissertation wurde eigenständig und ohne unerlaubte Hilfe erarbeitet.

München, den 13.04.2018

.....

Larissa Dorothea Knüppel

Dissertation eingereicht am: 13.04.2018

1. Gutachter: Prof. Dr. Karl-Peter Hopfner

2. Gutachter: PD Dr. Dietmar Martin

Mündliche Prüfung am: 13.06.2018

„What we know is a drop, what we don't know is an ocean“

Sir Isaac Newton

This is a cumulative thesis based on the following publications and manuscripts:

Chapter 2.1

Staab-Weijnitz, C.A., Fernandez IE, Knüppel L, Maul J, Heinzelmann K, Juan-Guardela BM, Hennen E, Preissler G, Winter H, Neurohr C, Hatz R, Lindner M, Behr J, Kaminski N, Eickelberg O. FK506-Binding Protein 10, a Potential Novel Drug Target for Idiopathic Pulmonary Fibrosis. *American Journal of Respiratory and Critical Care Medicine*, 2015.

Chapter 2.2

Knüppel L, Heinzelmann K, Lindner M, Hatz R, Behr J, Eickelberg O, Staab-Weijnitz C.A. FKBP10 regulates fibroblast migration via synthesis of collagen VI. *Respiratory Research*, 2018.

Chapter 2.3

Knüppel L, Ishikawa Y, Aichler M, Heinzelmann K, Hatz R, Behr J, Walch A, Bächinger HP, Eickelberg O, Staab-Weijnitz CA. A Novel Antifibrotic Mechanism of Nintedanib and Pirfenidone: Inhibition of Collagen Fibril Assembly. *American Journal of Respiratory Cell and Molecular Biology*, 2017.

Table of Contents

Summary

Idiopathic pulmonary fibrosis (IPF) is an incurable interstitial lung disease, characterized by an excessive deposition of extracellular matrix (ECM) proteins, mainly collagens, leading to an irreversible distortion of the lung architecture. The median survival after diagnosis is 3-5 years with increasing incidence worldwide. Therefore, the need for effective treatment options is huge.

In **chapter 2.1**, we proposed FK506-binding protein 10 (FKBP10), an endoplasmatic reticulum (ER) resident collagen chaperone and peptidyl-prolyl isomerase (PPIase) as a novel drug target in IPF. FKBP10 is upregulated in IPF patients and bleomycin-induced lung fibrosis and mainly expressed by (myo)fibroblasts, the ECM producing cell type in IPF. *In vitro* siRNA mediated knockdown of FKBP10 in primary human lung fibroblasts (phLF) of IPF patients reduced fibrotic marker expression and collagen secretion.

Another important characteristic of IPF, besides excessive collagen accumulation, is aberrant fibroblast adhesion and migration. **Chapter 2.2** examined the effects of FKBP10 loss on these processes. Interestingly, FKBP10 deficiency in phLF reduced the capacity of the cells to adhere and to migrate. Key molecules of adhesion and migration were mostly upregulated upon FKBP10 loss, whereas collagen VI expression was reduced. As the effects on migration and adhesion were 2-phosphoascorbate dependent, it was likely that collagen synthesis constituted the underlying mechanism. This was confirmed by coating culture dishes with collagen VI and collagen I. Collagen VI coating abolished the inhibitory effect of FKBP10 loss on migration completely, whereas the compensation by collagen I was less pronounced, but still visible.

In 2014 the U.S. Food and Drug Administration approved nintedanib and pirfenidone for IPF treatment, but their precise mechanisms of action are not completely resolved. **Chapter 2.3** directly compares the effects of both drugs on collagen synthesis and maturation in donor and IPF phLF. Nintedanib reduced the expression of collagen I, V, fibronectin (FN) and FKBP10 in IPF phLF and downregulated the secretion of collagen I and III. Pirfenidone reduced collagen V expression but was less effective in general. By and large, the effects between donor and IPF phLF were comparable. Within this publication we were able to reveal a novel antifibrotic mechanism of action of both drugs,

namely the inhibition of collagen I fibril formation. Both therapeutics reduced the amount and changed the appearance of collagen fibril bundles. Taken together nintedanib and pirfenidone interfere with important regulatory steps during collagen biosynthesis and maturation.

In conclusion, this thesis presents the inhibition of intracellular collagen biosynthesis and extracellular collagen fibril formation as promising approaches for IPF treatment and highlights FKBP10 as an important regulator of the ECM. By comparison of the effects of FKBP10 deficiency with other inhibitors of collagen biosynthesis and maturation, FKBP10 loss alone already reveals various beneficial antifibrotic effects, which strengthens FKBP10 as novel drug target to prevent IPF disease progression.

Zusammenfassung

Idiopathische pulmonale Fibrose (IPF) ist eine unheilbare interstitielle Lungenkrankheit, welche durch eine enorme Akkumulation von Extrazellulärer Matrix (ECM), hauptsächlich von Kollagenen, charakterisiert ist. Diese Ablagerungen führen letztendlich zu einer irreversiblen Zerstörung der Lungenarchitektur. Die durchschnittliche Lebenserwartung nach diagnostizierter IPF beträgt 3-5 Jahre. Das Krankheitsaufkommen steigt stetig, wodurch der Bedarf für neue therapeutische Ansätze erhöht ist.

In **Kapitel 2.1** wird FK506-binding Protein 10 (FKBP10) als neues Wirkstoffziel vorgestellt. Bei FKBP10 handelt es sich um ein im endoplasmatischen Retikulum (ER) lokalisiertes Protein mit Kollagenchaperonfunktion und Peptidyl-Prolyl-Isomerase Aktivität. FKBP10, hauptsächlich exprimiert von (Myo-)Fibroblasten, dem ECM produzierendem Zelltyp, ist hochreguliert in IPF Patienten und in Bleomycin induzierter Lungenfibrose. Der durch siRNA vermittelte *in vitro* Verlust von FKBP10 in primären humanen Lungenfibroblasten (phLF), isoliert von IPF Patienten, führte zu einer Reduktion fibrotischer Marker sowie der Kollagensekretion.

Neben enormer Kollagenakkumulation ist ein weiteres Charakteristikum von IPF die aberrante Adhäsion und Migration von Lungenfibroblasten. **Kapitel 2.2** untersucht die Effekte des FKBP10-Verlusts auf diese Prozesse. Interessanterweise war das Vermögen zur Adhäsion und Migration von FKBP10 defizienten Fibroblasten vermindert. Schlüsselmoleküle dieser Prozesse wurden größtenteils durch den Verlust von FKBP10 hochreguliert, während die Kollagen VI-Expression herunterreguliert wurde. Die Abhängigkeit der verminderten Adhäsion und Migration bei FKBP10 Verlust von 2-Phosphoascorbat ließ auf einen Kollagen-abhängigen Mechanismus schließen. Diese Hypothese wurde durch Beschichtung der Zellkulturschalen mit Kollagen VI und I bestätigt. Durch Kollagen VI Beschichtung konnte der inhibitorische Effekt des FKBP10 Verlustes vollständig aufgehoben werden, wohingegen die Kollagen I Beschichtung einen geringeren, jedoch sichtbaren kompensatorischen Effekt hatte.

Im Jahre 2014 wurden zwei Therapeutika, Nintedanib und Pirfenidon von der U.S. Food and Drug Administration zur Behandlung von IPF zugelassen, wobei der genaue Wirkungsmechanismus beider Medikamente nicht vollständig bekannt ist. In **Kapitel 2.3**

wurden die Effekte beider Therapeutika in Bezug auf ihre Wirkung auf die Kollagensynthese und Reifung in Donor- und IPF-Fibroblasten direkt miteinander verglichen. Nintedanib reduzierte die Expression von Kollagen I, V, Fibronektin und FKBP10 in IPF-Fibroblasten und regulierte die Sekretion von Kollagen I und III herunter. Pirfenidon-Behandlung führte zu einer Verminderung der Kollagen V-Expression, jedoch war dieses Therapeutikum im Großen und Ganzen weniger effektiv. Im Wesentlichen waren die Effekte auf Donor- und IPF-Fibroblasten vergleichbar. Darüber hinaus konnten wir in dieser Veröffentlichung die Inhibierung der Kollagen I-Fibrillenbildung als einen bisher unbekannten Wirkungsmechanismus beider Therapeutika aufklären und eine Reduktion in der Anzahl sowie ein verändertes Erscheinungsbild der Kollagenfibrillenbündel durch Behandlung mit beiden Medikamenten aufzeigen. Zusammenfassend lässt sich sagen, dass beide Therapeutika wichtige regulatorische Prozesse der Kollagensynthese und -reifung beeinträchtigen.

Alles in allem wird im Zuge dieser Arbeit die Inhibierung der intrazellulären Kollagenbiosynthese und der extrazellulären Kollagenfibrillenbildung als vielversprechender Ansatzpunkt der IPF-Behandlung präsentiert und FKBP10 als ein wichtiger Regulator der ECM hervorgehoben. Vergleicht man die Effekte des FKBP10-Verlustes mit anderen bekannten Inhibitoren der Kollagenbiosynthese und -reifung, so kristallisiert sich heraus, dass FKBP10-Verlust alleine schon vielzählige antifibrotische Effekte aufweist, was FKBP10 als neue therapeutische Zielstruktur für die Hemmung des Krankheitsverlaufs von IPF hervorhebt.

1. Introduction

1.1 Idiopathic Pulmonary Fibrosis (IPF)

Idiopathic pulmonary fibrosis (IPF), an incurable and irreversible lung disease that increases with age, is a diffuse interstitial lung disease (ILD) displaying the histopathological features of usual interstitial pneumonia with unknown etiology (Dancer *et al.*, 2011; Wolters *et al.*, 2014). The survival prognosis is between 30-50% within the first 5 years after diagnosis and patients dye upon asphyxiation due to the disruption of gas exchange (Kim *et al.*, 2006; Wolters *et al.*, 2014). The underlying pathogenic processes that cause the fibrotic response are not completely understood, but there is evidence that repeated micro-injuries of the alveolar epithelium lead to abnormal activation of alveolar epithelial cells (King *et al.*, 2011; Fernandez and Eickelberg, 2012; Tanjore *et al.*, 2012). These abnormally activated alveolar epithelial cells produce fibrotic mediators which may induce epithelial to mesenchymal transition, fibrocyte recruitment, as well as activation, proliferation and differentiation of fibroblasts into myofibroblasts (King *et al.*, 2011), resulting in an aberrant wound response (Renzoni *et al.*, 2014).

1.1.1 Epidemiology of IPF

The prevalence of IPF, the most common type of ILD, increases from year to year. IPF possibly has contributed substantially to the increases in ILD-related mortality detected from 1990 to 2013 (Kreuter *et al.*, 2015; Mortality and Causes of Death, 2015).

During disease progression, that can be either fast or slow, patients suffer from progressive breathlessness and lung function decline. The median survival is 2-3 years after diagnosis. Men are more affected by the disease than women (Navaratnam *et al.*, 2016).

As indicated by “idiopathic“, it is not well understood what causes the disease; however, there are several risk factors like smoking, environmental factors (metal dust, wood dust, chemicals) or gastroesophageal reflux that might cause the disease. Furthermore, genetics can also play a role in sporadic forms of IPF; mutations in genes like *MUC5B* or *TOLLIP* were found in these cases (Seibold *et al.*, 2011; Fingerlin *et al.*, 2013; Noth *et al.*, 2013; Mathai *et al.*, 2015; Allen *et al.*, 2017). Interestingly, patients that have a single nucleotide polymorphism in the *MUC5B* promotor region possess an increased survival

compared to patients without this mutation (Navaratnam *et al.*, 2016). IPF was reported to have an increase in comorbid illnesses like cardiovascular disease, gastroesophageal reflux disease (GERD) or lung cancer (Kreuter *et al.*, 2016; Navaratnam *et al.*, 2016).

1.1.2 Pathology of IPF

The main pathological characteristic of IPF is a heterogeneous pattern displaying subpleural and paraseptal areas of active fibrosis with septal thickening, honeycombing, and fibrotic areas termed as fibroblast foci combined with regions of normal parenchyma (King *et al.*, 2011).

Honeycombs are grounded in enlarged spaces bordered by areas of fibrosis (Fernandez and Eickelberg, 2012). Fibroblastic foci are characterized by regions of highly proliferative myofibroblast with neighboring areas of hyperplastic and/or apoptotic alveolar epithelial cells (Fernandez and Eickelberg, 2012). This results in the distortion of the normal architecture of the lung (Wilson and Wynn, 2009).

1.1.3 Pathogenesis of IPF

IPF pathogenesis is defined by a malfunctioning interplay of the epithelium and the mesenchyme.

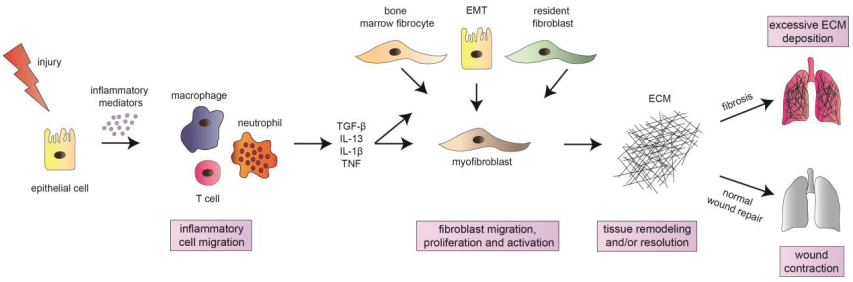

Figure 1. Stages in the process of normal and abnormal wound healing. Wound healing can be divided into four stages: Clotting and coagulation (not shown), inflammatory cell migration, fibroblast migration, proliferation and activation followed by tissue remodeling and/or resolution. Dysregulation of one of these stages or persistent lung injury can lead to tissue fibrosis. (Figure modified from Wynn *et al.*, 2011).

The initial injury induces a stress response leading to ER stress and apoptosis of alveolar type II cells. Epithelial and endothelial cells secrete inflammatory cytokines triggering the antifibrinolytic coagulation cascade inducing platelet activation and blood clotting. The

permeability of blood vessels increases facilitating leucocyte recruitment to the injury site followed by the release of profibrotic cytokines like transforming growth factor β (TGF-β), a key player in IPF and the main myofibroblast inducer. In the next phase local mesenchymal cells differentiate into myofibroblasts. Additionally, fibroblasts may get recruited from bone marrow-derived fibrocytes and/or via epithelial to mesenchymal transition (EMT), a process in which epithelial cells gain a mesenchymal phenotype. Upon activation, fibroblasts differentiate into α-smooth muscle (α-SMA) expressing myofibroblasts that migrate into the wound to promote wound contraction followed by regeneration of the injured tissue. During a persistent injury, myofibroblasts begin to synthesize excessive amounts of extracellular matrix (ECM) proteins, like collagen type I, III, V and fibronectin (FN) (tissue remodeling phase) leading to scarring and distortion of the normal lung architecture (Figure 1, adapted from (Wynn, 2011)) (Hinz *et al.*, 2007; King *et al.*, 2011; Rock *et al.*, 2011; Wynn, 2011; Fernandez and Eickelberg, 2012). Throughout the whole repair process TGF-β can be found in the wound fluid (Leask and Abraham, 2004).

1.1.4 Fibroblast migration – an important feature of IPF

One important feature of fibrosis is the abnormal regulation of fibroblast adhesion and migration (Verrecchia and Mauviel, 2007; Chang *et al.*, 2008; King *et al.*, 2011), which is controlled by cytokines like TGF-β1 and by the mechanical microenvironment (Hinz *et al.*, 2007).

Cell migration is a dynamic process regulated by assembly and disassembly of focal adhesions (FA). The attachment to the ECM is facilitated by transmembrane receptors, called integrins that build the link between the ECM and intracellular FA complexes (Carragher and Frame, 2004). Clustering of integrins upon ECM attachment induces signaling cascades inside the cell involving amongst others focal adhesion kinase (FAK) (Nagano *et al.*, 2012), which induces FA turnover. Besides the regulation of cell migration by FA molecules, properties of the ECM like topology, stiffness (determined by collagen deposition) and composition influences cell migration as well. Important adhesion ligands for integrins are *e.g.* collagens and FN (Charras and Sahai, 2014; Burgess *et al.*, 2016).

1.2 Collagens

Throughout the body collagens are the most abundant proteins as well as the major component of the ECM. However, not all collagen types are ECM proteins. Collagens are built up out of a repeating left-handed helix of Gly-X-Y triplets, whereby X and Y are mostly proline and hydroxyproline residues. Three left handed helices form a right handed triple helix and both homo- and heterotrimeric forms exist. Twenty-nine different collagen types are known to date maintaining different supramolecular structures like fibrillar collagens (type I, II, III, V, XI, XXIV, XXVII), network forming collagens (type IV, VIII, X), fibril-associated collagen with interrupted triple helices collagens (type IX, XII, XIV, XVI, XIX, XX, XXI, XXII), anchoring collagens (type VII), multiple triple helix domains and interruptions collagens (type XV, XVIII), beaded filament collagens (type VI, XXVI, XXVIII) and transmembrane collagens (type XIII, XVII, XXIII, XXV). All these collagen proteins comprise three polypeptide chains with a minimum of one section of triple helix; non-triple helical domains are N- and C-terminal telopeptides or structural domains like FN type III repeats. The structural variety of collagen leads to different tasks of collagen types including functions in tissue repair, adhesion and migration (Hulmes, 2002; Canty and Kadler, 2005; Ishikawa and Bächinger, 2013; Muiznieks and Keeley, 2013).

1.2.1 Collagens in IPF

In healthy lungs, collagen is the main ECM component and can be found in airways, basement membranes and in the interstitium. In the tissue of the human lung, about 15% of the dry weight is made up by collagens. Collagen type I and III are the most abundant collagens that can be found in the lung. Changes in structure, amount or topography of collagens lead to alterations in lung function (Laurent, 1986).

Excessive collagen deposition is one central characteristic of IPF. Collagens were reported to be the main component of newly synthesized ECM during the process of lung fibrosis (Decaris *et al.*, 2014). In areas of early stages of fibrosis collagen type III is primarily expressed, in contrast to areas of later stages of fibrosis in which collagen type I expression is increased (Kaarteenaho-Wiik *et al.*, 2004).
The excessive amount of collagen is largely produced by myofibroblasts, responsible for the synthesis of collagen I, III, V and VI in the lung (Laurent, 1986).

1.2.2 Collagen biosynthesis and maturation

Collagen biosynthesis and maturation are complex processes (Figure 2, adapted from (Chen and Raghunath, 2009)) which have mostly been described for type I collagen, but are otherwise incompletely understood (Ishikawa *et al.*, 2015). After gene transcription, procollagen is co-translationally translocated into the rough endoplasmic reticulum (rER) were the molecule is assembled either as homo- or as heterotrimer via its C-propeptides in a zipper-like style from its carboxyterminus to its aminoterminus (Hulmes, 2002). Before the triple helix can form, several steps are needed. First, unfolded procollagen is co-translationally hydroxylated via prolyl 4-hydroxlases (P4Hs), prolyl 3-hydroxlases (P3Hs), and lysyl hydroxylases (LHs), which all require ascorbic acid as cofactor. Posttranslational modifications (PTMs) like hydroxylation of prolines and lysines are indispensable for correct stability and triple helix formation and therefore for collagen secretion and its final supramolecular structure assembly. (Weis *et al.*, 2010; Hudson and Eyre, 2013; Ishikawa and Bächinger, 2013; Pokidysheva *et al.*, 2013)

Second, some hydroxylysines of the procollagen molecule are additionally modified by the attachment of β-galactose and α-glucose. Changes in collagen glycosylation levels have been associated with *Osteogenesis imperfecta* (OI) and other bone/skeletal disorders. Several functions of collagen glycosylation were suggested including the control of collagen fibrillogenesis or remodeling. However, a precise function is not fully elucidated (Yamauchi and Sricholpech, 2012; Ishikawa and Bächinger, 2013).

Third, N-terminal and especially C-terminal propeptides are folded under the assistance of general rER resident molecular chaperones like Binding immunoglobulin protein (BiP), Protein disulfide isomerase (PDI) and cyclophilin B. C-propeptide folding is important for the chain selection and includes disulfide bond formation, peptidyl-prolyl *cis-trans* isomerization, and N-linked glycosylation (Ishikawa and Bächinger, 2013).

To ensure a proper triple helix formation, all proline residues need to be isomerized from *cis* into *trans* conformation, which makes the isomerization the rate limiting step in this process. Three rER resident peptidyl-prolyl cis/trans isomerases (PPIases) (Cyclophilin B, FK(506)binding protein 10 and 14) catalyze this process.

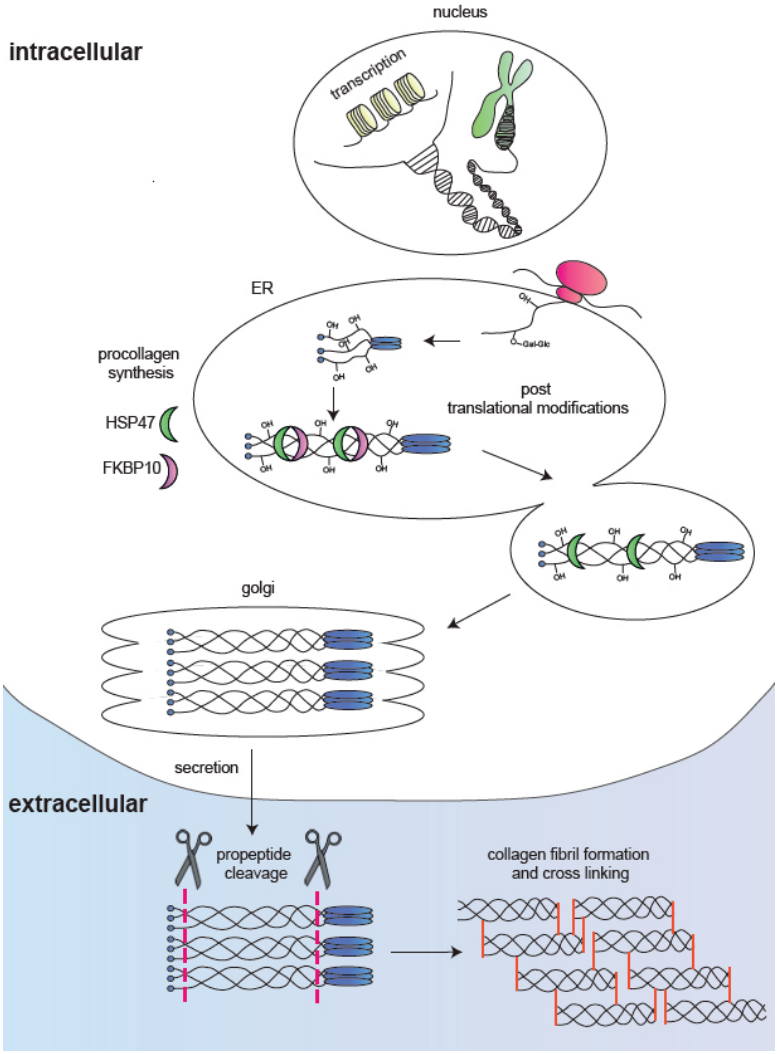

Figure 2. Pathway of collagen synthesis and maturation. The process starts in the cell with the transcription and translation of procollagen. Procollagen is co-translationally translocated into the rER where PTMs are executed. Several enzymes and molecular chaperones like HSP47 and FKBP10 assist in procollagen maturation and triple helical folding. Procollagen is translocated to the golgi via vesicles and further modified. After secretion propeptides are cleaved resulting in tropocollagen. Fibrils assemble in an entropy-driven process. Fibrils form into fibers and finally build fiber bundles. Crosslinking of the telopeptides of tropocollagen is catalyzed by lysyl oxidases and transglutaminase 2. (Figure adapted from Chen *et al*, 2009)

Moreover, collagen chaperones like FKBP10 and heat shock protein 47 (HSP47) are also important players to prevent premature association of the triple helices before collagen secretion (Ishikawa and Bächinger, 2013; Ishikawa *et al.*, 2015).

HSP47 binds to triple helical procollagen and accompanies it from the rER to the golgi where HSP47 dissociates and is recycled back via COPI vesicles. In the golgi more PTM occur and proteins are transported via vesicles from the *cis* to the *trans* golgi and in the last step procollagen bundles are secreted to the ECM (Ishikawa and Bächinger, 2013).

Outside the cell, propeptides of procollagen are cleaved by N- and C-procollagen proteinases generating tropocollagen having telopeptides on their cleaved ends. This initiates an entropy-driven process of spontaneous self-assembly of the tropocollagen triple helices into collagen fibrils. Crosslinking of collagen fibrils strengthens the fibrils. This reaction is executed by lysyl oxidases (LOs) and transglutaminase 2 (TG2), enzymes that catalyze the deamidation of specific hydroxylysines and lysines. The fibrils (10-300nm) further build collagen fibers (1-20 µm) which may associate in turn in large fiber bundles (up to 500 µm) (Kadler *et al.*, 1996; Kagan and Li, 2003; Muiznieks and Keeley, 2013).

1.2.3 Regulation of collagen fibril formation by ECM components and integrins

Collagen I was found to be incorporated into fibrils with either collagen III, which regulates the fibril diameter of collagen I or with collagen V, important for fibrillogenesis and fiber size (Birk *et al.*, 1988; Wenstrup *et al.*, 2004; Parra *et al.*, 2006; Muiznieks and Keeley, 2013; Vittal *et al.*, 2013).
Besides collagens, also proteoglycans, like biglycan and decorin can interact with collagens to regulate collagen fibril formation. Both proteoglycans are key regulators of lateral collagen fibril assembly. Moreover, both proteins interact with collagen VI. Collagen VI in turn interacts with many ECM protein, including collagen I and FN, through its beaded structure (Karsdal *et al.*, 2013).

The assembly of collagen I *in vivo* is not only triggered by propeptide cleavage, in contrast to in *vitro studies*. Collagen I fiber assembly *in vivo* is controlled by FN and FN- and collagen-binding integrins. Fibril formation is inhibited in the absence of FN, FN- and collagen binding integrins as well as in absence of collagen V (Kadler *et al.*, 2008). *In vivo* there are a lot of potential binding partners for collagen (approximately around 50 that

bind to fibrillary collagens). Kadler and colleagues proposed collagen V as potential nucleator for collagen fibril assembly and suggested that FN and integrins might be needed for the assembly site specification. (Kadler *et al.*, 2008)

1.2.4 Regulation of collagen homeostasis

Matrix turnover is regulated by a lot of different players including cytokines like TGF-β and cysteine (e.g. cathepsin K) and serine proteases (e.g. plasminogen activator) (Everts *et al.*, 1996). Under homeostasis, collagen production and degradation are coordinated to prevent fibrosis. The regulation can be performed either by intracellular or extracellular collagen degradation (Clarke *et al.*, 2013).

Few extracellular proteases, including several matrix metalloproteinases (MMPs), some serine proteases and cathepsin K can degrade fibrillar collagens. Fibroblast activation into myofibroblasts leads, besides to ECM protein expression, also to the expression of ECM regulating enzymes like matrix metalloproteinases (MMPs) and serine proteases (Lauer-Fields *et al.*, 2002; Song *et al.*, 2006; Clarke *et al.*, 2013; McKleroy *et al.*, 2013). During a pathologic state, the homeostasis of collagen deposition and degradation is aberrant. Plasminogen activator inhibitor 1 (Pai-1), upregulated in IPF, is an inhibitor of a signaling cascade that finally leads to the activation of specific MMPs and ultimately to collagen degradation (Ghosh and Vaughan, 2012; McKleroy *et al.*, 2013).

MMPs play a central role in connective tissue remodeling concerning development, homeostasis and wound healing (Lauer-Fields *et al.*, 2002).
In normal lungs, collagen degradation is dynamically regulated by MMPs as well as by tissue inhibitors of MMPs (TIMPs) (Dancer *et al.*, 2011). MMPs are extracellular endopeptidases that can be secreted or bound to the membrane, responsible for the degradation of connective tissue matrices, specifically ECM constituents. They can be divided into several subgroups according to their substrate specificity and structure (Bhattacharyya *et al.*, 2007). MMPs are either anti- or profibrotic; however in the development of fibrosis MMPs and their inhibitors are deregulated (Giannandrea and Parks, 2014).

Interestingly, besides collagen cleavage, MMPs are also able to activate latent TGF-β, a key regulator of collagen production. TGF-β is secreted as a pro-form and bound

together in a complex with latent associated protein $\beta 1$, $\beta 2$ and $\beta 3$ (small latent complex; SLC) to the ECM; latent TGF-β binding proteins (LTBPs) link the SLC to the ECM via association with ECM proteins like FN (Clarke *et al.*, 2013). Latent TGF-β is activated by MMPs by proteolytic cleavage of this inhibitory protein-protein interaction. (Bhattacharyya *et al.*, 2007; Clarke *et al.*, 2013)

Intracellular collagen degradation is executed by specific receptors like $\alpha 2\beta 1$ integrin on the cell surface recognizing collagen fibrils (Lee *et al.*, 1996; Arora *et al.*, 2000). After endocytosis, degradation of collagen is executed in the lysosomal network of the cell (Everts *et al.*, 1996).

To date there is the belief that extracellular and intracellular collagen degradation pathways collaborate with each other. After extracellular collagen degradation, fragments are internalized for further degradation via the lysosomal network given that extracellular collagen fragments can cause acute inflammation (Riley *et al.*, 1988; Weathington *et al.*, 2006).
Overall, in IPF all these accurately balanced processes can be dysregulated which result in excessive ECM deposition and distortion of the tissue (Clarke *et al.*, 2013).

1.3 Treatment options in IPF

IPF is characterized by lung tissue remodeling which leads to the distortion of the normal lung architecture by excessive ECM deposition.
In recent years, IPF was considered as a disease caused by chronic inflammation. Based on that belief, IPF patients were treated with corticosteroid and immunosuppressant drugs, but the lack of efficacy with this therapy guided the way to new treatment approaches (Datta *et al.*, 2011; Fujimoto *et al.*, 2015).
Based on the current concept that repeated microinjuries of the alveolar epithelium generate a fibrotic response, drug development was shifted to an antifibrotic strategy. However, in the guideline of 2011 no pharmacological treatment was recommended, except a weak recommendation for antacid therapy (Figure 1) (Kreuter *et al.*, 2015). Care options for IPF patients included palliation and lung transplantation (Raghu *et al.*, 2011).
Many compounds have been promising in the beginning like warfarin, ambrisentan (entothelin antagonist), imatinib (tyrosine kinase inhibitor) or the combination of corticosteroids and N-acetylcysteine (NAC) with the immunosuppressant azathioprine,

but were now not further recommended to treat IPF patients or even considered as harmful in the case of the last mentioned drug combination as published with the 2015s update of the clinical practice guidelines of 2011 (Table 1, adapted from (Kreuter *et al.*, 2015)), (Kreuter *et al.*, 2015). In 2014, two drugs, nintedanib and pirfenidone have been approved for IPF treatment by the FDA.

Additionally, there are many promising drug targets either preclinical or already in clinical trials like single component drugs that target extracellular factors implicated in fibrosis comprising amongst others extracellular TGF-β signaling inhibitors, receptor tyrosine kinase inhibitors (RTKs), cytokine inhibitors. Intracellular single component drug targets, mostly addressed by small molecules, are less accessible than extracellular targets, but nonetheless studies focusing on intracellular targets are increasing over the past few years; targets are classified as enzymes (e.g. Akt, FAK, MAPK), nuclear receptors (glucocorticoid receptor), epigenetic targets (miRNA) and other proteins (SMAD 2/3) (Li *et al.*, 2017).

Therapeutic Agent	2015 guideline	2011 guideline
Pirfenidone	Conditional recommendation for use *	Weak recommendation against use
Nintedanib	Conditional recommendation for use	Not addressed
Antiacid theraphy	Conditional recommendation for use	Weak recommendation for use
Phosphdiesterase-5 inhibitor (silenafil)	Conditional recommendation against use	Not addressed
Dual endothelin receptor antagonists	Conditional recommendation against use	Strong recommendation against use
N-acetylcysteine (NAC)	Conditional recommendation against use	Weak recommendation against use
Azathioprine + corticosteroids + NAC	Strong recommendation against use	Weak recommendation against use
Warfarin	Strong recommendation against use	Weak recommendation against use
Imatinib	Strong recommendation against use	Not addressed
Selective endothelin receptor anatgonist (ambrisentan)	Strong recommendation against use	Not addressed

*conditional recommendations are synonymous with weak recommendation

Table 1. Key recommendations on pharmacological treatment of IPF according to current guidelines (adapted from Kreuter, *et al.*, 2015)

The current guideline of 2015 recommends three options for IPF treatment, namely antacid therapy, nintedanib and pirfenidone which are introduced in the following paragraphs.

1.3.1 Antacid Therapy

Gastroesophageal reflux may contribute to IPF pathogenesis due to chronic micro aspiration of the refluxate. In animal models, repeated micro aspiration lead to increased collagen III, IV and FN expression via TGF-β and TNF-α regulation. Moreover, bile salts were reported to upregulate TGF-β production in human epithelial cells (Adamali and Maher, 2012).

Interestingly, half of the IPF patients treated against gastric reflux disease (GERD) were asymptomatic. A study revealed that the treatment with an antacid therapy, like proton pump inhibitors and histamine-2 receptor antagonists, is connected to a lower radiological fibrosis score which lead to a better survival in IPF patients (Adamali and Maher, 2012; Kreuter *et al.*, 2015).

Another study did not show any benefit of an antacid therapy; however, the 2015 guidelines give a conditional recommendation for use in IPF (Kreuter *et al.*, 2015).

1.3.2 Pirfenidone

Pirfenidone (5-methyl-1-phenylpyridin-2[1H]-one) is a synthetic pyridone analogue which was first discovered in 1976, with antifibrotic, antioxidant, and anti-inflammatory properties. It proved beneficial in different types of fibrosis, including lung, renal, hepatic and cardiac fibrosis; however, its precise mechanisms of action remain elusive. (Datta *et al.*, 2011; Schaefer *et al.*, 2011; Myllarniemi and Kaarteenaho, 2015)

In the 1990s researchers discovered that pirfenidone reduced profibrotic factors in lung tissue and diminished procollagen I, III and TGF-β accumulation as well as reduced the hydroxyproline content in lung tissue in bleomycin induced lung fibrosis in hamsters. Over the years, many other studies of bleomycin induced lung fibrosis in mice or cats could reproduce this outcome (Myllarniemi and Kaarteenaho, 2015).

In studies of (primary) human lung fibroblasts, pirfenidone treatment lead to reduced HSP47, FN, α-SMA levels and inhibited collagen I expression. Moreover, pirfenidone inhibited fibroblast proliferation and reduced PDGF, TNF-α and INF-γ levels (Nakayama *et al.*, 2008; Conte *et al.*, 2014; Lehtonen *et al.*, 2016).

The efficacy of pirfenidone was examined in four randomized, placebo controlled clinical 3 trials in IPF patients, in which three trials were able to show a slowdown in IPF

progression as measured by reduced decline in lung function (Maher, 2010; Blackwell *et al.*, 2014; Kreuter *et al.*, 2015).
Pirfenidone was approved for IPF treatment already in 2008 in Japan, followed by Europe in 2011 and finally in the U.S. in 2014 (Kreuter *et al.*, 2015). During standard treatment, patients receiving three daily doses of pirfenidone of 801 mg each and the serum levels are around 100 µM in patients (Wollin L, 2015). Reported side effects of the therapy include nausea, dizziness, vomiting and anorexia, but in general, pirfenidone is well tolerated, (Maher, 2010; Kreuter *et al.*, 2015).

1.3.3 Nintedanib

Nintedanib (BIBF1120), a small molecule developed by Boehringer-Ingelheim, is a receptor tyrosine kinase inhibitors (RTK) inhibitor against vascular endothelial growth factor, fibroblast growth factor and platelet-derived growth factor receptor. Nintedanib was originally designed as an anticancer drug and the clinical development for the treatment of cancers like breast-, ovarian- or gastrointestinal cancers is still ongoing. (Myllarniemi and Kaarteenaho, 2015; Wollin *et al.*, 2015).
Given that IPF and cancer share commonalities and nintedanib inhibits platelet-derived growth factor receptor, a receptor maintaining an important role in IPF disease progression, it was chosen as a possible treatment method for IPF (Wollin *et al.*, 2015).

In several preclinical studies, nintedanib revealed antifibrotic and anti-inflammatory properties. Nintedanib inhibits RTK receptors by blocking the intracellular ATP-binding pocket. Additionally, nintedanib can inhibit Src family kinases that are important players in processes like cell proliferation, migration and differentiation. PDGF stimulated motility was inhibited and TGF-β induced α-SMA expression was reduced in phLF of IPF patients upon nintedanib administration (Wollin *et al.*, 2015; Lehtonen *et al.*, 2016).

Nintedanib downregulated collagen secretion and deposition in phLF as well as FN and TIMP-2 and increased MMP-2 levels (Hostettler *et al.*, 2014; Wollin *et al.*, 2014; Rangarajan *et al.*, 2015).

Two identical international, randomized, placebo controlled, double-blind clinical phase III studies on nintedanib revealed a reduction in lung function decline compared to the placebo group. Patients are treated twice per day with 150 mg nintedanib each, whereby

the serum levels of 70 nM were reached. Nintedanib was approved in 2014 for IPF treatment in the USA and Europe (Richeldi *et al.*, 2014; Wollin *et al.*, 2015; Wollin L, 2015).
Overall nintedanib was well tolerated with reported drug related side effects like diarrhea and vomiting. The 2015 guideline recommends the use of nintedanib for IPF treatment (Kreuter *et al.*, 2015; Wollin *et al.*, 2015).

1.3.4 Targeting the ECM in lung fibrosis therapy

The primary goal of IPF therapy is to prevent progression, like during nintedanib and pirfenidone treatment. Nonetheless, the distortion of the normal lung architecture cannot be reverted to the normal state by this therapy, which might be the secondary goal.

To restore normal lung architecture, the disruption of a positive feedback loop in which the ECM composition induces the expression of more ECM proteins in myofibroblasts, might be a promising approach. Lung fibroblast seeded on decellularized IPF patient's matrix produced increased myofibroblast markers compared to control (Booth *et al.*, 2012). This observation was confirmed by another study revealing micro RNA 29 (miR29) a negative regulator of ECM genes, as a potential regulator of this feedback loop. In IPF and control fibroblasts that were grown on IPF derived ECM, miR29 was downregulated and thereby ECM protein expression not repressed (Parker *et al.*, 2014). These results highlight that the composition of the ECM is of importance for IPF disease progression and the disruption of this feedback loop might be potent strategy in IPF.

This might be archived by restoring the pathological ECM to the normal state and thereby repressing the feedback mechanism that leads to excessive ECM protein expression. Important players in this process are molecules implicated in collagen biosynthesis, maturation and degradation which comprise promising drug targets to interrupt this positive feedback loop.

To date, studies are ongoing on multicomponent drugs that either are one or several compounds that affect multiple targets, including compounds that target MMPs/TIMPs or TGF-β mechanisms (Li *et al.*, 2017). However, a study in phase II of a monoclonal antibody against LOXL2, an enzyme important for collagen crosslinking, was recently ended due to lack of efficacy; nonetheless other clinical trials are still ongoing focusing LOXL2 inhibition as therapy against IPF (Gilead Sciences, 2016; Li *et al.*, 2017).

One potential candidate for the disruption of the positive feedback loop can be FKBP10 as its deficiency can interfere with collagen synthesis and maturation as well as with fibrotic marker expression.

1.4 FK506 binding proteins

FK506 binding proteins (FKBPs) are intracellular proteins that belong to the family of immunophilins. They function as peptidyl-prolyl-isomerases (PPIs), catalyzing the *cis/trans* isomerization of proline (Figure 3, adapted from (Lu *et al.*, 2007)) and are molecular chaperones (Kang *et al.*, 2008). Immunophilins are targeted by the immunosuppressant drugs cyclosporine A and FK506 (tacrolimus), that are structurally not related but their mode of action is comparable as they both inhibit the PPIase activity (Kang *et al.*, 2008). According to their binding partners, immunophilins can be divided into two classes, cyclophilin bind to cyclosporine A and FKBPs bind to FK506 (Ishikawa *et al.*, 2008). The best known FKBP is FKBP1A (FKBP1, FKBP12). The complex of FKBP12/FK506 has immunosuppressive activity as it inhibits the phosphatase activity of calcineurin, resulting in impeded activation of the transcription factor nuclear factor of activated T cells (NFAT). NFAT is responsible for the activation of the transcription of the interleukin-2 gene during T-cell activation (Jorgensen *et al.*, 2003).

The FK506 binding domain (FKBD) of FKBPs is conserved from *archaea* to primates (Kang *et al.*, 2008).

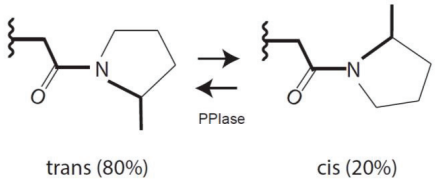

Figure 3. PPIase activity. PPIases catalyze the *cis/trans* isomerization of proline residues. (Figure adapted from Lu, *et al.*, 2007)

FKBPs are divided into four subgroups according to the regions next or within the PPI domains, covering the nuclear, the cytoplasmic, the tetracorticopeptide (TPR) domain as well as the secretory-pathway FKBPs (Rulten *et al.*, 2006). FKBP family members of

small molecular weight possess only the FK506-binding domain (FKBD), in contrast to FKBPs with larger molecular weight that own amongst others calcium binding domains or TPR repeats (Figure 4, adapted from (Rulten *et al.*, 2006)).

FKBPs maintain many different functions like protein trafficking and folding or receptor signaling (Kang *et al.*, 2008). The mammalian FKBP family is divided into four groups in accordance to their protein domains: FKBP1A (FKBP12) belongs to the cytoplasmic FKBPs, FKBP3 (FKBP25) is a member of the nuclear FKBPs, FKBP5 (FKBP51) can be included in the TPR repeats FKBPs and FKBP10 (FKBP65) belongs to the largest group of FKBPs, the secretory pathway FKBPs (Figure 4 adapted from (Rulten *et al.*, 2006)).

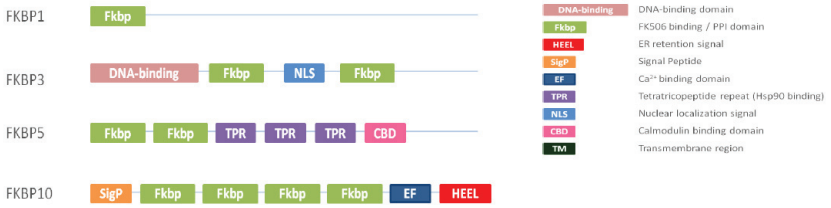

Figure 4. Examples of FKBP members of each subgroup. FKBP1 and FKBP1B belong to the cytoplasmatic FKBPs. FKBP3 and 15 are nuclear FKBPs. FKBP4, 5, 6, 8 contain a tetratricopeptide (TRP) domain and are therefore grouped as TRP-domain containing FKBPs. FKBP7, 9, 10, 11, 14 belong to the secretory pathway FKBPs. (Figure adapted from Rulten, *et al.*, 2006).

1.4.1 FKBP10

FKBP10 is an ER resident PPIase and collagen chaperone that is developmentally regulated and is an important player in folding and trafficking of secretory proteins (Patterson *et al.*, 2005; Ishikawa *et al.*, 2008). In the lung it is expressed with the same developmental pattern as tropoelastin and collagen I after bleomycin exposure in mice (Patterson *et al.*, 2005). Additionally, the PPIase activity of FKBP10 was proposed to be important for tropoelastin folding, a proline rich molecule and an FKBP10 ligand (Davis *et al.*, 1998).

The rate of collagen triple helix formation, which is limited by the process of *cis-trans* isomerization, was only marginally influenced by FKBP10 (Bächinger *et al.*, 1980; Bächinger *et al.*, 1993; Zeng *et al.*, 1998).

FKBP10 interacts with unfolded and triple helical collagen and its function as collagen chaperone is important in collagen stabilization and maturation (Ishikawa *et al.*, 2008). The chaperone activity of FKBP10 was not disrupted by the addition of FK506, probably because only one of four FKBDs in FKBP10 is blocked by FK506. Like HSP47, FKBP10 might inhibit premature procollagen association inside the cell (Ishikawa *et al.*, 2008). During post translational maturation of procollagen I, FKBP10 and HSP47 act cooperatively (Duran *et al.*, 2015).

FKBP10 interacts with ERp29, a PDI family member, and with lysyl hydroxylase 2 (LH2). Activation of LH2 needs dimerization that requires FKBP10, indicating FKBP10 important for LH2 activity (Barnes *et al.*, 2012; Schwarze *et al.*, 2013; Zhou *et al.*, 2014; Ishikawa *et al.*, 2015; Gjaltema *et al.*, 2016).

Connective tissue disorders arising from the disruption of collagen biosynthesis are commonly caused by mutations in genes encoding collagens or collagen biosynthetic enzymes. Mutations in *FKBP10* for example lead to Bruck and Kuskokwim syndrome and to a recessive form of OI, also called the brittle bone disease that is caused by structural defects of collagen I (Rauch and Glorieux, 2004; Ishikawa *et al.*, 2015). Therefore, FKBP10 is a crucial player in collagen biosynthesis and maintains an important role in collagen related diseases.

Besides OI or Bruck syndrome, IPF is also a collagen related disorder (Fernandez and Eickelberg, 2012). The PPIase inhibitory drug FK506, which inhibits one FKBD of FKBP10, was reported to execute antifibrotic action in lung fibrosis (Inase *et al.*, 2003; Nagano *et al.*, 2006; Horita *et al.*, 2011; Correale *et al.*, 2013). Reported effects *in vitro* ranged from reduced collagen synthesis to the inhibition of TGF-β1 receptor expression in dermal and lung fibroblasts, but the mechanism of action remains mainly unsolved (Nagano *et al.*, 2006; Dancer *et al.*, 2011; Wu *et al.*, 2012; Lan *et al.*, 2014).

1.5 Objectives of this thesis

IPF is a collagen related disorder characterized by excessive deposition of ECM, mainly collagen, resulting in an irreversible distortion of the lung architecture. FKBP10, a PPIase and collagen chaperone, maintains a major role in other collagen related disorders like OI. Additionally, the treatment with FK506, the inhibitor of one of FKBP10 FKBD, was

reported to have antifibrotic effects but the mechanism of action is unknown (Inase *et al.*, 2003; Nagano *et al.*, 2006; Dancer *et al.*, 2011; Horita *et al.*, 2011; Wu *et al.*, 2012; Correale *et al.*, 2013; Lan *et al.*, 2014). Therefore, the first aim of this thesis was to assess the localization, regulation and function of FKBP10 in the context of IPF (Chapter 2.1).

Based on the antifibrotic effects of FKBP10 loss in Chapter 2.1, and the fact that abnormal fibroblast adhesion and migration are known features of IPF pathogenesis, the second aim of this thesis was to examine the effect of FKBP10 deficiency on fibroblast adhesion and migration as well as to solve the underlying mechanism of action (Chapter 2.2).

Nintedanib and pirfenidone two therapeutics that were recently approved for the treatment of IPF, slow down disease progression, but their precise mechanism of action is incompletely understood. The third aim of this thesis was to comprehensively analyze and directly compare the effects of nintedanib and pirfenidone on collagen biosynthesis and secretion in phLF to get a better understanding of their mechanism of action (Chapter 2.3). Based on these results the effects of nintedanib and pirfenidone and other collagen synthesis and maturation inhibitors in comparison to the effects of FKBP10 loss are discussed in this thesis (Chapter 3).

2. Publications

2.1 FK506-Binding Protein 10, a Potential Novel Drug Target for Idiopathic Pulmonary Fibrosis

This publication reveals FKBP10 as potential novel drug target in IPF. FKBP10 is highly expressed in IPF patients and bleomycin-induced lung fibrosis. FKBP10 was found to be expressed by (myo)fibroblasts and $CD68^{+}$ macrophages. Knockdown experiments of FKBP10 in phLF lead to a reduction of fibrotic marker expression and decreased collagen secretion. In comparison with nintedanib, a recently approved IPF therapeutic, FKBP10 deficiency had a similar inhibitory effect on collagen secretion.

Contribution:
The author of this thesis helped with the experimental work, analysis and interpretation as well as drafting the manuscript.

Staab-Weijnitz, C.A., Fernandez IE, Knüppel L, Maul J, Heinzelmann K, Juan-Guardela BM, Hennen E, Preissler G, Winter H, Neurohr C, Hatz R, Lindner M, Behr J, Kaminski N, Eickelberg O. FK506-Binding Protein 10, a Potential Novel Drug Target for Idiopathic Pulmonary Fibrosis. *American Journal of Respiratory and Critical Care Medicine*, 2015. 192(4): p. 455-67.

The *American Journal of Respiratory and Critical Care Medicine* is an official journal of the American Thoracic Society.

ORIGINAL ARTICLE

FK506-Binding Protein 10, a Potential Novel Drug Target for Idiopathic Pulmonary Fibrosis

Claudia A. Staab-Weijnitz[1], Isis E. Fernandez[1], Larissa Knüppel[1], Julia Maul[1], Katharina Heinzelmann[1], Brenda M. Juan-Guardela[2], Elisabeth Hennen[1], Gerhard Preissler[3], Hauke Winter[3], Claus Neurohr[4], Rudolf Hatz[3,5], Michael Lindner[5], Jürgen Behr[4,5], Naftali Kaminski[2], and Oliver Eickelberg[1]

[1]Comprehensive Pneumology Center, Helmholtz Zentrum München, Member of the German Center of Lung Research (DZL), Munich, Germany; [2]Pulmonary, Critical Care and Sleep Medicine, Yale School of Medicine, New Haven, Connecticut; [3]Thoraxchirurgisches Zentrum, Klinik für Allgemeine, Viszeral, Transplantations, Gefäß- und Thoraxchirurgie, Klinikum Großhadern, Ludwig-Maximilians-Universität, Munich, Germany; [4]Medizinische Klinik und Poliklinik V, Klinikum der Ludwig-Maximilians-Universität, Member of the German Center of Lung Research (DZL), Munich, Germany; and [5]Asklepios Fachkliniken München-Gauting, Munich, Germany

Abstract

Rationale: Increased abundance and stiffness of the extracellular matrix, in particular collagens, is a hallmark of idiopathic pulmonary fibrosis (IPF). FK506-binding protein 10 (FKBP10) is a collagen chaperone, mutations of which have been indicated in the reduction of extracellular matrix stiffness (e.g., in osteogenesis imperfecta).

Objectives: To assess the expression and function of FKBP10 in IPF.

Methods: We assessed FKBP10 expression in bleomycin-induced lung fibrosis (using quantitative reverse transcriptase–polymerase chain reaction, Western blot, and immunofluorescence), analyzed microarray data from 99 patients with IPF and 43 control subjects from a U.S. cohort, and performed Western blot analysis from 6 patients with IPF and 5 control subjects from a German cohort. Subcellular localization of FKBP10 was assessed by immunofluorescent stainings. The expression and function of FKBP10, as well as its regulation by endoplasmic reticulum stress or transforming growth factor-β_1, was analyzed by small interfering RNA–mediated loss-of-function experiments, quantitative reverse transcriptase–polymerase chain reaction, Western blot, and quantification of secreted collagens in the lung and in primary human lung fibroblasts (phLF). Effects on collagen secretion were compared with those of the drugs nintedanib and pirfenidone, recently approved for IPF.

Measurements and Main Results: FKBP10 expression was up-regulated in bleomycin-induced lung fibrosis and IPF. Immunofluorescent stainings demonstrated localization to interstitial (myo)fibroblasts and $CD68^+$ macrophages. Transforming growth factor-β_1, but not endoplasmic reticulum stress, induced FKBP10 expression in phLF. The small interfering RNA–mediated knockdown of FKBP10 attenuated expression of profibrotic mediators and effectors, including collagens I and V and α-smooth muscle actin, on the transcript and protein level. Importantly, loss of FKBP10 expression significantly suppressed collagen secretion by phLF.

Conclusions: FKBP10 might be a novel drug target for IPF.

Keywords: FKBP65; peptidyl-prolyl isomerase; lung fibrosis; collagen cross-linking; extracellular matrix

(Received in original form December 15, 2014; accepted in final form May 18, 2015)

Supported by the Helmholtz Association, the German Center for Lung Research, and National Institutes of Health grants RO1HL108642 and RC2HL101715 (N.K.).

Author Contributions: Conception and design: C.A.S.-W., I.E.F., K.H., J.B., N.K., and O.E. Experimental work, analysis, and interpretation: C.A.S.-W., I.E.F., L.K., J.M., K.H., B.M.J.-G., E.H., G.P., H.W., C.N., R.H., M.L., N.K., and O.E. Drafting the manuscript and intellectual content: C.A.S.-W., I.E.F., L.K., K.H., N.K., and O.E.

Correspondence and requests for reprints should be addressed to Oliver Eickelberg, M.D., Comprehensive Pneumology Center, Ludwig-Maximilians-Universität and Helmholtz Zentrum München, Max-Lebsche-Platz 31, 81377 München, Germany. E-mail: oliver.eickelberg@helmholtz-muenchen.de

This article has an online supplement, which is accessible from this issue's table of contents at www.atsjournals.org

Am J Respir Crit Care Med Vol 192, Iss 4, pp 455–467, Aug 15, 2015

Originally Published in Press as DOI: 10.1164/rccm.201412-2233OC on June 3, 2015
Internet address: www.atsjournals.org

At a Glance Commentary

Scientific Knowledge on the Subject: Accumulation of extracellular matrix plays an important role in idiopathic pulmonary fibrosis (IPF) disease progression. Deficiency of the chaperone FK506-binding protein 10 (FKBP10) has been reported to attenuate collagen secretion and decrease extracellular collagen cross-linking in, for example, osteogenesis imperfecta.

What This Study Adds to the Field: FKBP10 is specifically up-regulated in interstitial fibroblasts in IPF. Inhibition of FKBP10 in primary IPF fibroblasts attenuates gene expression of various profibrotic genes and decreases collagen secretion.

Idiopathic pulmonary fibrosis (IPF) is the most fatal interstitial lung disease, with a 5-year survival rate of 30 to 50% and few treatment options (1). The etiology of IPF is poorly understood. The current concept involves repeated alveolar injuries of unclear nature, providing signals for fibroblast activation, proliferation, and differentiation to myofibroblasts (2–6). The latter overgrow the delicate alveolar lung tissue and secrete increased amounts of extracellular matrix (ECM) proteins. According to a recently published study, the ECM appears to play a major role not only in the composition but also in the maintenance of the fibrotic phenotype in IPF, contributing to the irreversibility of the disease (7). Therefore, matrix and matrix-processing enzymes will provide promising novel drug targets for IPF. For instance, inhibition of the collagen cross-linking enzyme lysyl oxidase-like 2 (LOXL2) is currently investigated as an IPF treatment option in a phase II trial (8).

Pirfenidone and nintedanib, two drugs recently approved by the U.S. Food and Drug Administration for IPF therapy, decelerate but do not attenuate disease progression in patients with IPF, by decreasing lung function decline. They also show considerable side effects, and their mechanism of action is incompletely understood (9, 10). As such, the need to identify novel drug targets for IPF remains imperative, as we require alternative treatment options for nonresponders, cell-type–specific targeted therapy, and combination therapy options.

The intracellular chaperone FK506-binding protein 10 (FKBP10, also termed FKBP65) has been reported to directly interact with collagen I (11). FKBP10 belongs to the FKBP subfamily of immunophilins, molecular chaperones with peptidyl-prolyl isomerase activity, which bind the immunosuppressive drug FK506 (tacrolimus) (12, 13). Collagen triple helix formation heavily relies on proline isomerization to *trans*-proline as a prerequisite of linear chain assembly (14). Mutations in *FKBP10* lead to collagen-related disorders such as osteogenesis imperfecta, and studies in the last 4 years have suggested an association of these mutations with attenuated collagen secretion and diminished collagen I cross-linking in dermal fibroblasts and bone (15–18). A recent study showed that $Fkbp10^{-/-}$ mouse embryos are postnatally lethal and display reduced collagen cross-linking in calvarial bone (19).

Given that FKBP10 is a collagen-processing enzyme with potential impact on ECM protein secretion and cross-linking, we sought to assess its role in IPF. We analyzed *FKBP10* expression in lungs of mice subjected to bleomycin and patients with IPF. Loss-of-function studies were performed in primary human lung fibroblasts (phLF) to investigate the effect of FKBP10 on ECM protein synthesis and secretion.

Methods

For more details on methods, *see* the online supplement. Statistical analysis was performed in GraphPadPrism 5 (GraphPad Software, San Diego, CA). Results are given as mean ± SEM, and paired *t* test was used for statistical analysis, if not mentioned otherwise.

Induction and Measurement of Murine Pulmonary Fibrosis

Pulmonary fibrosis was induced in female C57BL/6 mice (10–12 wk old) by a single intratracheal instillation of 50 μl of bleomycin (3 U/kg; Sigma Aldrich, Taufkirchen, Germany) dissolved in sterile saline and applied using the MicroSprayer Aerosolizer, Model IA-1C (Penn-Century, Wyndmoor, PA). Control mice were instilled with 50 μl of saline. After instillation, mice were kept for 14, 28, and 56 days. Before death, mice were anesthetized with ketamine/xylazine followed by lung function measurement and tissue harvesting as previously described (20). Fibrosis was further assessed by bronchoalveolar lavage cell counts and histology evaluation. All animal experiments were conducted under strict governmental and international guidelines and were approved by the local government for the administrative region of Upper Bavaria, Germany.

Gene Expression Data

Data for FKBP10 in IPF lungs (n = 99) and normal histology control lungs (n = 43) was extracted from the gene expression microarray data generated by us on lung samples obtained from the National Lung, Heart, and Blood Institute–funded Tissue Resource Consortium, as described previously (21, 22). Gene expression microarray data (Agilent Technologies, Santa Clara, CA), and associated clinical data are available on the Lung Genomics Research Consortium website (https://www.lung-genomics.org/research/) as well as on accession number GSE47460 or the Lung Tissue Research Consortium website (http://www.ltrcpublic.com). Significance was calculated using *t* statistics, and multiple testing was controlled by the false discovery rate method at 5% (23).

Human Material

Resected human lung tissue and lung explant material were obtained from the Asklepios biobank for lung diseases at the Comprehensive Pneumology Center. Biopsies were obtained from six patients with IPF (usual interstitial pneumonia pattern, mean age 54 ± 9 yr, five men, one woman). All participants gave written informed consent, and the study was approved by the local ethics committee of Ludwig-Maximilians University of Munich, Germany.

Isolation and Culture of phLF

For FKBP10 knockdown, phLF were isolated from IPF biopsies (n = 4), the adjacent normal region of a lung tumor resection (n = 2), and donor tissue (n = 3). For more details, *see* the online supplement.

Treatment of phLF with Transforming Growth Factor-β_1, Nintedanib, or Pirfenidone

Cells were seeded at a density of 20,000 to 25,000 cells/cm^2, starved for 24 hours in Dulbecco's modified Eagle medium/F12 with 0.5% fetal bovine serum and 0.1 mM 2-phospho-L-ascorbic acid, followed by treatment with the indicated concentrations of transforming growth factor (TGF)-β_1 (R&D Systems, Minneapolis, MN), nintedanib, and pirfenidone (both Selleck, Houston, TX) in starvation medium for the indicated time points. For more details, *see* the online supplement.

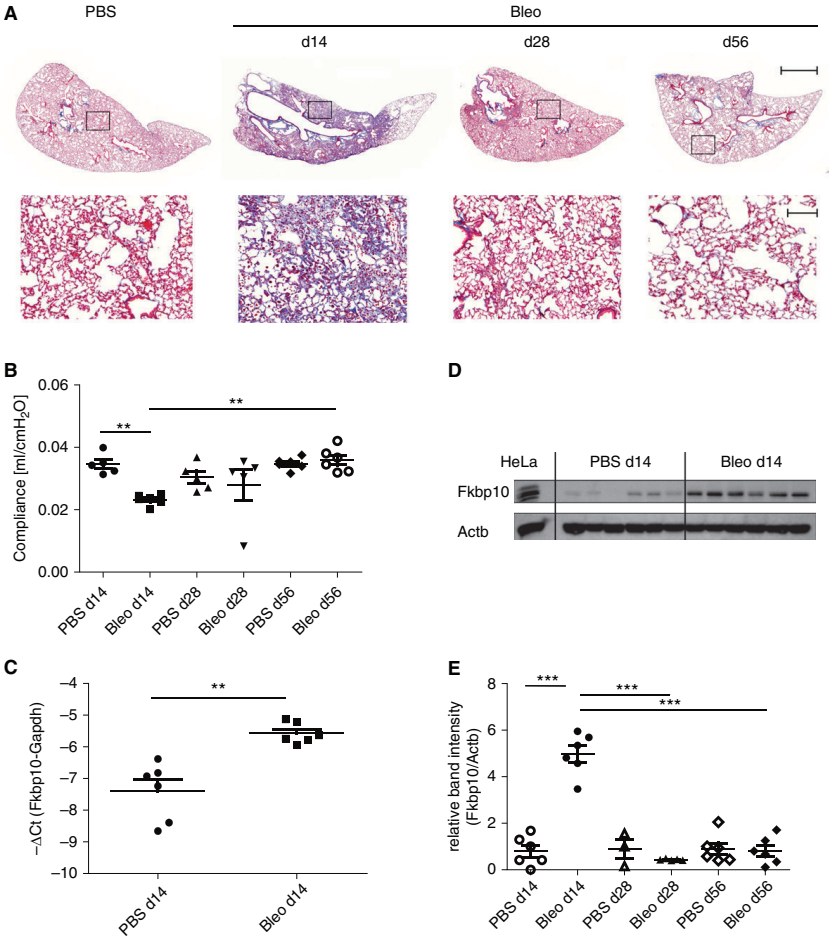

Figure 1. FK506-binding protein 10 (FKBP10) is up-regulated in a mouse model of bleomycin-induced lung fibrosis. (*A*) Representative Masson trichrome staining demonstrating that increased collagen deposition peaked at Day 14 and was gradually lost afterward. *Bottom row* shows magnification of the *boxed areas* in the *top row*. *Upper scale bar* = 1,000 μm; *lower scale bar* = 100 μm. (*B*) Bleomycin instillation led to a significant decrease in lung compliance at Day 14, which was completely restored after 56 days. (*C*) *FKBP10* gene expression was up-regulated at Day 14 after bleomycin instillation. (*D*) Representative Western blot showing that FKBP10 levels in total lung homogenate were significantly increased at Day 14 after bleomycin instillation; HeLa lysate was used as positive control. (*E*) Quantification by densitometric analysis demonstrating that FKBP10 levels returned to baseline at Day 28 and Day 56. Data shown are mean ± SEM, and a two-tailed Mann-Whitney test was used for statistical analysis for comparison between bleomycin groups (Bleo) at different time points and phosphate-buffered saline (PBS) control vs. bleomycin for each time point. Actb = β-actin as loading control. Gapdh = glyceraldehyde phosphate dehydrogenase. $^{**}P < 0.01$, $^{***}P < 0.001$.

Transfection of phLF

Cells were reverse transfected either with human FKBP10 small interfering RNA (siRNA) (s34171; Life Technologies, Carlsbad, CA) or negative control siRNA No. 1 (Life Technologies). Twenty-four hours after transfection, cells were starved for another 24 hours in Dulbecco's modified Eagle medium/F-12 including 0.5% fetal bovine serum and 0.1 mM 2-phospho-L-ascorbic acid, followed by treatment with 2 ng/ml TGF-β_1 in starvation medium. Twenty-four and 48 hours after beginning the TGF-β_1 treatment, cells and cell culture supernatants were harvested for RNA and protein analysis. In total, eight completely independent knockdowns were performed in eight different human primary fibroblast lines.

After 24 hours of siRNA transfection, forward transfection with the mothers against decapentaplegic homolog (SMAD) signaling luciferase reporter plasmid was performed in three different cell lines with pGL3-CAGA(9)-luc (24) or pGL3 control vector (Promega, Madison, WI). After incubation for 6 hours, cells were starved for 18 hours, followed by treatment with 2 ng/ml TGF-β_1. Luminescence was recorded in a TriStar LB 941 Multimode Reader (Berthold Technologies, Bad Wildbad, Germany), and results were normalized to pGL3 control luciferase activity.

For more details, *see* the online supplement.

Real-Time Quantitative Reverse Transcriptase Polymerase Chain Reaction Analysis

Relative transcript abundance of a gene is expressed as $-\Delta C_t$ values ($\Delta C_t = C_t^{\text{target}} - C_t^{\text{reference}}$) or as fold change derived from the relevant $\Delta\Delta C_t$ values, using $2^{-(\Delta\Delta Ct)}$. For specific gene amplification, primers listed in Table E1 in the online supplement were used. Glyceraldehyde phosphate dehydrogenase (GAPDH) and hypoxanthine-guanine phosphoribosyltransferase (HPRT) were used as endogenous controls for standardization of relative mRNA expression in mice and phLF, respectively. For more technical details on RNA isolation and quantitative reverse transcriptase polymerase chain reaction, *see* the online supplement.

Protein Isolation and Western Blot Analysis

See online supplement.

Quantification of Secreted Collagen

For quantification of total secreted collagen, the Sircol assay was performed according to manufacturer's instructions (Biocolor, Carrickfergus, UK).

For specific quantification of secreted collagen I, collagens were precipitated from cell culture supernatant as follows: Proteins were precipitated with 0.2 g/ml ammonium sulfate and incubated on ice for 30 minutes,

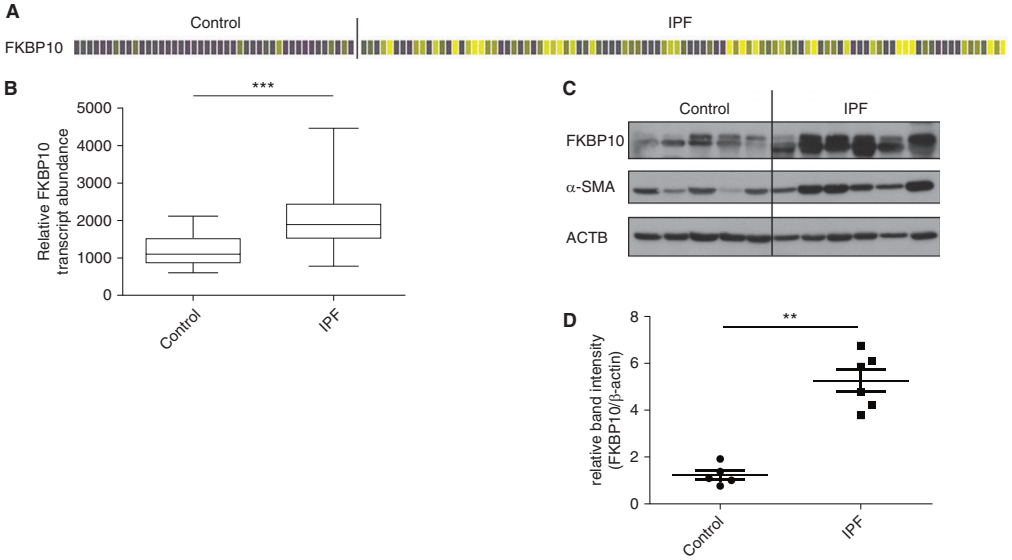

Figure 2. FK506-binding protein 10 (FKBP10) is up-regulated in idiopathic pulmonary fibrosis (IPF). (*A*) Heat map of *FKBP10* gene expression, extracted from microarray data of normal histology control (n = 43) and samples from patients with IPF (n = 99). Every column corresponds to a patient. Increases and decreases are denoted in increasing shades of *yellow* and *purple*, respectively, and *gray* is unchanged (false discovery rate < 5%). (*B*) Box-and-whisker plot for *FKBP10* gene expression data. The difference is highly significant (***$P < 1 \times 10^{-7}$). (*C*) Western blot analysis of total lung tissue homogenate showed up-regulation of FKBP10 in patients with IPF relative to donor samples in an independent cohort. (*D*) Densitometric analysis of the Western blot showed that FKBP10 up-regulation in IPF is highly significant. Data shown are mean ± SEM, and a two-tailed Mann-Whitney test was used for statistical analysis (**$P < 0.01$). α-SMA = α-smooth muscle actin; ACTB = β-actin as loading control.

followed by centrifugation at 20,000 × *g* at 4°C for 30 minutes. The pellet was dissolved in 0.1 M acetic acid containing 0.1 mg/ml pepsin (Thermo Fisher Scientific, Waltham, MA) and incubated overnight at 4°C. Then, 5 M NaCl was added to yield a final concentration of 0.7 M, followed by incubation on ice for 30 minutes and centrifugation at 20,000 × *g* at 4°C for 30 minutes. The pellet containing collagen I was resuspended in 0.1 M acetic acid and analyzed by immunoblotting.

Immunofluorescent and Masson Trichrome Stainings

Cultured phLF were seeded on coverslips, and immunostaining was performed as described previously (25). For staining of tissue sections, human and murine lung tissue was fixed in 10% formalin before paraffin embedding. Three-micron sections were prepared and mounted on slides, followed by deparaffinization and immunofluorescent staining or Masson trichrome staining according to a standard protocol. For more details, *see* the online supplement.

Subcellular Fractionation

Protein fractionation was performed with a Subcellular Protein Fractionation Kit for Cultured Cells (Thermo Fisher Scientific) according to the manufacturer's instructions. Purity of the fractions was assessed using the following marker proteins for Western blot analysis of the obtained fractions: calreticulin and protein disulfide isomerase 3 (PDIA3) for the membrane extract, glyceraldehyde phosphate dehydrogenase (GAPDH) for the cytosolic extract, and lamin A/C for the nuclear and chromatin-bound extract.

Results

FKBP10 Expression Is Increased in Lung Fibrosis

We first studied FKBP10 expression in the mouse model of bleomycin-induced lung fibrosis. Bleomycin instillation led to increased ECM deposition, as demonstrated by Masson trichrome staining, and a significant decrease in lung compliance at Day 14, which was completely restored after 56 days (Figures 1A and 1B). Western blot analysis showed a clear increase of FKBP10 protein levels in total lung lysates at Day 14 after instillation of bleomycin (Figure 1D). After resolution of fibrosis, at Day 56, FKBP10 expression had returned to baseline levels (*cf.* Figures 1A, 1B, and 1E). With a fold change of 3.6, up-regulation of FKBP10 at Day 14 occurred in part on the transcriptional level (Figure 1C).

Next, we studied FKBP10 gene expression in IPF. Analysis of microarray data of 99 IPF samples and 43 normal histology control samples revealed significant up-regulation of FKBP10 (fold change, 1.7; false discovery rate $< 5\%$; $P < 1 \times 10^{-7}$) (Figures 2A and 2B). Up-regulation of FKBP10 was confirmed on the protein level using lung homogenates from patients with IPF of an independent cohort: FKBP10 was highly increased in comparison with donor samples (Figures 2C and 2D). Moreover, FKBP10 levels appeared to correlate with levels of α-smooth muscle actin (α-SMA), a marker of myofibroblasts (Figure 2C).

FKBP10 Is Expressed in Interstitial Fibroblasts, Including Myofibroblasts

Immunofluorescent stainings of lung tissue sections from the bleomycin-treated mice and patients with IPF confirmed increased expression of FKBP10 in fibrotic lungs, with little staining of FKBP10 in phosphate-buffered saline–instilled control mice or donor lungs. FKBP10 expression was predominantly localized to interstitial fibroblasts, as evidenced by colocalization with α-SMA (Figures 3 and 4A) or desmin (Figure 4A), both markers of myofibroblasts. In addition, a fraction of FKBP10-expressing cells were found to be interstitial macrophages (evidenced by $CD68^+$ staining; Figure 4B).

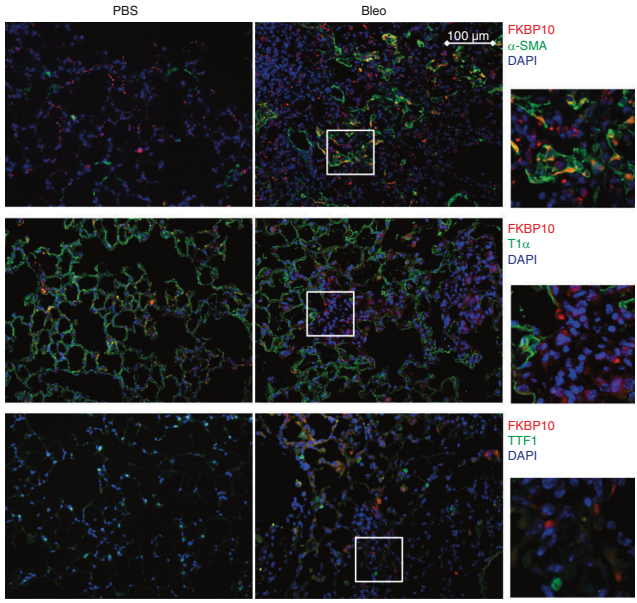

Figure 3. FK506-binding protein 10 (FKBP10) is expressed in interstitial fibroblasts, including myofibroblasts, in a mouse model of bleomycin-induced lung fibrosis. Immunofluorescent stainings of paraffin sections from control (phosphate-buffered saline [PBS], *left panels*) and bleomycin-treated (Bleo, *right panels*) mice at Day 14 after bleomycin instillation. Representative Fkbp10 immunostaining is shown in *red*, α-smooth muscle actin (α-SMA), podoplanin (T1α), or thyroid transcription factor 1 (TTF1) in *green*, and 4′,6-diamidino-2-phenylindole (DAPI) in *blue*, as indicated on the *right side*. *White squares* in the Bleo stainings are shown enlarged to the *right*. Sections shown are representative stainings from three PBS- and three bleomycin-treated mice.

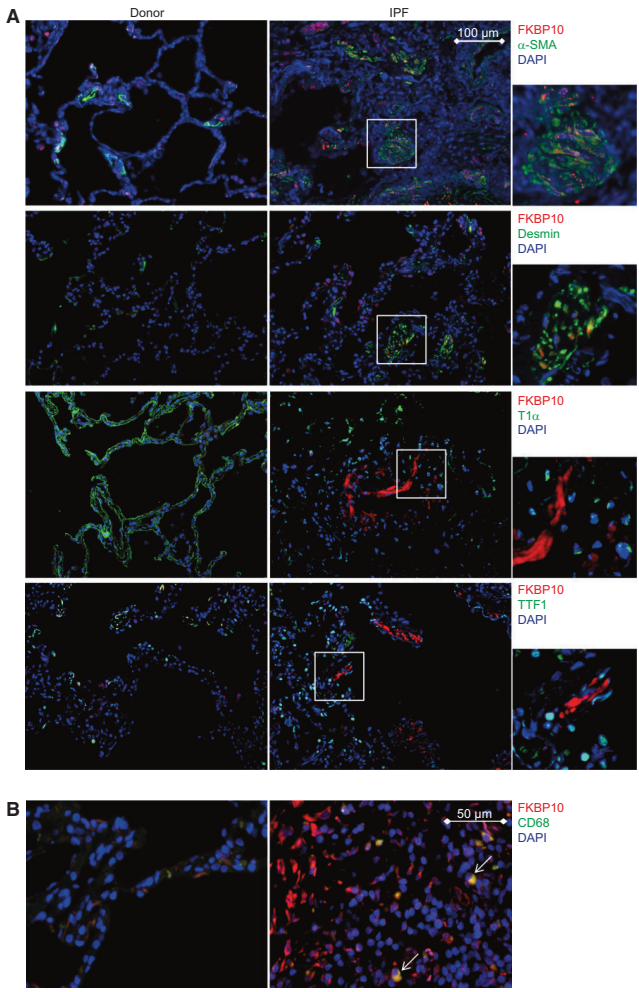

Figure 4. FK506-binding protein 10 (FKBP10) is expressed in interstitial fibroblasts, including myofibroblasts, and interstitial CD68$^+$ macrophages in human idiopathic pulmonary fibrosis (IPF). Representative immunofluorescent stainings of paraffin sections from donor (*left panels*) and IPF tissue (*right panels*). Representative FKBP10 immunostaining is always shown in *red* and 4′,6-diamidino-2-phenylindole (DAPI) in *blue*. (*A*) Representative immunofluorescent costainings with α-smooth muscle actin (α-SMA), desmin, podoplanin (T1α), and thyroid transcription factor 1 (TTF1) in *green* show FKBP10 expression in interstitial fibroblasts but not in alveolar epithelial cells. *White squares* in the IPF stainings are shown enlarged to the *right*. *Scale bar* = 100 μm. (*B*) Representative immunofluorescent costainings with CD68 show FKBP10 expression in interstitial macrophages (indicated by white arrows). Sections shown are representative stainings from three donors and three patients with IPF. *Scale bar* = 50 μm.

In contrast, FKBP10 did not colocalize with T1α (AT1 cells) or TTF1 (AT2 cells) (Figures 3 and 4A).

FKBP10 Is an Endoplasmic Reticulum Resident Protein but Not Up-regulated by ER Stress in Primary Human Lung Fibroblasts

In immunofluorescent stainings of phLF, FKBP10 localized mainly to the cytoplasm and showed colocalization with PDIA3, an endoplasmic reticulum (ER)-resident protein (Figure 5A). In some cells, positive FKBP10 staining was also observed in the nucleus. In contrast, costaining with a marker for the Golgi apparatus, Golgin subfamily A member 1 (GOLGA1) showed no colocalization (Figure 5B). Subcellular fractionation of phLF resulted in a clear enrichment of FKBP10 in the ER/membrane extract (Figure 5C). Additionally, FKBP10 was also weakly detected in the cytosolic and the nuclear extract.

Although tunicamycin and thapsigargin up-regulated the ER stress markers BiP, ATF4, and CHOP, FKBP10 levels were drastically decreased by both (*see* Figure E1 in the online supplement). FKBP10 usually migrated at approximately 70 kD, but in the presence of tunicamycin an additional FKBP10 band appeared at approximately 65 kD, in agreement with the theoretical size of the unmodified protein (cf. Figure E1A).

TGF-β_1 Up-regulates FKBP10 Expression in phLF

TGF-β_1 induced FKBP10 expression in a dose-dependent manner, with a clearly visible up-regulation for concentrations of 1 ng/ml and higher after 48 hours of treatment (Figure 6A). Efficacy of TGF-β_1 treatment was confirmed by Western blot analysis of phosphorylated and total SMAD3 (Figure 6A). From these initial experiments, an effective concentration of 2 ng/ml TGF-β_1 was derived and used in the following FKBP10 knockdown experiments, where the TGF-β_1 effect on FKBP10 expression was also quantified (Figure 6B). Results in Figure 6B are based on results with control siRNA from the loss-of-function experiments (*cf.* Figure 6C for a representative Western blot). Induction of FKBP10 expression by TGF-β_1 was already observed at transcript level (Figure E2).

Loss of FKBP10 in IPF Fibroblasts Attenuates ECM Protein Synthesis and Decreases Levels of Secreted Collagen Independent of TGF-β Signaling

The siRNA-mediated knockdown of FKBP10 in IPF fibroblasts showed significant down-regulation of collagen I, collagen V, and fibronectin protein levels in crude cell lysates after 48 hours of TGF-β_1 treatment (Figures 6C and 6D). Interestingly, TGF-β_1 partly counteracted this effect for collagen I, but not for collagen V or fibronectin (Figure 6D). Moreover, levels of the myofibroblast marker α-SMA were also significantly decreased by knockdown of FKBP10 in the presence of TGF-β_1 (Figure 6D, *bottom right panel*). The effects observed for collagen I and V manifested at transcript level already and also transcription of the TGF-β target gene *PAI1* were decreased by knockdown of FKBP10, suggestive of an effect on overall TGF-β signaling (Figure 7A). However, the corresponding TGF-β–induced transcript fold changes did not indicate attenuation of TGF-β signaling in the FKBP10 knockdown (Figure 7B), and neither a Smad signaling luciferase reporter assay (Figure 7C) nor analysis of SMAD 3 phosphorylation or protein levels (Figure 7D and Figure E3) showed an appreciable effect of FKBP10 knockdown on canonical TGF-β signaling.

Finally, we assessed levels of secreted collagen in these experiments by two approaches. First, specifically collagen type I levels were semiquantified using Western blot analysis followed by densitometry (Figures 8A and 8B); second, total secreted collagen was quantified using the Sircol assay (Figure 8C). Both approaches showed significant decreases of secreted collagen in the FKBP10 knockdown in absence and presence of TGF-β_1.

In our efforts to interpret the relevance of FKBP10 knockdown in IPF fibroblasts in the context of currently approved IPF therapeutics, we used the same experimental setup to address inhibition of total collagen secretion in IPF fibroblasts by nintedanib and pirfenidone. Importantly, FKBP10 knockdown significantly decreased total collagen secretion by about 20%, in an amount similar to the effects observed with nintedanib, whereas we did not observe any effect of pirfenidone on total collagen secretion (Figure 9).

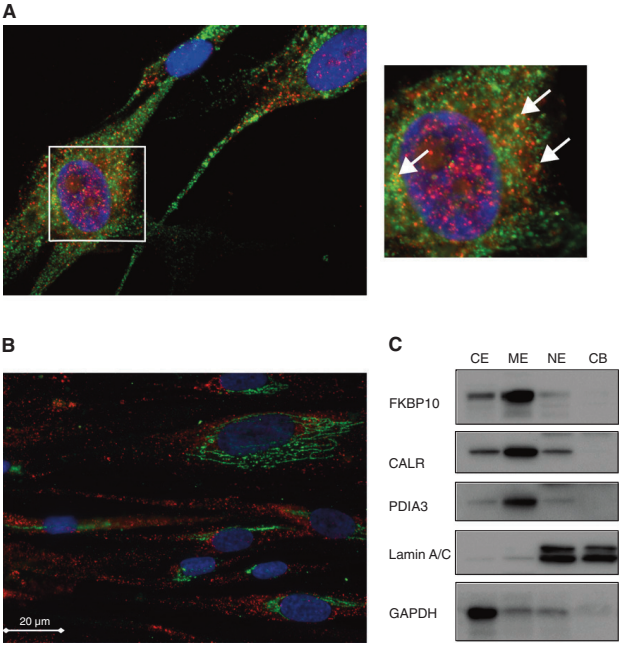

Figure 5. FK506-binding protein 10 (FKBP10) is mainly an endoplasmic reticulum (ER)-resident protein and does not localize to the Golgi apparatus. (*A*) Immunostaining of FKBP10 and the ER-marker protein disulfide isomerase A3 (PDIA3) is shown in *red* and *green*, respectively. 4′,6-diamidino-2-phenylindole (DAPI) staining is shown in *blue*. The *white square* was chosen as the region of interest and enlarged to the *right*. *Arrows* in the region of interest depict examples for colocalization of FKBP10 and PDIA3. While the staining shown to the *left* is an extended-focus picture generated from a z-stack, the enlarged figure to the *right* shows one focal plane from the z-stack only. (*B*) Immunostaining of FKBP10 and the Golgi-marker protein Golgin subfamily A member 1 is shown in *red* and *green*, respectively. DAPI staining is shown in *blue*. The presented staining is an extended-focus picture generated from a z-stack. (*C*) Western blot analysis of subcellular fractionation of primary human lung fibroblasts. FKBP10 is enriched in the membrane extract (ME), similar to the ER-resident proteins calreticulin (CALR) and PDIA3. FKBP10 was additionally found in the cytosolic extract (CE) and the nuclear extract (NE) but not in the chromatin-bound fraction (CB). Lamin A/C and glyceraldehyde phosphate dehydrogenase (GAPDH) were used as marker proteins for NE/CB and CE, respectively.

Discussion

In the present study, we show that FKBP10 is up-regulated in bleomycin-induced lung fibrosis and IPF. FKBP10 is predominantly expressed in interstitial (myo)fibroblasts and $CD68^+$ macrophages. TGF-β_1, but not ER stress, induced *FKBP10* expression in phLF. Loss of FKBP10 in phLF led to attenuation of collagen synthesis and secretion and reduced the expression of α-SMA and PAI1 independent of the TGF-β signaling pathway. Finally, FKBP10 knockdown inhibited collagen secretion with an efficiency similar to that of nintedanib.

FKBP10 was up-regulated in the mouse model of bleomycin-induced lung fibrosis and returned to baseline with resolution of the disease (Figure 1). In agreement, a previous study has indicated up-regulation of FKBP10 mRNA during bleomycin-induced lung injury (26). In this study, however, analysis was restricted to

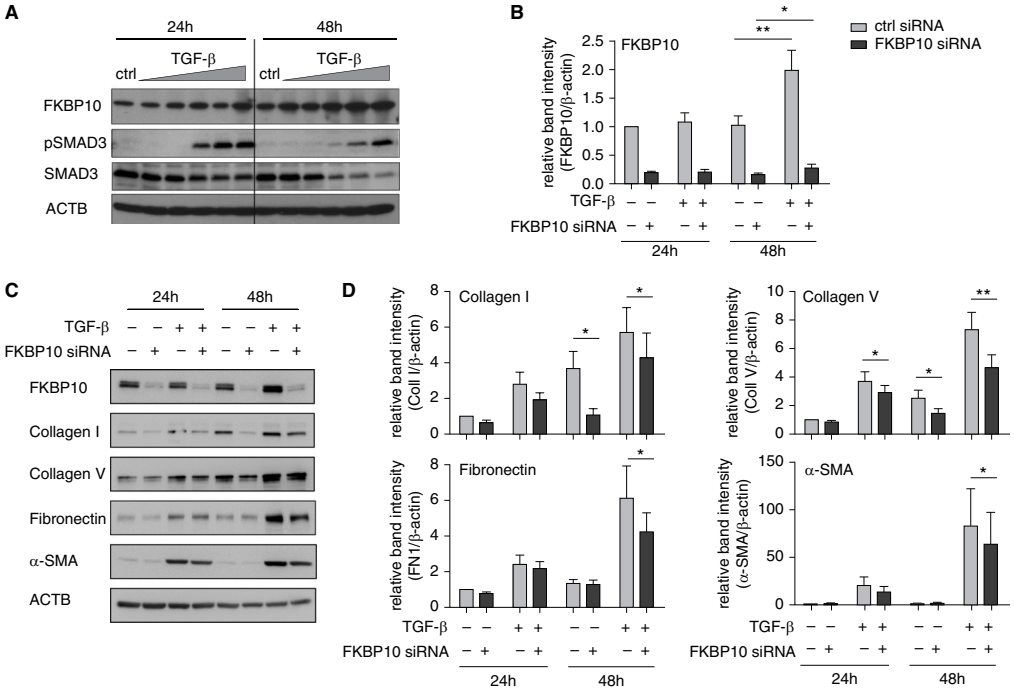

Figure 6. FK506-binding protein 10 (FKBP10) is up-regulated by transforming growth factor (TGF)-β_1 in primary human lung fibroblasts (phLF), and knockdown of FKBP10 attenuates synthesis of collagen I, collagen V, and α-smooth muscle actin (α-SMA). (*A*) Western blot analysis of phLF treated with increasing concentrations of TGF-β_1 (0.1, 0.2, 1.0, 2.0, and 5.0 ng/ml) shows up-regulation of FKBP10 at 48 hours in the presence of 1.0 ng/ml and higher TGF-β_1 concentrations. Efficacy of TGF-β_1 treatment was confirmed by monitoring phosphorylation of mothers against decapentaplegic homolog 3 (SMAD3, depicted as pSMAD3) in comparison with total SMAD3 levels (SMAD3). (*B*) 2.0 ng/ml TGF-β_1 significantly increased FKBP10 in phLF after 48 h, as quantified by densitometric analysis from Western blot analysis (*cf.* Figure 7*C* for representative Western blot, lanes with scrambled [−] small interfering RNA [siRNA] only). The effect of the knockdown was always significant ($P < 0.01$ or $P < 0.001$) but is not specified in the interest of clarity. (*C*) FKBP10 knockdown effects in phLF in combination with 24 and 48 hours of TGF-β_1 treatment (2.0 ng/ml). A representative Western blot analysis for detection of FKBP10, collagen I, collagen V, fibronectin, and α-SMA is shown. (*D*) Densitometric quantification of collagen I, collagen V, fibronectin, and α-SMA protein levels. β-actin (ACTB) was used as loading control. Scrambled siRNA was used as control. Data are based on eight completely independent experiments and are given as mean ± SEM. Statistical analysis for comparison of FKBP10 siRNA vs. scrambled siRNA control was performed by paired two-tailed *t* test. $^*P < 0.05$, $^{**}P < 0.01$. The well-known effect of TGF-β_1 on these proteins was mostly significant but is not specified in the interest of clarity. ctrl = control.

Day 10 after bleomycin administration, and up-regulation was merely assessed at transcript level. We clarify that FKBP10 overexpression occurs on the protein level and correlated with the fibrotic phase and lung function, both aspects of importance for the translation of these results to IPF, a state of presumably irreversible fibrosis. Most importantly, we show for the first time that FKBP10 expression is increased in IPF (Figure 2). This appears to be a universal phenomenon, as we discovered this in two completely independent cohorts, one in the United States and one in Europe, strongly arguing for an important function of FKBP10 in IPF. Immunofluorescent stainings of fibrotic mouse and IPF tissue sections revealed strong FKBP10 expression by interstitial fibroblasts, including myofibroblasts, the major ECM-producing cell type in fibrotic lung disease (Figures 3 and 4), indicating that FKBP10 might have a function in ECM protein synthesis in phLF. Notably, many myofibroblasts, both in the mouse model as well as in the IPF sections, were FKBP10-negative, highlighting the phenotypic diversity of interstitial mesenchymal cell types in fibrosis.

The subcellular localization provided an important clue for FKBP10 function in fibroblasts, as FKBP10 substrates proposed in the literature include not only ECM protein precursors, such as procollagen I or tropoelastin (11, 27), but also cytosolic proteins, such as HSP90 and c-Raf-1 (28).

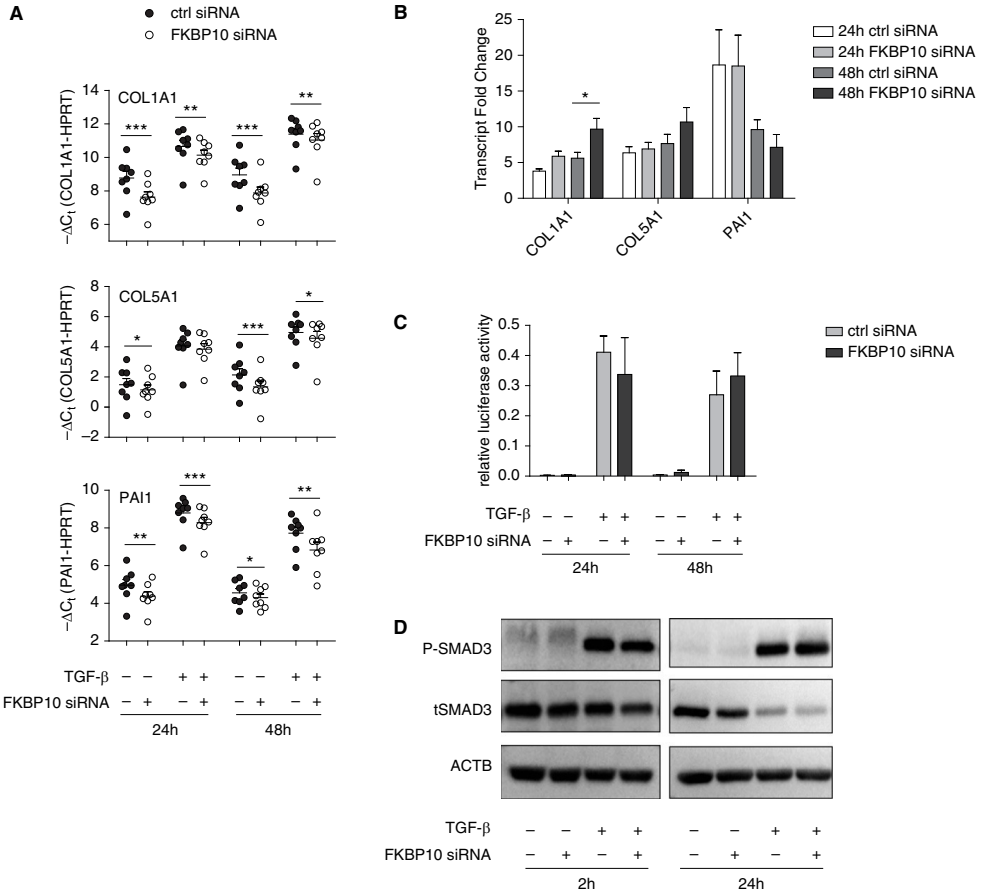

Figure 7. Transforming growth factor (TGF)-β_1 induces FK506-binding protein 10 (FKBP10) expression, and knockdown of FKBP10 in primary human lung fibroblasts (phLF) significantly decreases expression of collagen α-1(I) chain (COL1A1), collagen α-1(V) chain (COL5A1), and plasminogen activator inhibitor 1 (PAI1) on the transcriptional level independent of the canonical TGF-β signaling pathway. (*A*) Quantitative reverse transcriptase–polymerase chain reaction analysis of transcript levels of COL1A1 and COL5A1 (encoding the α1-chain of collagen I and V, respectively) and PAI1 as a representative TGF-β_1–transduced gene after FKBP10 knockdown in combination with 24 and 48 hours of TGF-β_1 treatment (2.0 ng/ml). Data are depicted as mean ± SEM from eight independent experiments, and a paired two-tailed *t* test was used for statistical analysis for comparison of FKBP10 small interfering RNA (siRNA) vs. scrambled siRNA control. The well-known effect of TGF-β_1 on these transcripts was always highly significant ($P < 0.01$ or $P < 0.001$) but is not specified in the interest of clarity. Hypoxanthine-guanine phosphoribosyltransferase (HPRT) was used as endogenous control. (*B*) TGF-β–induced transcript fold changes obtained from the same data do not show attenuation of TGF-β signaling. (*C*) Transfection of phLF with a mothers against decapentaplegic homolog (SMAD) signaling luciferase reporter plasmid during FKBP10 knockdown showed no effect on canonical TGF-β signaling (n = 3). (*D*) Western blot analysis (n = 3) demonstrated that FKBP10 knockdown did not affect levels of total and phosphorylated SMAD3. β-actin (ACTB) was used as loading control. For quantification of these data, *see* Figure E3 in the online supplement. $^*P < 0.05$, $^{**}P < 0.01$, $^{***}P < 0.001$. ctrl = control.

Here, we demonstrate that FKBP10 localized mainly to the ER in phLF (Figure 5). No colocalization was observed with the Golgi-specific protein GOLGA1 (29), indicating that FKBP10 is not associated with transport processes across the trans-Golgi network to the extracellular space. This suggests that FKBP10 mainly functions as an ER-resident chaperone and/or foldase in phLF, which agrees with previous studies in chondroblasts and embryonic fibroblasts (19, 27).

As there is evidence that ER stress contributes to IPF pathology (30, 31), we assessed whether FKBP10 is induced by ER

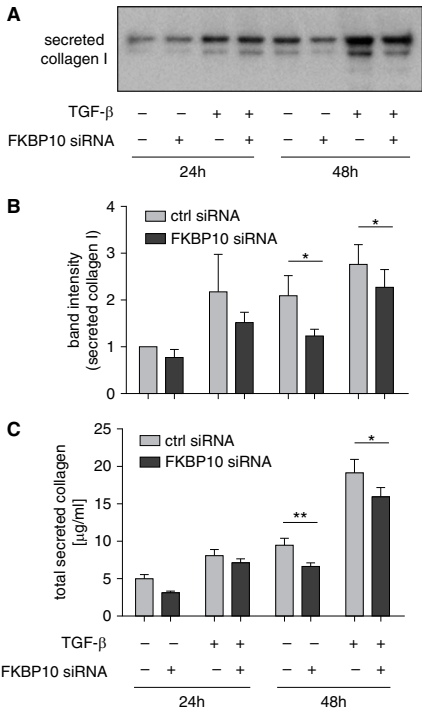

Figure 8. Knockdown of FK506-binding protein 10 (FKBP10) attenuates collagen secretion. (*A*) Western blot analysis of secreted collagen I. Collagen I was precipitated from cell culture supernatant after FKBP10 knockdown in combination with 24 and 48 hours of transforming growth factor (TGF)-β_1 treatment (2.0 ng/ml) and analyzed by Western blot analysis. (*B*) Densitometric analysis of secreted collagen I as detected in *A*. Data shown are based on seven independent experiments and given as mean ± SEM. (*C*) Results of a Sircol assay for assessment of total secreted collagen in cell culture supernatant after FKBP10 knockdown in combination with 24 and 48 hours of TGF-β_1 treatment. Data shown are based on eight independent experiments and given as mean ± SEM. Statistical analysis was performed using paired two-tailed *t* test for comparison of FKBP10 siRNA vs. scrambled siRNA control. ctrl = control; siRNA = small interfering RNA. $^*P < 0.05$, $^{**}P < 0.01$.

stress as a possible explanation for its increased expression in IPF. Interestingly, we observed a drastic decrease in FKBP10 levels (band at 70 kD; cf. Figure E1A) in response to tunicamycin, an inhibitor of N-protein glycosylation (32). This decrease was accompanied by the appearance of a lower band at the height of the predicted size of the unmodified protein (65 kD; cf. Figure E1A), in line with the previous identification of FKBP10 as an N-glycosylated protein (33). This is in agreement with a previous study showing that FKBP10 is degraded by the proteasome in response to ER stress (34). As the observed decrease of FKBP10 might reflect deglycosylation of the protein rather than an overall decrease in expression levels, a mechanistically independent ER stress inducer, thapsigargin, was used to confirm FKBP10 down-regulation in ER stress (Figure E1B). Hence, it is unlikely that the unfolded protein response contributes to FKBP10 up-regulation in IPF.

In contrast, TGF-β_1 significantly induced FKBP10 expression in phLF on the mRNA and protein level (*cf.* Figure E2, Figure 6B). This effect has previously only been observed in fetal lung fibroblasts (26) and implies that adult IPF phLF have retained the capacity to up-regulate FKBP10 under fibrotic conditions, supporting the use of this cell culture system for the functional analysis of FKBP10 *in vitro*. In agreement with a collagen chaperone function, inhibition of FKBP10 by an siRNA-mediated approach in this model resulted in a consistent decrease of collagen I and collagen V protein levels (*cf.* Figure 6C and 6D) as well as in decreased secreted collagen (Figure 8). In line with our results, deficiency of FKBP10 in osteogenesis imperfecta has been shown to attenuate collagen secretion and, moreover, decrease the extent of lysyl hydroxylation and extracellular collagen cross-linking and increase protease sensitivity of extracellular collagen I in dermal fibroblasts from patients with osteogenesis imperfecta (15, 17, 18).

Surprisingly, loss of FKBP10 affected collagen levels not only on protein but also on transcript levels (Figure 7A). This is unexpected, as FKBP10—as a chaperone and peptidyl-prolyl isomerase—is mainly ascribed a post-transcriptional role in procollagen I processing (11, 14, 15, 17, 18). Interestingly, loss of FKBP10 also attenuated the expression of the TGF-β–responsive genes PAI1 and α-SMA (Figures 6D and 7A). However, this was not due to inhibition of the canonical TGF-β signaling pathway (Figure 7B–7D). Hence, it appears that FKBP10 exerts a previously unappreciated function in signal transduction processes for the transcriptional regulation of profibrotic genes. Nevertheless, the data also show an increase in TGF-β–induced collagen expression and secretion, even in the context of FKBP10 knockdown, indicating that alternative, FKBP10-independent, profibrotic mechanisms contribute to overall ECM deposition.

Importantly, the effects of FKBP10 knockdown on TGF-β–induced collagen secretion in phLF were comparable to those of submicromolar concentrations of nintedanib (Figures 9A and 9B). In contrast, we did not observe any effect of pirfenidone in this context. Previous studies in human lung fibroblasts and A549 cells have shown moderate reduction of collagen I expression only at concentrations higher than those used in this study (1.0 mM vs. 1.6 and 2.7 mM pirfenidone, respectively [35, 36]). The effect of pirfenidone on TGF-β–induced collagen secretion *in vitro* has, to our knowledge, only been studied in trabecular meshwork

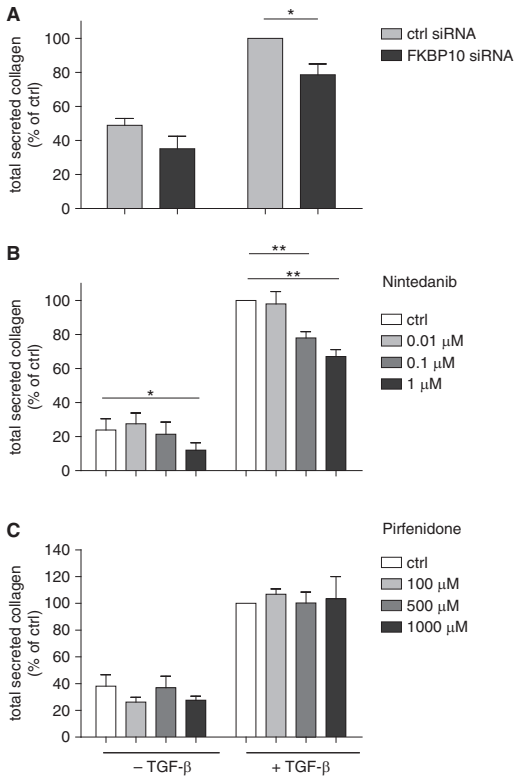

Figure 9. In idiopathic pulmonary fibrosis fibroblasts, FK506-binding protein 10 (FKBP10) knockdown inhibits collagen secretion with similar efficiency as nintedanib, whereas pirfenidone shows no effect. (*A–C*) Normalized levels of secreted collagen in response to (*A*) FKBP10 knockdown, (*B*) nintedanib, and (*C*) pirfenidone treatment at varying concentrations. In contrast to pirfenidone, nintedanib shows a dose-dependent effect. In comparison, FKBP10 knockdown performs with similar efficiency as submicromolar concentrations of nintedanib. For FKBP10 knockdown, scrambled small interfering RNA (siRNA) was used as control. Data shown are based on four independent experiments and given as mean ± SEM. Statistical analysis was performed using paired two-tailed *t* test. $^{*}P < 0.05$, $^{**}P < 0.01$. ctrl = control; TGF-β = transforming growth factor-β.

cells, where collagen secretion was significantly reduced at a concentration of 2.5 mM (37). These concentrations are hardly physiologically relevant, indicating that the well-known antifibrotic effects of pirfenidone *in vivo* (38) differ substantially in underlying mechanisms or involve metabolic activation.

The ability to bind the immunosuppressive drug FK506 (tacrolimus) via at least one peptidyl-prolyl isomerase domain is characteristic for all FKBPs, including FKBP10 (11, 39). Interestingly, immunosuppressive peptidyl-prolyl isomerase inhibitors like FK506 have been ascribed potent antifibrotic effects in lung fibrosis (40–43). FK506 suppresses collagen synthesis and expression of the TGF-β_1 receptor in dermal and lung fibroblasts, but the underlying mechanisms are largely unclear (41, 44, 45). Our findings put forward the possibility that inhibition of FKBP10 might contribute to the antifibrotic effects of FK506.

In conclusion, we show that FKBP10 is overexpressed in bleomycin-induced lung fibrosis and IPF. Up-regulation of FKBP10 expression is at least partly mediated by TGF-β_1. Loss of FKBP10 in phLF derived from patients with IPF or control patients attenuated ECM protein expression and secretion and suppressed fibroblast-to-myofibroblast differentiation/activation. Although FKBP10 has been suggested to be important for normal lung development, with little expression in normal adult tissues, its expression appears to be reactivated during lung fibrosis (26, 27). Considering the impact of FKBP10 on collagen cross-linking (15, 17, 18) and the effects described herein on collagen secretion, FKBP10 might provide a very specific and effective drug target for treatment of IPF. ■

Author disclosures are available with the text of this article at www.atsjournals.org.

Acknowledgment: The authors thank Daniela Dietel for excellent technical assistance, Mona Dotzler for initial contributions to this project, and Melanie Königshoff and Kathrin Mutze for valuable help and discussion.

References

1. Kim DS, Collard HR, King TE Jr. Classification and natural history of the idiopathic interstitial pneumonias. *Proc Am Thorac Soc* 2006;3:285–292.
2. Selman M, King TE, Pardo A; American Thoracic Society; European Respiratory Society; American College of Chest Physicians. Idiopathic pulmonary fibrosis: prevailing and evolving hypotheses about its pathogenesis and implications for therapy. *Ann Intern Med* 2001;134:136–151.
3. Renzoni E, Srihari V, Sestini P. Pathogenesis of idiopathic pulmonary fibrosis: review of recent findings. *F1000Prime Rep* 2014;6:69.
4. Wolters PJ, Collard HR, Jones KD. Pathogenesis of idiopathic pulmonary fibrosis. *Annu Rev Pathol* 2014;9:157–179.
5. Blackwell TS, Tager AM, Borok Z, Moore BB, Schwartz DA, Anstrom KJ, Bar-Joseph Z, Bitterman P, Blackburn MR, Bradford W, *et al*. Future directions in idiopathic pulmonary fibrosis research: an NHLBI workshop report. *Am J Respir Crit Care Med* 2014;189:214–222.

6. Selman M, Pardo A. Revealing the pathogenic and aging-related mechanisms of the enigmatic idiopathic pulmonary fibrosis. an integral model. *Am J Respir Crit Care Med* 2014;189: 1161–1172.
7. Parker MW, Rossi D, Peterson M, Smith K, Sikström K, White ES, Connett JE, Henke CA, Larsson O, Bitterman PB. Fibrotic extracellular matrix activates a profibrotic positive feedback loop. *J Clin Invest* 2014;124:1622–1635.
8. Ahluwalia N, Shea BS, Tager AM. New therapeutic targets in idiopathic pulmonary fibrosis: aiming to rein in runaway wound-healing responses. *Am J Respir Crit Care Med* 2014; 190:867–878.
9. King TE Jr, Bradford WZ, Castro-Bernardini S, Fagan EA, Glaspole I, Glassberg MK, Gorina E, Hopkins PM, Kardatzke D, Lancaster L, *et al*.; ASCEND Study Group. A phase 3 trial of pirfenidone in patients with idiopathic pulmonary fibrosis. *N Engl J Med* 2014;370: 2083–2092.
10. Richeldi L, du Bois RM, Raghu G, Azuma A, Brown KK, Costabel U, Cottin V, Flaherty KR, Hansell DM, Inoue Y, *et al*.; INPULSIS Trial Investigators. Efficacy and safety of nintedanib in idiopathic pulmonary fibrosis. *N Engl J Med* 2014;370: 2071–2082.
11. Ishikawa Y, Vranka J, Wirz J, Nagata K, Bächinger HP. The rough endoplasmic reticulum-resident FK506-binding protein FKBP65 is a molecular chaperone that interacts with collagens. *J Biol Chem* 2008;283:31584–31590.
12. Lu KP, Finn G, Lee TH, Nicholson LK. Prolyl cis-trans isomerization as a molecular timer. *Nat Chem Biol* 2007;3:619–629.
13. Kang CB, Hong Y, Dhe-Paganon S, Yoon HS. FKBP family proteins: immunophilins with versatile biological functions. *Neurosignals* 2008; 16:318–325.
14. Ishikawa Y, Bächinger HP. A molecular ensemble in the rER for procollagen maturation. *Biochim Biophys Acta* 2013;1833: 2479–2491.
15. Alanay Y, Avaygan H, Camacho N, Utine GE, Boduroglu K, Aktas D, Alikasifoglu M, Tuncbilek E, Orhan D, Bakar FT, *et al*. Mutations in the gene encoding the RER protein FKBP65 cause autosomal-recessive osteogenesis imperfecta. *Am J Hum Genet* 2010;86:551–559.
16. Kelley BP, Malfait F, Bonafe L, Baldridge D, Homan E, Symoens S, Willaert A, Elcioglu N, Van Maldergem L, Verellen-Dumoulin C, *et al*. Mutations in FKBP10 cause recessive osteogenesis imperfecta and Bruck syndrome. *J Bone Miner Res* 2011;26:666–672.
17. Barnes AM, Cabral WA, Weis M, Makareeva E, Mertz EL, Leikin S, Eyre D, Trujillo C, Marini JC. Absence of FKBP10 in recessive type XI osteogenesis imperfecta leads to diminished collagen cross-linking and reduced collagen deposition in extracellular matrix. *Hum Mutat* 2012;33:1589–1598.
18. Schwarze U, Cundy T, Pyott SM, Christiansen HE, Hegde MR, Bank RA, Pals G, Ankala A, Conneely K, Seaver L, *et al*. Mutations in FKBP10, which result in Bruck syndrome and recessive forms of osteogenesis imperfecta, inhibit the hydroxylation of telopeptide lysines in bone collagen. *Hum Mol Genet* 2013;22: 1–17.
19. Lietman CD, Rajagopal A, Homan EP, Munivez E, Jiang MM, Bertin TK, Chen Y, Hicks J, Weis M, Eyre D, *et al*. Connective tissue alterations in Fkbp10-/- mice. *Hum Mol Genet* 2014;23:4822–4831.
20. John G, Kohse K, Orasche J, Reda A, Schnelle-Kreis J, Zimmermann R, Schmid O, Eickelberg O, Yildirim AO. The composition of cigarette smoke determines inflammatory cell recruitment to the lung in COPD mouse models. *Clin Sci (Lond)* 2014;126:207–221.
21. Bauer Y, Tedrow J, de Bernard S, Birker-Robaczewska M, Gibson KF, Juan Guardela B, Hess P, Klenk A, Lindell KO, Poirey S, *et al*. A novel genomic signature with translational significance for human idiopathic pulmonary fibrosis. *Am J Respir Cell Mol Biol* 2015;52: 217–231.
22. Yang IV, Pedersen BS, Rabinovich E, Hennessy CE, Davidson EJ, Murphy E, Guardela BJ, Tedrow JR, Zhang Y, Singh MK, *et al*. Relationship of DNA methylation and gene expression in idiopathic pulmonary fibrosis. *Am J Respir Crit Care Med* 2014;190: 1263–1272.
23. Herazo-Maya JD, Noth I, Duncan SR, Kim S, Ma SF, Tseng GC, Feingold E, Juan-Guardela BM, Richards TJ, Lussier Y, *et al*. Peripheral blood mononuclear cell gene expression profiles predict poor outcome in idiopathic pulmonary fibrosis. *Sci Transl Med* 2013; 5:205ra136.
24. Dennler S, Itoh S, Vivien D, ten Dijke P, Huet S, Gauthier JM. Direct binding of Smad3 and Smad4 to critical TGF beta-inducible elements in the promoter of human plasminogen activator inhibitor-type 1 gene. *EMBO J* 1998;17:3091–3100.
25. Mise N, Savai R, Yu H, Schwarz J, Kaminski N, Eickelberg O. Zyxin is a transforming growth factor-β (TGF-β)/Smad3 target gene that regulates lung cancer cell motility via integrin α5β1. *J Biol Chem* 2012;287:31393–31405.
26. Patterson CE, Abrams WR, Wolter NE, Rosenbloom J, Davis EC. Developmental regulation and coordinate reexpression of FKBP65 with extracellular matrix proteins after lung injury suggest a specialized function for this endoplasmic reticulum immunophilin. *Cell Stress Chaperones* 2005;10:285–295.
27. Patterson CE, Schaub T, Coleman EJ, Davis EC. Developmental regulation of FKBP65: an ER-localized extracellular matrix binding-protein. *Mol Biol Cell* 2000;11:3925–3935.
28. Coss MC, Stephens RM, Morrison DK, Winterstein D, Smith LM, Simek SL. The immunophilin FKBP65 forms an association with the serine/threonine kinase c-Raf-1. *Cell Growth Differ* 1998;9:41–48.
29. Munro S. The golgin coiled-coil proteins of the Golgi apparatus. *Cold Spring Harb Perspect Biol* 2011;3:6.
30. Korfei M, Ruppert C, Mahavadi P, Henneke I, Markart P, Koch M, Lang G, Fink L, Bohle RM, Seeger W, *et al*. Epithelial endoplasmic reticulum stress and apoptosis in sporadic idiopathic pulmonary fibrosis. *Am J Respir Crit Care Med* 2008;178:838–846.
31. Tanjore H, Blackwell TS, Lawson WE. Emerging evidence for endoplasmic reticulum stress in the pathogenesis of idiopathic pulmonary fibrosis. *Am J Physiol Lung Cell Mol Physiol* 2012;302: L721–L729.
32. Elbein AD. Inhibitors of the biosynthesis and processing of N-linked oligosaccharides. *CRC Crit Rev Biochem* 1984;16:21–49.
33. Zhang H, Li XJ, Martin DB, Aebersold R. Identification and quantification of N-linked glycoproteins using hydrazide chemistry, stable isotope labeling and mass spectrometry. *Nat Biotechnol* 2003; 21:660–666.
34. Murphy LA, Ramirez EA, Trinh VT, Herman AM, Anderson VC, Brewster JL. Endoplasmic reticulum stress or mutation of an EF-hand Ca(2+)-binding domain directs the FKBP65 rotamase to an ERAD-based proteolysis. *Cell Stress Chaperones* 2011;16: 607–619.
35. Conte E, Gili E, Fagone E, Fruciano M, Iemmolo M, Vancheri C. Effect of pirfenidone on proliferation, TGF-β-induced myofibroblast differentiation and fibrogenic activity of primary human lung fibroblasts. *Eur J Pharm Sci* 2014;58:13–19.
36. Hisatomi K, Mukae H, Sakamoto N, Ishimatsu Y, Kakugawa T, Hara S, Fujita H, Nakamichi S, Oku H, Urata Y, *et al*. Pirfenidone inhibits TGF-β1-induced over-expression of collagen type I and heat shock protein 47 in A549 cells. *BMC Pulm Med* 2012;12:24.
37. Pattabiraman PP, Maddala R, Rao PV. Regulation of plasticity and fibrogenic activity of trabecular meshwork cells by Rho GTPase signaling. *J Cell Physiol* 2014;229:927–942.
38. Schaefer CJ, Ruhrmund DW, Pan L, Seiwert SD, Kossen K. Antifibrotic activities of pirfenidone in animal models. *Eur Respir Rev* 2011;20: 85–97.
39. Coss MC, Winterstein D, Sowder RC II, Simek SL. Molecular cloning, DNA sequence analysis, and biochemical characterization of a novel 65-kDa FK506-binding protein (FKBP65). *J Biol Chem* 1995;270: 29336–29341.
40. Horita N, Akahane M, Okada Y, Kobayashi Y, Arai T, Amano I, Takezawa T, To M, To Y. Tacrolimus and steroid treatment for acute exacerbation of idiopathic pulmonary fibrosis. *Intern Med* 2011;50: 189–195.
41. Nagano J, Iyonaga K, Kawamura K, Yamashita A, Ichiyasu H, Okamoto T, Suga M, Sasaki Y, Kohrogi H. Use of tacrolimus, a potent antifibrotic agent, in bleomycin-induced lung fibrosis. *Eur Respir J* 2006;27:460–469.

42. Correale M, Totaro A, Lacedonia D, Montrone D, Di Biase M, Barbaro Foschino MP, Brunetti ND. Novelty in treatment of pulmonary fibrosis: pulmonary hypertension drugs and others. *Cardiovasc Hematol Agents Med Chem* 2013;11: 169–178.
43. Inase N, Sawada M, Ohtani Y, Miyake S, Isogai S, Sakashita H, Miyazaki Y, Yoshizawa Y. Cyclosporin A followed by the treatment of acute exacerbation of idiopathic pulmonary fibrosis with corticosteroid. *Intern Med* 2003;42:565–570.
44. Lan CC, Fang AH, Wu PH, Wu CS. Tacrolimus abrogates TGF-beta1-induced type I collagen production in normal human fibroblasts through suppressing p38MAPK signalling pathway: implications on treatment of chronic atopic dermatitis lesions. *J Eur Acad Dermatol Venereol* 2014;28:204–215.
45. Wu CS, Wu PH, Fang AH, Lan CC. FK506 inhibits the enhancing effects of transforming growth factor (TGF)-β1 on collagen expression and TGF-β/Smad signalling in keloid fibroblasts: implication for new therapeutic approach. *Br J Dermatol* 2012;167:532–541.

ONLINE DATA SUPPLEMENT

FK506-BINDING PROTEIN 10 IS A POTENTIAL NOVEL DRUG TARGET FOR IDIOPATHIC PULMONARY FIBROSIS

Claudia A. Staab-Weijnitz, Isis E. Fernandez, Larissa Knüppel, Julia Maul, Katharina Heinzelmann, Brenda M. Juan-Guardela, Elisabeth Hennen, Gerhard Preissler, Hauke Winter, Claus Neurohr, Rudolf Hatz, Michael Lindner, Jürgen Behr, Naftali Kaminski, and Oliver Eickelberg*

*To whom correspondence should be addressed: Oliver Eickelberg, Comprehensive Pneumology Center, Ludwig-Maximilians-Universität and Helmholtz Zentrum München, Max-Lebsche-Platz 31, 81377 München, Germany, Tel.: 0049(89)31874666; Fax: 0049(89)31874661; Email: oliver.eickelberg@helmholtz-muenchen.de

MATERIALS AND METHODS

Animals

Pathogen-free female C57BL/6 mice (10–12 weeks old) were obtained from Charles River and housed in rooms maintained at constant temperature and humidity with a 12 h light cycle. Animals were allowed food and water *ad libitum*.

Isolation and culture of primary human lung fibroblasts (phLF)

Isolation of phLF from lung tissue was performed as follows: Human lung specimens were dissected into pieces of 1–2 cm^2 in size and digested by 1 mg/ml of Collagenase I (Biochrom, Cambridge, UK) at 37°C for 2 hours. Subsequently, samples were filtered through nylon filters with a pore size of 70 µm (BD Falcon, Franklin Lakes, NJ, USA). Filtrates, containing the cells, were centrifuged at 400 *g*, 4°C for 5 minutes. Pellets were resuspended in DMEM/F-12 medium (Life Technologies, Carlsbad, CA, USA) supplemented with 20% fetal bovine serum (Pan Biotech, Aidenbach, Germany) and Penicillin/Streptomycin (Life Technologies) and plated on 10 cm cell-culture dishes. Medium was changed after 2 days and cells were split after reaching a confluence of 80–90%. For the present study, phLF were used in passages 4-9. Fibroblasts were cultured in DMEM/F12 (Life Technologies) supplemented with 20% FBS (Pan Biotech) and Penicillin/Streptomycin. For assessment of collagen, 0.1 mM 2-phospho-L-ascorbic acid (Sigma-Aldrich, St. Louis, MO, USA) was included in the medium. Prior to TGF-β1 or ER stress inducer treatment, cells were starved with 0.5% FBS for 24h.

Treatment with TGF-β1, tunicamycin, thapsigargin, nintedanib, and pirfenidone

Experiments with ER stress inducers were performed in phLF derived from normal regions from lung tumor resections (n=2). Experiments with IPF therapeutics were performed in fibroblasts isolated from IPF patients (n=4). Cells were seeded at a density of 20.000 - 25.000

cells/cm², starved for 24 h in DMEM/F12 with 0.5% FBS and 0.1 mM 2-Phospho-L-ascorbic acid, followed by treatment with the indicated concentrations of TGF-β1 (R&D Systems, Minneapolis, MM, USA), tunicamycin (0.5 µg/ml, Sigma-Aldrich), thapsigargin (40 ng/ml, Santa Cruz Biotechnology, Dallas, TX, USA), nintedanib and pirfenidone (both Selleck, Houston, TX, USA) in starvation medium for the indicated time points. Tunicamycin, thapsigargin, nintedanib, and pirfenidone were dissolved in DMSO, and the final DMSO concentration in the medium was always 0.05% for ER stress inducers and 1% for IPF therapeutics.

Transfection of phLF

For reverse transfection with siRNA, cells were seeded at a density of 20.000 - 25.000 cells/cm² in 6-well plates and transfected either with 10 nM human FKBP10 siRNA (s34171, Life Technologies) or negative control siRNA No. 1 (Life Technologies) in the presence of Lipofectamine RNAiMAX (Life Technologies) according to the manufacturer's instructions. FKBP10 knockdown had no significant effect on cell viability (results not shown). 24 h after transfection, cells were starved for another 24 h in DMEM/F-12 including 0.5% FBS and 0.1 mM 2-Phospho-L-ascorbic acid, followed by treatment with 2 ng/ml TGF-β1 in starvation medium. 24 and 48 h after beginning of the TGF-β1 treatment, cells and cell culture supernatants were harvested for RNA and protein analysis. In total, eight completely independent knockdowns were performed in eight human primary fibroblast lines.

For transfection with the SMAD signaling luciferase reporter plasmid, reverse transfection with siRNA was performed as described above in 48-well-plates. 24h after siRNA transfection, three different primary fibroblast lines were forward transfected with 250 ng/well pGL3-CAGA(9)-luc (1) or the pGL3 control vector (Promega, Madison, WI, USA) in the presence of Lipofectamine 2000 (Life Technologies). After incubation for 6h,

cells were starved for 18 h, followed by treatment with 2 ng/ml TGF-β1. Luminescence was recorded in a TriStar LB 941 Multimode Reader (Berthold Technologies, Bad Wildbad, Germany) and results were normalized to pGL3 control luciferase activity.

RNA Isolation and Real-Time Quantitative Reverse-Transcriptase PCR (qRT-PCR) Analysis

Liquid nitrogen-frozen tissue was homogenized using a microdismembrator (Sartorius, Göttingen, Germany). RNA extraction from human and mouse tissue was performed using the Roti Quick Kit (Carl Roth, Karlsruhe, Germany) followed by RNA purification with the peqGold RNA isolation kit (Peqlab, Erlangen, Germany), according to manufacturers' instructions. For RNA extraction from cultured cells, the peqGold RNA isolation kit or the NucleoSpin RNA II (Macherey-Nagel, Düren, Germany) was used. RNA was reverse-transcribed in a 40-µl reaction using M-MLV reverse transcriptase and random hexamers, according to the manufacturer's protocol (Life Technologies). Quantitative real-time PCR (qRT-PCR) was performed using SYBR Green PCR master mix (Roche Applied Science, Mannheim, Germany) and primer mixtures as given in Table E1.

Protein Isolation and Western Blot Analysis

Liquid nitrogen-frozen tissue was homogenized using a microdismembrator (Sartorius, Göttingen, Germany). Protein from pulverized human and mouse tissue was taken up in Radio-Immunoprecipitation Assay (RIPA) buffer (50 mM Tris HCl pH 7.4, 150 mM NaCl, 1% Triton X100, 0.5% sodium deoxycholate, 1 mM EDTA, 0.1% SDS) containing a protease inhibitor and a phosphatase inhibitor cocktail (both Roche), incubated 30 min, followed by short sonification and centrifugation for 15 min at 13,000 rpm and 4°C to clarify the lysates. For protein extraction from cultured cells, cells were scraped into RIPA, incubated, and centrifuged as above, without sonification. Protein concentration of the supernatant was

determined using the Pierce BCA Protein Assay (Thermo Fisher Scientific; Waltham, USA). Samples were denatured in Laemmli buffer (65 mM Tris-HCl pH 6.8, 10% glycerol, 2% SDS, 0.01% bromophenolblue, 100 mM DTT) and proteins resolved by SDS-PAGE. Proteins were then transferred to polyvinylidene diflouride (PVDF) membranes. Nonspecific binding to membrane was blocked with 5% milk in TBS-T (0.1% Tween 20, TBS). Membranes were shortly rinsed and washed three times for 5 min in TBS-T and incubated with primary antibody (*cf*. Table E2 for details on the specific antibodies) overnight at 4°C. After washing with TBS-T, membranes were incubated with secondary antibody for 1 h at room temperature. Blots were rinsed with TBS-T and visualized with the enhanced chemiluminescence (ECL) system (Thermo Fisher Scientific, Waltham, MA, USA) and analyzed by exposure to film or, for quantification, with the ChemiDocXRS+ imaging system (Bio-Rad, Munich, Germany). Band quantification was performed in Image Lab (version 3.0, Bio-Rad, Hercules, CA).

Immunofluorescent stainings of tissue sections

For deparaffinization, the paraffin-embedded sections were placed at 60°C for at least 30 min, incubated twice in xylene (5 min each), and then transferred into 100% EtOH (2 min), 100% EtOH (2 min), 90% EtOH (1 min), 80% EtOH (1 min), and 70% EtOH (1 min) at room temperature. Sections were rinsed in deionized water and stored in 0.5 M Tris, 1.5 M NaCl, pH 6.8 (termed Tris buffer hereafter). For antigen retrieval, slides were immersed in citrate buffer pH 6,0 and heated in a Decloaking Chamber 30 seconds at 125°C, followed by 10 seconds at 90°C. Then, the slides were allowed to slowly cool down to room temperature. Slides were washed three times in Tris buffer and primary antibody dilutions were prepared in antibody diluent (Zytomed Systems, Berlin, Germany, *cf*. Table E2 for details on the specific antibodies), added to each tissue section in a wet chamber and incubated overnight. 1:250 dilution of each secondary antibody was applied (Alexa Fluor 488 goat anti-mouse IgG,

Alexa Fluor 568 goat anti-rabbit IgG, Alexa Fluor 488 donkey anti-sheep IgG, all Life Technologies). Slides were rinsed three times with Tris buffer and counterstained with DAPI (Sigma-Aldrich, 1:2500) for 1 min in darkness. Then slides were rinsed three times with Tris buffer, covered with Fluorescence Mounting Medium (Dako, Hamburg, Germany) and examined under an Axio Imager Microscope (Carl Zeiss, Jena, Germany).

CD68 stainings were performed with a primary antibody coupled to a red fluorophore, therefore, FKBP10 was originally detected with Alexa Fluor 488 goat anti-rabbit, but for consistency of data presentation, colors were inversed using the ZEN software (Carl Zeiss).

Masson's Trichrome Stainings

Masson's Trichrome stainings were performed using a Masson's Trichrome Staining kit (Sigma-Aldrich, Steinheim, Germany) according to the manufacturer's protocol. Briefly, slides were deparaffinized as described above, rinsed in deionized water, and put in preheated Bouin's solution at 56°C for 15 minutes. After cooling down in deionized water, slides were stained in Weigert's iron hematoxylin solution and Biebrich scarlet-acid Fuchsin. Slides were then placed in phosphotungstic/hosphomolybdic Acid, followed by Aniline blue solution, and Acetic Acid 1%, dehydrated through ethyl alcohol, and mounted.

TABLES

Table E1. Primer table for qRT-PCR. Primers were synthesized by MWG Eurofins (Ebersberg, Germany).

Target	**Species**	**Forward primer** (5′-3′)	**Reverse primer** (5′-3′)
ATF4	human	AACAACAGCAAGGAGGAT	AGGTCATCTATACCCAACAG
CHOP	human	CCTATGTTTCACCTCCTG	GACCTCTGCTGGTTCTG
COL1A1	human	TACAGAACGGCCTCAGGTACCA	ACAGATCACGTGATCGCACAAC
COL5A1	human	CTTCAAGGTTTACTGCAAC	CCCTTCGGACTTCTTG
FKBP10	human	CGACACCAGCTACAGTAAG	TAATCTTCCTTCTCTCTCCA
	mouse	GGACGTGTGGAACAAAGCAG	AGCGCACAAAGTCACTGTTC
FN1	human	CCGACCAGAAGTTTGGGTTCT	CAATGCGGTACATGACCCCT
GAPDH	human	TGACCTCAACTACATGGTTTACATG	TTGATTTTGGAGGGATCTCG
	mouse	TGTGTCCGTCGTGGATCTGA	CCTGCTTCACCACCTTCTTGA
HPRT	human	AAGGACCCCACGAAGTGTTG	GGCTTTGTATTTTGCTTTTCCA
	mouse	ATAGTGATAGATCCATTCCTATGACTG	TTCAACAATCAAGACATTCTTTCCA
PAI-1	human	GACATCCTGGAACTGCCCTA	GGTCATGTTGCCTTTCCAGT
	mouse	AGGTCAGGATCGAGGTAAACGAG	GGATCGGTCTATAACCATCTCCGT

Table E2. Primary antibodies used in the different applications. Secondary HRP-linked antibodies were from GE Healthcare Life Sciences (Freiburg, Germany). WB, Western Blot; IF, immunofluorescent staining

Target	Antibody	Provider	Application
α-SMA (ACTA2)	mouse monoclonal anti-ACTA2 antibody	Sigma Aldrich, Louis, MO, USA	WB, IF
β-actin (ACTB)	HRP-conjugated anti-ACTB antibody	Sigma Aldrich, Louis, MO, USA	WB
BiP	rabbit monoclonal anti-BiP antibody	Cell Signaling, Danvers, MA, USA	WB
Calreticulin	rabbit polyclonal anti-calreticulin antibody	Cell Signaling, Danvers, MA, USA	WB
CD68	APC anti-human CD68 Antibody	BioLegend, San Diego, CA, USA	IF
Collagen type I	rabbit polyclonal anti-Collagen I antibody	Rockland, Gilbertsville, PA, USA	WB, IF
Collagen type V	rabbit polyclonal anti-Collagen V antibody	Santa Cruz, Dallas, TX, USA	WB
Desmin (B7)	mouse monoclonal anti-desmin antibody	Santa Cruz, Dallas, TX, USA	IF
Fibronectin	rabbit polyclonal anti-Fibronectin antibody	Santa Cruz, Dallas, TX, USA	WB
FKBP10	rabbit polyclonal anti-FKBP10 antibody	ATLAS, Stockholm, Sweden	WB[1], IF
FKBP10	rabbit polyclonal anti-FKBP10 antibody	Acris Antibodies, San Diego, CA, USA	WB[2]
GAPDH	HRP-conjugated anti-GAPDH antibody	Cell Signaling, Danvers, MA, USA	WB
GOLGA1	mouse monoclonal anti-GOLGA1 antibody	Life Technologies, Carlsbad, CA, USA	IF
Lamin A/C	rabbit polyclonal anti-Lamin A/C antibody	Cell Signaling, Danvers, MA, USA	WB
PDIA3	mouse monoclonal anti-Erp57 antibody	Abcam, Cambridge, UK	WB, IF
P-SMAD3	rabbit monoclonal anti-Smad 3 (phospho Ser423/Ser425) antibody	Abcam, Cambridge, UK	WB
SMAD3	rabbit polyclonal anti-total SMAD3 antibody	Abcam, Cambridge, UK	WB
mouse T1α (podoplanin)	goat polyclonal anti-mouse podoplanin antibody	R&D, Minneapolis, MN, USA	IF
human T1α (podoplanin)	Sheep polyclonal anti-human podoplanin antibody	R&D, Minneapolis, MN, USA	IF
TTF1	mouse monoclonal anti-TTF antibody	Santa Cruz	IF

[1] used for WB analysis of human samples

[2] used only for WB analysis of mouse samples

SUPPLEMENTAL FIGURE LEGENDS

Figure E1: FKBP10 is downregulated by the ER stress inducers tunicamycin and thapsigargin. (A) Representative Western Blot of phLF treated with 0.5 µg/ml tunicamycin in presence and absence of TGF-β for 24 and 48 h. (B) Representative Western Blot of phLF treated with 40 ng/ml thapsigargin in presence and absence of TGF-β for 24 and 48 h. BiP (also termed GRP78) is used as positive control for ER stress induction. (C) Transcript analysis of the classical ER stress mediator ATF4 by qRT-PCR for tunicamycin (TM) and thapsigargin (TG) treatment in absence and presence of TGF-β for 24 and 48 h. (D) Transcript analysis of the classical ER stress mediator CHOP by qRT-PCR for tunicamycin (TM) and thapsigargin (TG) treatment in absence and presence of TGF-β for 24 and 48 h.

Figure E2: TGF-β1 induces FKBP10 expression on transcript level. qRT-PCR analysis of FKBP10 transcript after FKBP10 knockdown in combination with 24 and 48h of TGF-β1 treatment (2.0 ng/ml). The effect of the knockdown was always highly significant ($p<0.001$), but is not specified in the interest of clarity.

Figure E3: FKBP10 knockdown does not affect levels of total or phosphorylated SMAD3. Densitometric quantification of levels of P-SMAD3 (left panel) and total SMAD3 (right panel), normalized to band intensities of total SMAD and β-actin, respectively. Data are based on three independent experiments and shown as mean ± SEM. A representative Western Blot is given in Figure 7D.

REFERENCES

E1. Dennler S, Itoh S, Vivien D, ten Dijke P, Huet S, Gauthier JM. Direct binding of Smad3 and Smad4 to critical TGF beta-inducible elements in the promoter of human plasminogen activator inhibitor-type 1 gene. *EMBO J* 1998; 17: 3091-3100.

2.2 FKBP10 regulates fibroblast migration via synthesis of collagen VI

In this manuscript, further effects of FKBP10 deficiency in phLF were examined in addition to its regulatory effects on collagen synthesis and secretion. The influence of FKBP10 on fibroblast migration and adhesion, important features in IPF disease progression, was examined. FKBP10 loss in phLF resulted in a decrease in cell adhesion and migration. Key molecules implicated in cell adhesion and migration were mainly upregulated. The effects were dependent on the addition of 2-phosphoascorbate, indicating collagen synthesis as the regulating mechanism. FKBP10 knockdown decreased, besides collagen I and FN expression (Chapter 2.1), the expression of collagen VI. The inhibitory effect of FKBP10 deficiency was compensated by coating culture dishes with collagen I and more pronounced by collagen VI, indicating decreased collagen VI synthesis as a result of FKBP10 deficiency as the underlying mechanism of action.

Contribution:
The author of this thesis contributed to conception and design of this study, to the experimental work, analysis and interpretation as well as drafting the manuscript and the intellectual content.

Knüppel L, Heinzelmann K, Lindner M, Hatz R, Behr J, Eickelberg O, Staab-Weijnitz C.A. FKBP10 regulates fibroblast migration via synthesis of collagen VI. *Respiratory Research*, 2018, 19:67.

Knüppel et al. Respiratory Research (2018) 19:67
https://doi.org/10.1186/s12931-018-0768-1

Respiratory Research

RESEARCH Open Access

FK506-binding protein 10 (FKBP10) regulates lung fibroblast migration via collagen VI synthesis

Larissa Knüppel[1,2], Katharina Heinzelmann[1,2], Michael Lindner[3], Rudolf Hatz[3,4], Jürgen Behr[3,5], Oliver Eickelberg[1,2,6] and Claudia A. Staab-Weijnitz[1,2*]

Abstract

Background: In idiopathic pulmonary fibrosis (IPF), fibroblasts gain a more migratory phenotype and excessively secrete extracellular matrix (ECM), ultimately leading to alveolar scarring and progressive dyspnea. Here, we analyzed the effects of deficiency of FK506-binding protein 10 (FKBP10), a potential IPF drug target, on primary human lung fibroblast (phLF) adhesion and migration.

Methods: Using siRNA, FKBP10 expression was inhibited in phLF in absence or presence of 2ng/ml transforming growth factor-β1 (TGF-β1) and 0.1mM 2-phosphoascorbate. Effects on cell adhesion and migration were monitored by an immunofluorescence (IF)-based attachment assay, a conventional scratch assay, and single cell tracking by time-lapse microscopy. Effects on expression of key players in adhesion dynamics and migration were analyzed by qPCR and Western Blot. Colocalization was evaluated by IF microscopy and by proximity ligation assays.

Results: FKBP10 knockdown significantly attenuated adhesion and migration of phLF. Expression of collagen VI was decreased, while expression of key components of the focal adhesion complex was mostly upregulated. The effects on migration were 2-phosphoascorbate-dependent, suggesting collagen synthesis as the underlying mechanism. FKBP10 colocalized with collagen VI and coating culture dishes with collagen VI, and to a lesser extent with collagen I, abolished the effect of FKBP10 deficiency on migration.

Conclusions: These findings show, to our knowledge for the first time, that FKBP10 interacts with collagen VI and that deficiency of FKBP10 reduces phLF migration mainly by downregulation of collagen VI synthesis. The results strengthen FKBP10 as an important intracellular regulator of ECM remodeling and support the concept of FKBP10 as drug target in IPF.

Keywords: FKBP10, FKBP65, migration, focal adhesion, collagen VI, lung fibrosis, fibroblast, fibulin

Background

Patients suffering from idiopathic pulmonary fibrosis (IPF), a highly progressive interstitial lung disease, have a median survival prognosis of 2-5 years after diagnosis [1]. The pathogenic processes are not completely understood. It is currently believed that the fibrotic response is caused by repeated micro-injuries of the respiratory epithelium [2] which leads to the release of profibrotic mediators like transforming growth factor β1 (TGF-β1), followed by myofibroblast differentiation, increased fibroblast migration, and, ultimately, excessive deposition of extracellular matrix (ECM) in the alveolar region [3–6]. More recent evidence suggests that the composition of the ECM strongly affects fibroblast phenotypes and therefore plays a crucial role in disease progression [4, 7, 8].

Aberrant fibroblast adhesion and migration are common features of fibrosis [9–11] and targeting fibroblast migration, *e.g.* by inhibition of focal adhesion kinase (FAK) or of integrins, has been proposed as a treatment strategy [12, 13]. For instance, myofibroblasts possess an increased ability to adhere to the ECM, which is

* Correspondence: staab-weijnitz@helmholtz-muenchen.de
[1]Comprehensive Pneumology Center, Ludwig-Maximilians-Universität and Helmholtz Zentrum Munich, Max-Lebsche-Platz 31, 81377 Munich, Germany
[2]Member of the German Center of Lung Research (DZL), Munich, Germany
Full list of author information is available at the end of the article

mediated by focal adhesions (FA) attaching the actin cytoskeleton to the matrix [14]. Cell attachment to the ECM via clustering of integrins leads to the recruitment of numerous FA proteins with adapter, structural, and enzymatic functions [15, 16]. For instance, structural proteins like talin, vinculin and α-actinin facilitate the connection between integrins and actin fibers and provide the basis for the transmission of mechanical forces between cell and ECM [17]. To enable cell migration, turnover of FA is necessary. Several factors are involved in FA disassembly, like actin dynamics, FAK and Src phosphorylation, and ERK/MAP kinase-mediated activation of calpain-2, a calcium-dependent protease [15].

Finally, migration is strongly influenced by topology and composition of the ECM including integrin ligands like collagen, fibronectin (FN), and laminin [7]. Collagen type VI appears to play a particularly important role in this context, as several studies indicate a central, albeit context-dependent and tissue-specific role of collagen VI for migration and adhesion [18–20].

FK506-binding protein 10 (FKBP10, also termed FKBP65), a member of the family of immunophilins, is an endoplasmic reticulum (ER) -resident peptidyl prolyl isomerase and a collagen I chaperone [21]. We have previously reported upregulation of FKBP10 in experimental lung fibrosis and IPF, where it is mainly expressed by (myo)fibroblasts [22]. Deficiency of FKBP10 by siRNA-mediated knockdown in primary human lung fibroblasts (phLF) reduced the expression of profibrotic markers like α-smooth muscle actin (α-SMA), FN and collagen I, and suppressed collagen secretion [22].

As properties of the ECM play an important role in adhesion dynamics and FKBP10 has been identified previously as a regulator of collagen biosynthesis in phLF, the aim of this study was to assess the effect of FKBP10 deficiency on adhesion and migration in phLF. To elucidate the underlying mechanisms, we analyzed the effect of siRNA-mediated knockdown of FKBP10 on intracellular and membrane-spanning components of the FA complex, on regulatory events of FA turnover, on proteins involved in actin dynamics, and, finally, on a selection of ECM proteins with important emerging functions in migration.

Methods

Material

Primers were obtained from MWG Eurofins (Ebersberg, Germany) and are shown in Table 1. Table 2 contains used primary antibodies. HRP-linked and fluorescent labeled secondary antibodies were purchased from GE Healthcare Life Sciences (Freiburg, Germany).

Statistical Analysis

Statistical analysis was performed in GraphPadPrism 5 (GraphPad Software, San Diego, CA, USA). Results are shown as mean ± SEM. Paired t-test was used for statistical analysis. Notably, analysis using a Wilcoxon signed rank test yielded very similar results except for the scratch assays shown in Fig. 5a where results just failed significance (not shown). Significance is indicated as follows: *p<0.05, **p<0.01, ***p<0.001.

Human Lung Material, Isolation and Culture of phLF

Primary human lung fibroblasts (phLF) were isolated from human lung tissue and derived from in total eight different patients. The tissue derived from human lung explant material of IPF patients or histologically normal regions adjacent to resected lung tumors was obtained from the BioArchive CPC-M for lung diseases at the Comprehensive Pneumology Center (CPC Munich, Germany). The study was approved by the local ethics committee of the Ludwig-Maximilians University of

Table 1 Primer table for Real-Time Quantitative Reverse-Transcriptase PCR (qRT-PCR). Primers were synthesized by MWG Eurofins (Ebersberg, Germany).

Target	Species	Forward primer (5′-3′)	Reverse primer (5′-3′)
CAPNS1	human	GACGCTACTCAGATGAAAGT	TCTTTGTCAAGAGATTTGAAG
CAV1	human	TCACTGTGACGAAATACTG	CGTAGATGGAATAGACACG
COL6A1	human	GACGCACTCAAAAGCA	ATCAGGTACTTATTCTCCTTCA
COL6A2	human	AGAAAGGAGAGCCTGCGGAT	AGGTCTCCCTCACGTAGGTC
COL6A3	human	CTCTACCGAGCCCAGGTGTT	ATGAGGGTGCGAACGTACTG
CORO1C	human	GTTAACAAATGTGAGATTGC	TGGAAAAGGTCAGACTTC
DHX8	human	TGACCCAGAGAAGTGGGAGA	ATCTCAAGGTCCTCATCTTCTTCA
ERK1	human	TTCGAACATCAGACCTACT	AGGTCCTGCACAATGTAG
FBLN1C	human	GCCCTGAGAACTACCG	GAGAGGTGGTAGTAGGTTATTC
FKBP10	human	CGACACCAGCTACAGTAAG	TAATCTTCCTTCTCTCTCCA
ITGB1	human	TTACAAGGAGCTGAAAAACT	AAAATGACTTCTGAGGAAAG
TLN1	human	GCTCTTTCTGTCAGATGAT	CATAGTGTCCCCATTTC

Table 2 Primary antibodies used in Western Blot analysis, Immunofluorescence and Proximity Ligation Assays

Target	Abbreviation	Antibody	Provider	Application
β-actin	ACTB	HRP-conjugated anti-ACTB antibody	Sigma Aldrich, St. Louis, USA	WB
Calpain-4	CAPNS1	mouse monoclonal anti-Calpain-4	Abnova, Taipei City, Taiwan	WB, IF, PLA
Caveolin-1	CAV1	rabbit monoclonal anti-Caveolin-1 antibody	Cell Signaling, Boston, USA	WB
Collagen VI α1	COL6A1	mouse monoclonal anti-Collagen VI A1 antibody	Santa Cruz, Dallas, USA	WB, IF, PLA
Collagen VI α3	COL6A3	mouse monoclonal anti-Collagen VI A3 antibody	Santa Cruz, Dallas, USA	IF, PLA
Coronin 1C	CORO1C	mouse monoclonal anti-CORO1C antibody	Santa Cruz, Dallas, USA	WB, IF, PLA
Extracellular Signaling Related Kinase 1	ERK1	mouse monoclonal anti-ERK1 antibody	BD Biosciences, New Jersey, USA	WB
ER protein 57 (Protein disulfide-isomerase A3)	ERp57	mouse monoclonal anti-ERp57	Abcam, Cambridge, UK	PLA
Fibulin-1	FBLN1	mouse monoclonal anti-FBLN1 antibody	Santa Cruz, Dallas, USA	WB, IF, PLA
FK506-binding protein 10	FKBP10	rabbit polyclonal anti-FKBP10 antibody	ATLAS, Stockholm, Sweden	WB, IF, PLA
Focal Adhesion Kinase	FAK	rabbit polyclonal anti-FAK antibody	Santa Cruz, Dallas, USA	WB
Golgin97	CDF4	mouse monoclonal anti-Golgin97 antibody	Invitrogen, Carlsbad, USA	PLA
mouse IgG (neg. ctrl)	mouse IgG	mouse IgG1κ isotype control	eBioscience, San Diego, USA	PLA
Integrin-β1	ITGB1	mouse monoclonal anti-ITGB1 antibody	Abcam, Cambridge, UK	WB
Phosphorylated Extracellular Signaling Related Kinase 1/2	p-ERK1/2	rabbit monoclonal anti-pERK1/2 (Thr202/Tyr204)	Cell Signaling, Boston, USA	WB
Phosphorylated Focal Adhesion Kinase	p-FAK Y397	rabbit monoclonal anti-pFAK (Tyr397)	Cell Signaling, Boston, USA	WB
Phosphorylated Focal Adhesion Kinase	p-FAK Y566/577	rabbit monoclonal anti-pFAK (Tyr576/Tyr577)	Biomol, Hamburg, Germany	WB
Phosphorylated SRC Proto-Oncogene, Non-Receptor Tyrosine Kinase	p-Src	rabbit polyclonal anti-pSrc (Tyr416)	Cell Signaling, Boston, USA	WB
SRC Proto-Oncogene, Non-Receptor Tyrosine Kinase	Src	mouse monoclonal anti-Src	Cell Signaling, Boston, USA	WB
Talin 1	TLN1	mouse monoclonal anti-TLN1	Sigma Aldrich, Dt. Louis, USA	WB, IF, PLA

Secondary HRP-linked antibodies and secondary antibodies (Alexa Fluor 488 goat anti-mouse IgG, Alexa Fluor 568 goat anti-rabbit IgG) for IF were purchased from GE Healthcare Life Sciences (Freiburg, Germany). 4',6-Diamidino-2-phenylindole (DAPI) was used for nuclear staining (Sigma-Aldrich, St. Louis, USA)

Munich, Germany, and all participants gave written informed consent. Isolation and culture of phLF was performed as described previously [22, 23]. Notably, in previous studies, we have never seen consistent expression differences between control and IPF fibroblasts, neither in terms of basal and TGF-β1-induced gene expression of collagens and collagen biosynthetic enzymes, nor in terms of collagen secretion [22, 23].

Transfection of phLF and TGF-β1 Treatment

Cells were seeded at a density of 20.000–25.000 cells/cm^2. Reverse transfection was carried out with human small interfering RNA of FKBP10 (siRNA) (s34171; Life Technologies, Carlsbad, CA) or negative control siRNA. Twenty-four hours later starvation for another 24 hours in Dulbecco's modified Eagle medium/F-12 including 0.5% fetal bovine serum and 0.1 mM 2-phospho-L-ascorbic acid was performed. Then, cells were treated with 2 ng/ml TGF-β1 (R&D Systems, Minneapolis, MN) in starvation medium for another 24 - 48 h, followed by harvesting for RNA and protein analysis. Unless stated otherwise, all data is derived from eight independent knockdown experiments in at least three and maximally in eight different human primary fibroblast lines. For fibroblast lines that had been used for more than one knockdown experiment in different passages, typically a mean was formed for these experiments prior to statistical analysis to avoid overrepresentation of one biological replicate in the data.

RNA Isolation and Real-Time Quantitative Reverse-Transcriptase PCR (qRT-PCR) Analysis

RNA isolation and qRT-PCR analysis were performed as described previously [22, 23].

Protein Isolation and Western Blot analysis

Protein isolation and Western Blot analysis were performed as described previously [22, 23].

Cell Fixation and Immunofluorescent Stainings

Cells were seeded on FN-coated coverslips (6 μg/mL, Sigma-Aldrich, St. Louis, USA), followed by serum starvation and TGF-β1 treatment for 48h as described above. The fixation method was chosen accordingly to the used antibodies. For methanol fixation, cells were washed once in 1x phosphate-buffered saline (PBS), followed by fixation with 100% methanol for 2 minutes on ice and three additional washing steps with 1x PBS to remove the residual methanol.

For para-formaldehyde (PFA) fixation, cells were washed once with 1x PBS and 4% PFA was added to the cells followed by incubation at room temperature for 20 minutes. Residual PFA was removed by three washing steps with 1x PBS. Staining of the cover slips was performed as described before [22]. Immunofluorescence (IF) was examined by acquiring z-stack images with an Axio Imager M2 Microscope (Carl Zeiss, Jena, Germany) and analysed by AxioVision 4.8 software.

Proximity Ligation Assay (PLA)

Cells were seeded, treated with TGF-β1 for 48h, and methanol-fixed as described above. The Duolink® PLA Kit (Sigma Aldrich, St. Louis, USA) was used and carried out according to the manufacturer's protocol. Interaction of FKBP10 with target proteins was visualized using an Axio Imager M2 Microscope (Carl Zeiss, Jena, Germany).

Cell Adhesion Assay

For analysis of cell attachment in FKBP10-deficient phLF, cells were seeded and treated as described above. After 48h of TGF-β1 treatment and 96h of siRNA knockdown, cells were trypsinized and counted. Per condition, four replicates with 100.000 cells per 48-well were seeded and incubated for 1 hour at 37°C, 5% CO_2. Wells were carefully washed once with 1 x PBS to remove non-adherent cells and attached cells were fixed with 4% PFA as described before. Cells were stained with 4′,6-Diamidin-2-phenylindol (DAPI) and Phalloidin, labeled with Alexa Fluor 568 (Invitrogen) followed by imaging using an LSM T-PMT microscope (Carl Zeiss, Jena, Germany). Attached cells were counted using IMARIS Software 9.0. Results were normalized to non-treated control and visualized as percentage of attached cells.

Scratch Assay

Cells were seeded at a density of 35.000 cells/cm^2 and siRNA-mediated knockdown of FKBP10 was performed as described above. To reach 100% confluency, cells were grown for 48h followed by starvation for 24h. A scratch was executed using a 1000 μL pipette tip and TGF-β1 was added. Images were taken at time point 0h using an inverse microscope (Primovert, Carl Zeiss, Jena, Germany) and the section was marked by a black dot. After 24h, additional images were taken to compare wound closure between control and FKBP10 deficient cells. Results are given in percent of wound closure normalized to untreated control.

Single Cell Migration Assay Using Time Lapse Microscopy

Cells were seeded at a density of 5.500 cells/cm^2 on uncoated, collagen I-coated (~50 μg/mL, Sigma-Aldrich, St. Louis, USA), or collagen VI-coated (10 μg/mL, Abcam, Cambridge, UK) wells. Knockdown by siRNA of FKBP10 was performed as described above. After 24h, cells were serum-starved for another 24h followed by TGF-β1 treatment (2 ng/mL) for 24h. Movies were generated over a period of 12h - 24h using Axio Observer Z1 microscope equipped with an AxioCam camera (Carl Zeiss, Jena, Germany) and images were taken in 20 min intervals. Single cell movement was analyzed using the cell tracking tool of the AxioVision 4.8 software (Carl Zeiss, Jena, Germany).

Results

Deficiency of FKBP10 attenuates migration and adhesion of primary human lung fibroblasts

SiRNA-mediated knockdown of FKBP10 expression in phLF was highly efficient on both protein and mRNA level (Fig. 1a, b, knockdown efficiency 86% ± 5%). Wound closure in a conventional scratch assay was significantly reduced in FKBP10-deficient cells compared to control in absence of TGF-β1. A similar trend was observed in presence of TGF-β1, which just failed significance (Fig. 1c, d). These results were confirmed with an independent and more accurate method, namely a single cell migration assay using time-lapse microscopy to track individual cells. In this assay, FKBP10-deficient cells showed a highly significant reduction of mean velocity both in absence and presence of TGF-β1 (Fig. 1e).

Next, we investigated the effect of siRNA-mediated knockdown of FKBP10 on adhesion of phLF using an IF-based attachment assay. In presence of TGF-β1, FKBP10 deficiency significantly reduced the ability of phLF to adhere to the cell culture dish surface (Fig. 1f).

While TGF-β1 had no significant effect on migration, neither in the scratch nor in the single cell tracking assay, TGF-β1 significantly increased fibroblast adhesion.

Deficiency of FKBP10 upregulates expression of key molecules of adhesion and migration in primary human lung fibroblasts, but does not alter the activation of focal adhesion kinase and downstream pathways

To gain a better understanding of the effect of FKBP10 deficiency on adhesion and migration, we analyzed several selected proteins with key functions in these processes. In terms of altered gene expression of focal

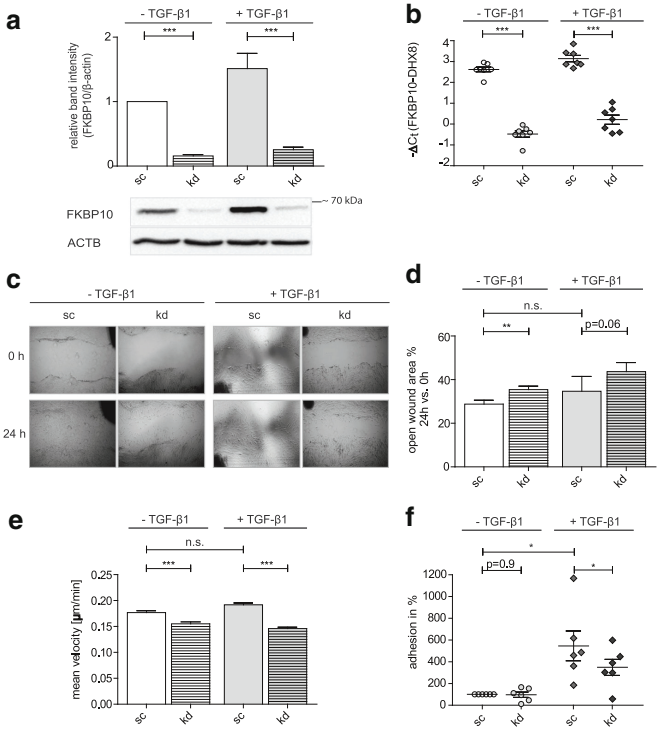

Fig. 1 Knockdown of FKBP10 reduces migration and adhesion of phLF. **a** Western Blot analysis of phLF treated with scrambled siRNA as control (sc) or FKBP10 siRNA (kd) and 2-phosphoascorbate (0.1 mM) in absence and presence of TGF-β1 (2 ng/mL) for 48h. Densitometric analysis and representative blots show the effect of FKBP10 knockdown on the expression of FKBP10 relative to β-actin as loading control (ACTB). **b** Quantitative reverse transcriptase-polymerase chain reaction analysis of phLF treated with sc siRNA as control or FKBP10 siRNA (kd) and 2- phosphoascorbate (0.1 mM) in absence and presence of TGF-β1 (2 ng/mL) for 48h. Transcript levels are shown as -ΔCt values. DEAH (Asp-Glu-Ala-His) Box Polypeptide 8 (DHX8) was used as endogenous control. Data (**a**, **b**) is based on eight independent experiments. **c** Representative images of a scratch assay of phLF treated with sc siRNA as control or FKBP10 and 2- phosphoascorbate (0.1 mM) in absence or presence of TGF-β1 (2 ng/mL). Images were taken at 0h and after 24h. **d** Analysis of open wound areas as shown in (**c**) normalized to controls at 0h (100%), given in % of the remaining wound area. Data is based on four independent experiments. **e** SCM assay of phLF treated with sc siRNA as control or FKBP10 siRNA and 2- phosphoascorbate (0.1 mM) in absence and presence of TGF-β1 (2 ng/mL). Cells were tracked over a period of 12h - 24h. Results of five independent experiments are shown as mean velocity of around 80 tracked cells per condition. **f** Cell attachment assay of phLF treated with sc siRNA as control or FKBP10 siRNA in absence or presence of TGF-β1 (2 ng/mL) for 48h. Results originate from six independent experiments and are visualized as percentage of cell adhesion normalized to non TGF-β1-treated cells. Statistical significance between control and FKBP10 kd is indicated by horizontal brackets and asterisks

adhesion and ECM components, we only observed marginal differences between fibroblasts isolated from normal histology control or from IPF lung tissue and therefore decided to pool the data. Deficiency of FKBP10 in phLF led to induction of the focal adhesion component talin-1 (TLN1) on protein and mRNA level in absence and presence of TGF- β1 (Fig. 2a, b). Next, we investigated the effect of FKBP10 knockdown on calpain-4 (CAPNS1), the small regulatory subunit of calpain-1 and calpain-2, which is indispensable for formation and strengthening of adhesions and for mechanosensing during fibroblast migration [24]. Similar to TLN1, CAPNS1 expression was significantly upregulated in absence and presence of TGF-β1 on transcript level (Fig. 2c, d); this effect, however, translated to the protein level only in absence of TGF-β1. Moreover, FKBP10

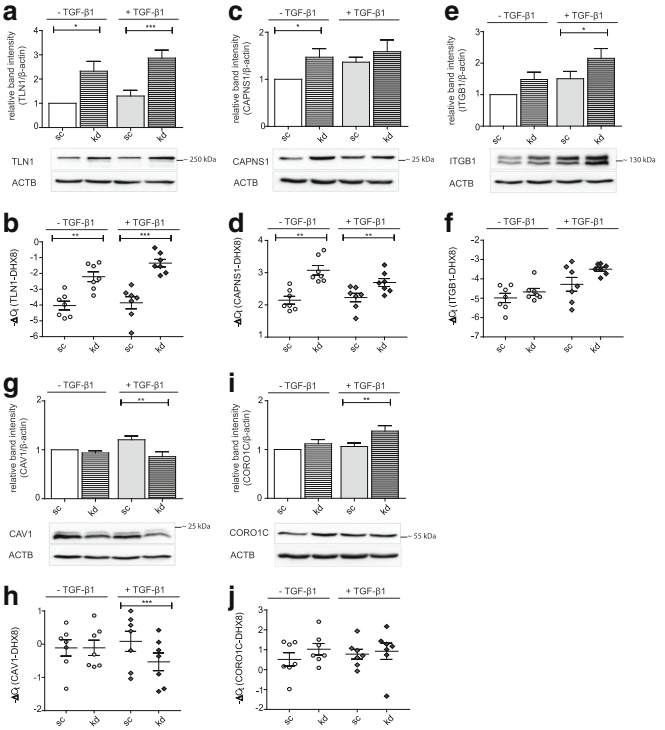

Fig. 2 FKBP10 deficiency alters the expression of molecules implicated in adhesion and migration. **a, c, e, g, i** Western Blot analysis of phLF treated with scrambled siRNA as control (sc) or FKBP10 siRNA (kd) and 2- phosphoascorbate (0.1 mM) in absence and presence of TGF-β1 (2 ng/mL) for 48h. Densitometric analysis and representative blots show the effect of FKBP10 kd on the expression of talin-1 (TLN1) (**a**), calpain-4 (CAPNS1) (**c**), integrin β1 (ITGB1) (**e**), caveolin-1 (CAV1) (**g**) and coronin 1C (CORO1C) (**i**) relative to β-actin as loading control (ACTB). **b, d, f, h, j** Quantitative reverse transcriptase-polymerase chain reaction analysis of phLF treated with scrambled siRNA as control (sc) or FKBP10 siRNA (kd) and 2- phosphoascorbate (0.1 mM) in absence and presence of TGF-β1 (2 ng/mL) for 48h. Transcript levels are presented as -**Δ**Ct values showing the effect of siRNA mediated kd of FKBP10 on talin-1 (TLN1) (**b**), calpain-4 (CAPNS1) (**d**), integrin β1 (ITGB1) (**f**), caveolin-1 (CAV1) (**h**) and coronin 1C (CORO1C) (**j**). DEAH (Asp-Glu-Ala-His) Box Polypeptide 8 (DHX8) was used as endogenous control. All data is based on eight (protein) or seven (mRNA) independent experiments. Statistical significance between control and FKBP10 kd is indicated by horizontal brackets and asterisks

knockdown also increased protein levels of the transmembrane collagen receptor integrin-β1 (ITGB1), particularly in presence of TGF-β1 (Fig. 2e), while transcript levels were not significantly changed (Fig. 2f). Finally, two modulators of cytoskeleton dynamics, caveolin-1 (CAV1) and coronin-1C (CORO1C), were regulated in opposite directions: Whereas CAV1 expression (protein and mRNA) was downregulated upon FKBP10 knockdown in presence of TGF-β1 (Fig. 2g, h), CORO1C protein levels were upregulated (Fig. 2i, j).

FAK activation by either integrins or growth factors leads to autophosphorylation of Tyr 397 in FAK, creating a motif which results in binding and conformational activation of proto-oncogene tyrosine-protein kinase Src. Active Src triggers further FAK phosphorylation on Tyr sites like Tyr 576/577, starting the ras-raf-MEK-ERK signal transduction cascade which is implicated in many processes including cell adhesion and migration. MEK1/2 catalyzes ERK1/2 phosphorylation on specific Tyr and Thr residues essential for enzyme activity [25, 26].

Deficiency of FKBP10 slightly upregulated total FAK levels (Fig. 3a); however, there was no significant effect on the phosphorylation on Tyr 397 or Tyr 576/577 of

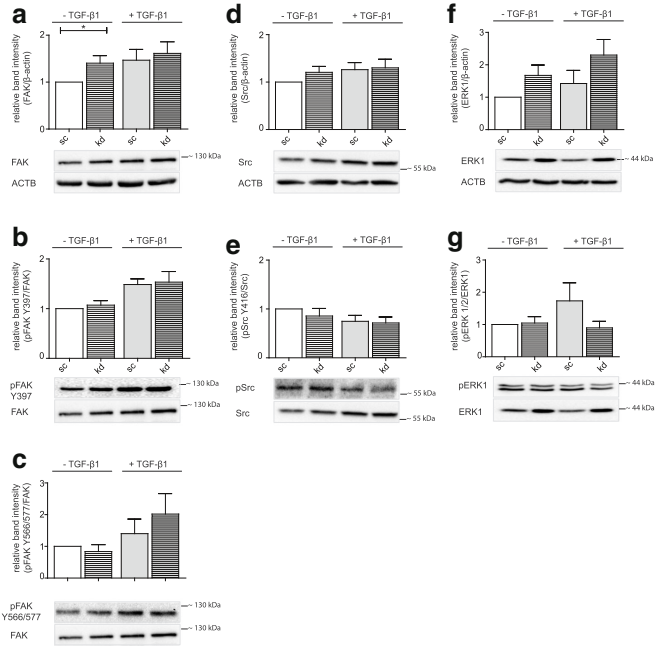

Fig. 3 Neither FAK, Src, nor ERK1/2 activation is affected by FKBP10 kd. Western Blot analysis of phLF treated with scrambled siRNA as control (sc) or FKBP10 siRNA (kd) and 2- phosphoascorbate (0.1 mM) in absence and presence of TGF-β1 (2 ng/mL) for 48h. Densitometric analysis and representative blots show the effect of FKBP10 kd on the expression of FAK (**a**), Src (**d**) and ERK1 (**f**) relative to β-actin as loading control (ACTB). **b, c** Densitometric analysis and representative blots showing the effect of FKBP10 kd on the phosphorylation of FAK (Y397) (**b**) and FAK (Y576/577) (**c**) relative to FAK. **e, g** Densitometric analysis and representative blots showing the effect of FKBP10 kd on the phosphorylation of Src (Y416) (**e**) relative to Src and pERK1/2 (T202/Y204) (**g**) relative to ERK1. All data is based on eight independent experiments. Statistical significance between control and FKBP10 kd is indicated by horizontal brackets and asterisks

FAK (Fig. 3b, c). Similarly, none of the assessed downstream signaling pathways appeared affected: Neither levels of total Src and phospho-Src nor levels of total ERK1 and phosphorylated ERK1/2 changed upon FKBP10 knockdown (Fig. 3d-g).

FKBP10 interacts with type VI collagen and fibulin-1 and regulates their expression

As changes in expression of focal adhesion complex components and in events during FAK signaling did not explain the observed attenuated migration upon FKBP10 knockdown, we reasoned that changes in ECM composition could be the main cause of reduced migration velocity. Besides the ECM proteins collagen I and FN, which we reported to be downregulated upon FKBP10 knockdown previously [22], collagen VI and fibulin-1 also have been described to maintain important roles in the process of cell migration [18, 27]. Here, we found that collagen VI and fibulin-1 expression were regulated in different directions in response to FKBP10 knockdown. Collagen 6A1 was significantly reduced on protein level in FKBP10 deficient phLF with and without TGF-β1, whereas *COL6A1* transcript was only reduced in presence of TGF-β1 (Fig. 4a, b). Interestingly, mRNA levels of *COL6A2* and *COL6A3* chains were not influenced by FKBP10 deficiency (Fig. 4c, d). In contrast, fibulin-1 protein expression was increased in response to FKBP10 knockdown in absence and presence of TGF-β1; transcript levels of *FBLN1C* were significantly upregulated under basal conditions upon FKBP10 knockdown (Fig. 4e, f).

Co-localization of FKBP10 with both, collagen VI (COL6A1 and COL6A3) (Fig. 4g, h) and fibulin-1 (Fig. 4i) was examined by IF stainings and PLA (Fig. 4j). Negative

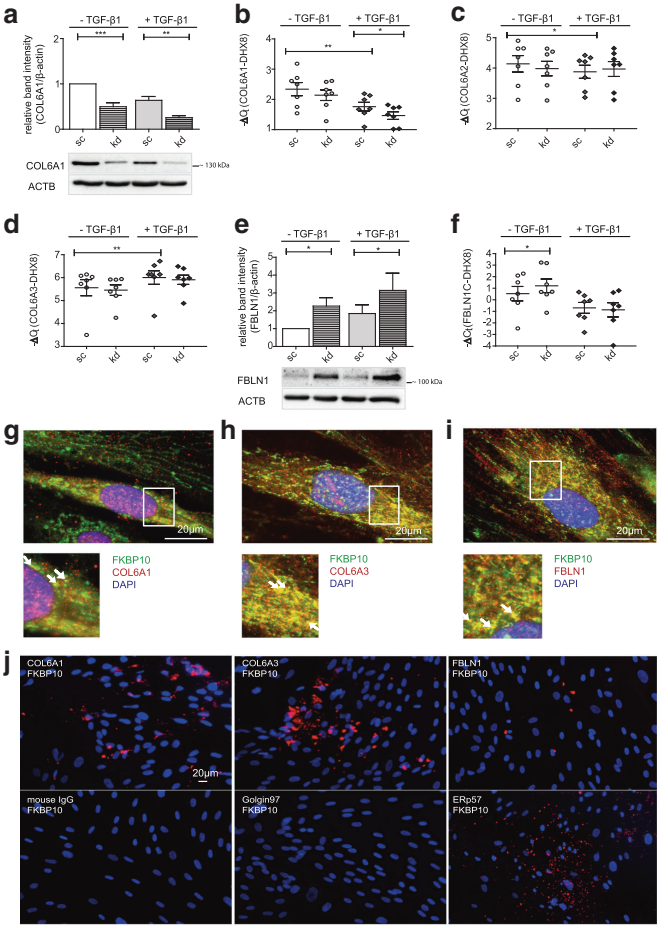

Fig. 4 FKBP10 interacts with COL6A1 and FBLN1 and regulates their expression. **a, e** Western Blot analysis of phLF treated with scrambled siRNA as control (sc) or FKBP10 siRNA (kd) and 2- phosphoascorbate (0.1 mM) in absence and presence of TGF-β1 (2 ng/mL) for 48h. Densitometric analysis and representative blots showing the effect of FKBP10 kd on the expression of Collagen VI alpha1 (COL6A1) (**a**) and fibulin-1 (FBLN1) (**e**) relative to β-actin as loading control (ACTB). **b, c, d, f** Quantitative reverse transcriptase-polymerase chain reaction analysis of phLF treated with sc siRNA as control or FKBP10 siRNA and 2-phosphoascorbate (0.1 mM) in absence and presence of TGF-β1 (2 ng/mL) for 48h. Transcript levels are shown as -ΔCt values of showing the effect of FKBP10 kd on collagen VI alpha 1 (COL6A1) (**b**), collagen VI alpha 2 (COL6A2) (**c**), collagen VI alpha 3 (COL6A3) (**d**) and fibulin-1C (FBLN1C) (**f**). DEAH (Asp-Glu-Ala-His) Box Polypeptide 8 (DHX8) was used as endogenous control. All data is based on eight (protein) or seven (mRNA) independent experiments. Statistical significance is indicated by horizontal brackets and asterisks. **g-i** Immunofluorescence staining of FKBP10 (green) and COL6A1 (red) (**g**), COL6A3 (red) (**h**) and FBLN1 (red) (**i**). 4`, 6-diamidino-2-phenylindole (DAPI) staining is shown in blue. The region of interest is indicated by a white square and enlarged in the picture below. White arrows specify examples for co-localization of FKBP10 with COL6A1, COL6A3 or FBLN1. Stainings were taken as z-stack and the enlarged pictures show one focal plane from this z-stack. Representative images were selected from three independent experiments. **j** Representative images of *in situ* localization of the interaction of FKBP10 and COL6A1, COL6A3, FBLN1, mouse IgG1κ (negative control), Golgin97 (negative control) and ERp57 (positive control), assessed by proximity ligation assay. Representative images were selected from three independent experiments, except for IgG negative control (n=1)

controls (mouse IgG and Golgin97) did not show any interaction with FKBP10. Endoplasmic Reticulum Protein 57 (ERp57), previously reported by IF to co-localize with FKBP10 [22] was used as positive control and showed proximity to FKBP10. Positive signals were also observed for COL6A1, COL6A3 and FBLN1, indicating interaction with or proximity to FKBP10.

The effects of FKBP10 deficiency on migration and adhesion depend on 2-phosphoascorbate and are abolished by coating cell culture dishes with collagen VI

Post-translational modifications (PTM) like proline and lysine hydroxylation of collagens (including collagen VI) are crucial steps in collagen biosynthesis and catalyzed by ascorbate-dependent prolyl and lysyl hydroxylases [28–30]. In contrast, FBLN1 biosynthesis is not dependent on ascorbate [31]. Therefore, we reasoned that exclusion of ascorbate from the culture medium would give us a first indication whether decreased biosynthesis of collagen or increased biosynthesis of fibulin may underlie the observed effects of FKBP10 deficiency on migration and adhesion. Notably, in absence of 2-phosphoascorbate the effect of FKBP10 deficiency in phLF on adhesion and migration was lost, in comparison to the results in presence of 2-phosphoascorbate (Fig. 5), pointing towards a collagen-dependent mechanism.

As both collagen I and collagen VI are downregulated upon FKBP10 deficiency [22], we coated dishes with either collagen I or collagen VI and analyzed migration in a single-cell migration approach. Notably, the effect of FKBP10 deficiency in phLFs on migration was completely lost when culture dishes were coated with collagen VI (Fig. 6b) when compared to uncoated dishes

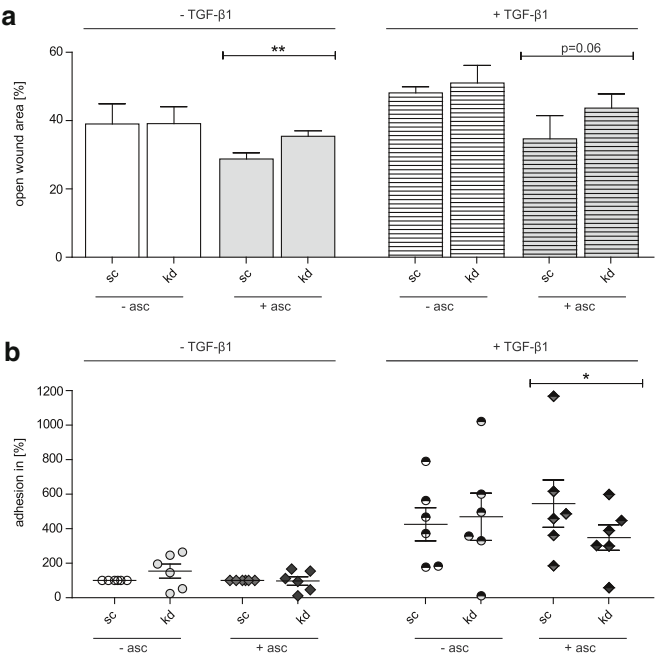

Fig. 5 The inhibitory effect of FKBP10 deficiency on migration and adhesion is 2-phosphoascorbate dependent. **a** Analysis of open wound areas in scratch assays of phLF treated with scrambled siRNA (sc) as control or FKBP10 siRNA (kd) in absence and presence of TGF-β1 (2 ng/mL) and 0.1 mM 2-phosphoascorbate. Images were taken at 0h and after 24h. Data is normalized to controls at 0h (100%), given in % of the remaining wound area and based on four independent experiments. **b** Cell attachment assay of phLF treated with scrambled siRNA (sc) as control or FKBP10 siRNA (kd) in absence or presence of TGF-β1 (2 ng/mL) and 2-phosphoascorbate (0.1 mM) for 48h. Results originate from six independent experiments and are visualized as percentage of cell adhesion normalized to non TGF-β1 treated. Experiments without and with 2- phosphoascorbate were performed in parallel

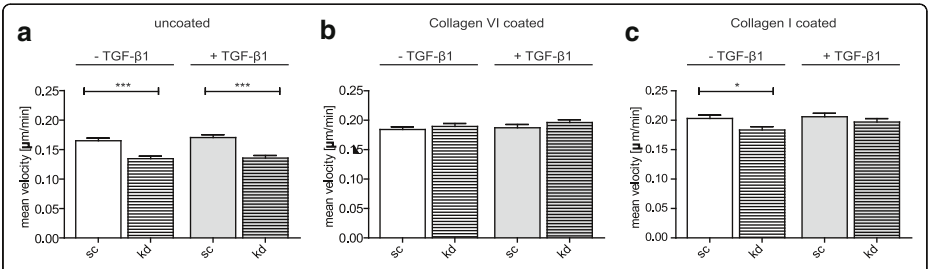

Fig. 6 Coating of dishes with collagen VI abolishes the inhibitory effect of FKBP10 knockdown on migration. SCM assay of phLF treated with scrambled siRNA as control (sc) or FKBP10 siRNA (kd) and 2- phosphoascorbate (0.1 mM) in absence and presence of TGF-β1 (2 ng/mL). Cells were tracked over a period of 12h -24h. Results of three independent experiments are shown as mean velocity of around 80 tracked cells per condition. Effect of collagen VI coated dishes on mean velocity of phLF is shown in (**b**) and of collagen I coated dishes in (**c**) compared to uncoated dishes for control (**a**). Statistical significance between control and FKBP10 kd is indicated by horizontal brackets and asterisks

(Fig. 6a). Some compensation was also visible in collagen I-coated dishes, albeit not that pronounced (Fig. 6c).

Discussion

In this study we demonstrated that FKBP10 deficiency inhibited phLF adhesion and migration. This effect could neither be explained by changes in expression or activation of components of the FA complex, nor by changes in FAK downstream signaling events, nor by changes in regulators of actin dynamics. Instead, we found that the effect of FKBP10 deficiency on migration and adhesion depended on 2-phosphoascorbate, pointing towards a central role of collagen biosynthesis in this context. Loss of FKBP10 downregulated the expression of collagen VI, a collagen type increasingly recognized as a central player in migration, and coating culture dishes with collagen VI completely abolished the effect of FKBP10 deficiency on phLF migration.

Next to excessive ECM deposition by interstitial fibroblasts, aberrant fibroblast adhesion and increased migration are also important features of IPF [6, 9–11]. Here we show that loss of the collagen chaperone FKBP10, which we previously identified as potential IPF drug target due to its role in ECM synthesis and secretion [22], inhibited wound closure and reduced the mean velocity and adhesion capacity of phLF (Fig. 1). This observation is in line with the very recent report by Liang *et al.*, showing that siRNA-mediated knockdown of FKBP10 led to reduced migration in human hypertrophic scar fibroblasts [32]. Collectively, these studies are confirmative of our concept of FKBP10 as potential drug target in fibrotic disease.

We assessed fibroblast migration both in a conventional scratch assay as well as by tracking individual cells with videomicroscopy in time-lapse experiments, a more accurate approach. Overall, both assays consistently showed reduced migration under conditions of FKBP10 deficiency, even if the scratch assay results in presence of TGF-β1 failed significance (p=0.06). We believe that this minor discrepancy reflects the well-known disadvantages of the scratch assay, most importantly variations in gap width due to the manually applied and therefore often uneven scratch, the fact that ECM substrate is equally scraped off together with the cells, and also the mechanical cell damage which may introduce artifacts. These technical drawbacks may explain the greater variations observed in this assay, leading to results that just fail significance.

Our finding that TGF-β1 did not affect fibroblast migration is in agreement with previous studies by others [33–35]. Increased fibroblast adhesion in presence of TGF-β1 may in part reflect increased expression of β1-integrin (this work, cf. Fig. 2e, f, scr ctrl *vs.* scr TGF-β1, p=0.0642) and/or β3-integrins [36].

Initially, we sought to assess the effect of FKBP10 deficiency on several regulatory levels of FA turnover to elucidate the mechanism underlying attenuated migration. Cell migration is a complex cyclic process starting with the extension of membrane protusions (*lamellipodia*) at the leading edge followed by their adhesion to the ECM and retraction of the cell tail [37]. During cell migration assembly and disassembly of FA is dynamically regulated. The process of cell attachment to the ECM is initiated by clustering of integrins on the cell surface, heterodimeric transmembrane receptors consisting of α and β subunits. The intracellular domains of the clustered integrins serve as a platform for FA protein recruitment and ultimately link the ECM via FA to actin stress fibers [38]. In this context, TLN1 mediates the initiation of FA assembly by interacting with the cytoplasmic domain of the integrin β subunit on the one hand and with actin and actin-binding proteins on the other [15]. Another initial event upon integrin clustering is activation of FAK including autophosphorylation of Tyr

397 and Src-mediated phosphorylation of additional tyrosine residues within FAK (*e.g.* Y 566 and 577), which are essential for full FAK activity. Active FAK interacts with multiple signalling molecules including Grb7, PI3K, paxillin, MLCK and ERK, activating signalling pathways which result in protrusion extension, increased FA turnover, and therefore, ultimately, in increased cell motility [15, 39–42]. The protease calpain 2, a heterodimer consisting of a catalytic subunit and a regulatory subunit (calpain-4, CAPNS1) plays a central role in this context as it, when recruited by FAK and activated by ERK/MAP kinase, mediates amongst others proteolysis of TLN1 and FAK, considered the rate-limiting step in FA turnover [15, 38, 39, 43, 44]. Finally, directional cell migration is strongly dependent on polarized actin dynamics. Rho-like GTPases like RhoA and Rac1 control cytoskeleton contractility, polymerization, and protrusion. The integral membrane protein caveolin-1 (Cav-1), activated by small kinases like Src, is a central regulator of Rho-like GTPase signaling in this context [45, 46]. Another regulator of actin filament turnover in the *lamellipodia* during cell migration is the actin binding protein coronin 1C (CORO1C) [47].

FKBP10 deficiency led to several significant changes in expression of FA components on all levels assessed, *i.e.* upregulation of ITGB1, TLN1, CAPNS1, FAK, CORO1C and downregulation of CAV1 (Fig. 2). Upregulation of ITGB1 may associate with reduced FA turnover and slow migration [48–50] but impaired migration and adhesion has also been reported as a result of ITGB1 deficiency [51]. Collectively, these findings suggest that manipulation of ITGB1 protein levels in general is unfavorable to cell motility, regardless of direction of regulation. As ITGB1 functions as an adapter protein between the ECM and intracellular FA complexes, it is conceivable that its expression levels must be tightly regulated to allow for functional intermolecular interactions between different interacting partners.

The same may apply to TLN1, an adapter protein linking the cytoskeleton to ITGB1, where reports in the literature are also seemingly controversial: Upregulation of TLN1, but also suppression of TLN1 has been reported to reduce migration and adhesion [52–54]. Interestingly, downregulation of TLN1 has also been associated with increased migration [52, 55], which is in support of its function as a regulator of FA turnover together with its protease calpain-2 [15, 38, 39, 43, 44]. In our system, however, the simultaneous increase of the regulatory calpain 2 subunit CAPNS1, argues for overall little change in FA turnover, at least in absence of TGF-β1 (Fig. 2c, d). This is consistent with our observation that phosphorylation levels of FAK, Src, and ERK (Fig. 3), central signaling events in the process of FA turnover [39, 56–58] remained unchanged.

At first, observing inhibition of adhesion and migration in the absence of changes in activation of FAK and related signaling pathways seemed contradictory to us. However, similarly, Asano and colleagues have reported that siRNA-mediated knockdown of α-smooth muscle actin (α-SMA) in phLF led to inhibition of migration without affecting the FAK signaling pathway [59]. This observation suggested that changes in actin dynamics may underlie the observed inhibition of migration and, indeed, from our previous studies, we know that FKBP10 deficiency reduces α-SMA expression in phLF [22]. Also, deficiency of the actin binding protein CORO1C typically results in inhibition of migration; however, here, we observed a moderate increase of CORO1C protein rather than downregulation (Fig. 2i) [60, 61]. Expression of CAV1, deficiency of which typically results in decreased migratory speed in variable cell types [62–64], was only moderately downregulated in presence of TGF-β1 (Fig. 2g, h). Collectively, these observations do not argue for altered actin dynamics as a major mechanism underlying inhibition of migration in response to FKBP10 deficiency.

Importantly, cell migration is influenced by properties of the ECM, like density of adhesion ligands (collagen, FN), ECM composition, and stiffness [7, 65]. Previously, we have observed downregulation of expression and secretion of type I collagen and FN, both major components of the fibroblast ECM, in response to FKBP10 knockdown [22]. Here we extended this analysis and assessed additional ECM components with important roles in cell migration, namely type VI collagen and FBLN1. Both proteins colocalized with FKBP10 in phLF, as assessed by both immunofluorescence colocalization analysis and proximity ligation assay (Fig. 4g-j), indicating direct interaction with FKBP10 in the ER. Interestingly, we found that loss of FKBP10 significantly increased FBLN1 expression (Fig. 4e, f), but decreased protein levels of COL6A1 (Fig. 4a, b). Notably, COL6A1 deficiency is sufficient to inhibit collagen VI deposition in the ECM, as no triple helical molecules can be formed without the α1(VI)-chain [66]. These results suggest opposing functions of FKBP10 in FBLN1 and collagen VI biosynthesis in phLF. It is tempting to speculate, for instance, that FKBP10 acts as a FBLN1 chaperone, sequestering FBLN1 in the ER, prohibiting packing in vesicles for secretion or targeting FBLN1 for ER-associated protein degradation, while at the same time FKBP10 is likely required for efficient collagen VI triple helix formation, similar to collagen I and III [21, 67, 68]. These aspects will be interesting to explore in future studies.

As to function of these proteins in migration, reduced attachment and decreased migratory speed has been reported for a human breast cancer cell line (MDA MB231) in response to FBLN1 overexpression [27] and

siRNA mediated knockdown of FBLN1 in corneal fibroblasts upregulated cell migration [69]. Therefore, taken together, it was plausible that increased FBLN1 levels may underlie the observed inhibition of migration under conditions of FKBP10 deficiency.

While collagen VI begins to emerge as an important regulator of cell migration, reports on its direction of effect, inhibiting or promoting migration, are controversial [18–20]. For instance, collagen VI-deficient tendon fibroblasts show delayed wound closure, *i.e.* lower migration speed, in a scratch assay [18], while human dermal fibroblasts displayed higher migration speed on matrices derived from collagen VI-deficient cells [20]. These discrepancies may be a result of the divergent approaches in the mentioned studies (assessment of newly formed ECM versus assessment of ECM deposited within 10 days, respectively), different collagen VI chains assessed (COL6A1 versus COL6A2), but also of the different cell origins, thus possibly reflecting time-, chain-, and cell-specific effects of collagen VI.

Ascorbic acid is a cofactor necessary for proline and lysine hydroxylation during collagen synthesis [68] including collagen VI [30, 70], but not required for FBLN1 synthesis. Therefore, to differentiate between increased FBLN1 or decreased type VI collagen as the underlying mechanism of decreased adhesion and migration, we compared effects of FKBP10 knockdown on adhesion and migration in absence and presence of 2-phosphoascorbate, a stable analogue of ascorbic acid. Notably, neither migration nor adhesion were changed upon loss of FKBP10 when the cell culture medium was ascorbate-deficient (Fig. 5a, b). These results strongly indicated that the effect of FKBP10 deficiency on adhesion and migration was collagen-dependent. While coating with collagen VI abolished the effect of FKBP10 knockdown on migration completely, coating with collagen I only did so marginally (Fig. 6). Overall, this indicated that FKBP10 knockdown inhibits lung fibroblast migration by reduced collagen VI biosynthesis rather than reduced collagen I biosynthesis, an effect of FKBP10 deficiency which we have reported previously [22].

Conclusion

Collagen VI is an important regulator of the ECM organizing the three-dimensional meshwork of collagen and FN fibers [71, 72] and the topography of the fibrillar ECM network guides directional cell migration [73]. Therefore, our observations suggest that loss of FKBP10 results in reduced biosynthesis of collagen VI and, possibly in combination with decreased extracellular collagen I levels, leads to a disorganized ECM with changed adhesion ligand density, stiffness and composition, which may not provide sites for integrin clustering and does not favor directional cell migration. Upregulation of ITGB1, TLN1, CAPNS1, total FAK, and CORO1C may ultimately reflect an attempt of the cells to overcome decreased migration by overcompensation, increasing expression of ECM receptors or components of the FA turnover machinery.

Interestingly, FKBP10 mediates dimerization with collagen lysyl hydroxylase 2 and thus contributes to the generation of collagen hydroxylysines, which act as substrates for extracellular lysyl-oxidase-mediated collagen crosslinking [74–76]. Extracellular collagen lacking proper crosslinks is prone to proteolytic degradation and may not be able to contribute to the higher ordered organization of the ECM anymore [77–80]. Therefore, downregulation of FKBP10 may also contribute to disorganization of the ECM by providing less crosslinking sites in type I and type VI collagen.

In summary, we found that loss of FKBP10 in phLF results in decreased adhesion and migration. We found that the main underlying mechanism was reduced collagen VI biosynthesis, as both ascorbate deficiency and coating of cell culture dishes with collagen VI abolished the effect of FKBP10 knockdown on migration. As increased fibroblast migration is a characteristic of IPF, the results are in support of our concept of FKBP10 as a potential drug target for IPF.

Abbreviations

FKBP10: FK506-binding Protein 10; IPF: Idiopathic Pulmonary Fibrosis; ECM: Extracellular matrix; phLF: Primary Human Lung Fibroblast; TGF-β1: Transforming Growth Factor-β1; IF: Immunofluorescence; FAK: Focal Adhesion Kinase; FA: Focal Adhesions; Src: SRC Proto-Oncogene, Non-Receptor Tyrosine Kinase; ERK: Extracellular Signaling Related Kinase; MAP: Mitogen-activated Protein; FN: Fibronectin; ER: Endoplasmic Reticulum; α-SMA: α-smooth muscle actin; ACTB: β-actin; CAPNS1: Calpain-4; CAV1: Caveolin-1; COL6A1: Collagen VI α1; COL6A3: Collagen VI α3; CORO1C: Coronin 1C; ERp57: ER protein 57 (Protein disulfide-isomerase A3); FBLN1: Fibulin-1; ITGB1: Integrin-β1; TLN1: Talin 1; COL6A1: Collagen VI alpha 1; COL6A2: Collagen VI alpha 2; COL6A3: Collagen VI alpha 3; PTM: Post-translational Modification; sc: scrambled; kd: knockdown

Acknowledgements

We thank Elisabeth Hennen for excellent technical assistance, and Gerald Burgstaller for his support with single cell migration assays. Human samples for derivation of phLF were kindly provided by the CPC-M BioArchive.

Funding

This work was supported by the Friedrich-Baur-Stiftung (grant to CASW, 51/16), the Helmholtz Association, and the German Center for Lung Research (DZL).

Availability of data and materials

The datasets used or analyzed during the current study are available from the corresponding author on reasonable request.

Authors' contributions

Conception and design: LK, KH, ML, RH, JB, OE, CSW. *Experimental work, analysis, and interpretation:* LK, CSW. *Drafting the manuscript and intellectual content:* LK, OE, CSW. All authors read and approved the final manuscript.

Ethics approval and consent to participate

The study was approved by the local ethics committee of the Ludwig-Maximilians University of Munich, Germany (333-10), and all participants gave written informed consent.

Competing interests
The authors declare that they have no competing interests.

Publisher's Note

Springer Nature remains neutral with regard to jurisdictional claims in published maps and institutional affiliations.

Author details
[1]Comprehensive Pneumology Center, Ludwig-Maximilians-Universität and Helmholtz Zentrum Munich, Max-Lebsche-Platz 31, 81377 Munich, Germany. [2]Member of the German Center of Lung Research (DZL), Munich, Germany. [3]Asklepios Fachkliniken Munich-Gauting, Munich, Germany. [4]Thoraxchirurgisches Zentrum, Klinik für Allgemeine-, Viszeral-, Transplantations-, Gefäß- und Thoraxchirurgie, Klinikum Großhadern, Ludwig-Maximilians-Universität, Munich, Germany. [5]Medizinische Klinik und Poliklinik V, Klinikum der Ludwig-Maximilians-Universität, Munich, Germany. [6]Colorado Anschutz Medical Campus, Pulmonary and Critical Care Medicine University, Denver, Colorado, USA.

Received: 8 February 2018 Accepted: 2 April 2018
Published online: 19 April 2018

References

1. Meltzer EB, Noble PW. Idiopathic pulmonary fibrosis. Orphanet J Rare Dis. 2008;3:8.
2. Fernandez IE, Eickelberg O. New cellular and molecular mechanisms of lung injury and fibrosis in idiopathic pulmonary fibrosis. Lancet. 2012;380:680–8.
3. Wynn TA. Common and unique mechanisms regulate fibrosis in various fibroproliferative diseases. J Clin Invest. 2007;117:524–9.
4. Hinz B, Phan SH, Thannickal VJ, Galli A, Bochaton-Piallat ML, Gabbiani G. The myofibroblast: one function, multiple origins. Am J Pathol. 2007;170:1807–16.
5. Rock JR, Barkauskas CE, Cronce MJ, Xue Y, Harris JR, Liang J, Noble PW, Hogan BL. Multiple stromal populations contribute to pulmonary fibrosis without evidence for epithelial to mesenchymal transition. Proc Natl Acad Sci U S A. 2011;108:E1475–83.
6. Suganuma H, Sato A, Tamura R, Chida K. Enhanced migration of fibroblasts derived from lungs with fibrotic lesions. Thorax. 1995;50:984–9.
7. Burgess JK, Mauad T, Tjin G, Karlsson JC, Westergren-Thorsson G. The extracellular matrix - the under-recognized element in lung disease? J Pathol. 2016;240:397–409.
8. Parker MW, Rossi D, Peterson M, Smith K, Sikstrom K, White ES, Connett JE, Henke CA, Larsson O, Bitterman PB. Fibrotic extracellular matrix activates a profibrotic positive feedback loop. J Clin Invest. 2014;124:1622–35.
9. Chang YZ, Yang L, Yang CQ. Migration of hepatic stellate cells in fibrotic microenvironment of diseased liver model. Hepatobiliary Pancreat Dis Int. 2008;7:401–5.
10. King TE Jr, Pardo A, Selman M. Idiopathic pulmonary fibrosis. Lancet. 2011; 378:1949–61.
11. Verrecchia F, Mauviel A. Transforming growth factor-beta and fibrosis. World J Gastroenterol. 2007;13:3056–62.
12. Lagares D, Busnadiego O, Garcia-Fernandez RA, Kapoor M, Liu S, Carter DE, Abraham D, Shi-Wen X, Carreira P, Fontaine BA, et al. Inhibition of focal adhesion kinase prevents experimental lung fibrosis and myofibroblast formation. Arthritis Rheum. 2012;64:1653–64.
13. Henderson NC, Sheppard D. Integrin-mediated regulation of TGFbeta in fibrosis. Biochim Biophys Acta. 1832;2013:891–6.
14. Tomasek JJ, Gabbiani G, Hinz B, Chaponnier C, Brown RA. Myofibroblasts and mechano-regulation of connective tissue remodelling. Nat Rev Mol Cell Biol. 2002;3:349–63.
15. Nagano M, Hoshino D, Koshikawa N, Akizawa T, Seiki M. Turnover of focal adhesions and cancer cell migration. Int J Cell Biol. 2012;2012:310616.
16. Lo SH. Focal adhesions: what's new inside. Dev Biol. 2006;294:280–91.
17. Huttenlocher A, Horwitz AR. Integrins in cell migration. Cold Spring Harb Perspect Biol. 2011;3:a005074.
18. Sardone F, Santi S, Tagliavini F, Traina F, Merlini L, Squarzoni S, Cescon M, Wagener R, Maraldi NM, Bonaldo P, et al. Collagen VI-NG2 axis in human tendon fibroblasts under conditions mimicking injury response. Matrix Biol. 2016;55:90–105.
19. Soret R, Mennetrey M, Bergeron KF, Dariel A, Neunlist M, Grunder F, Faure C, Silversides DW, Pilon N, Ente-Hirsch Study G. A collagen VI-dependent pathogenic mechanism for Hirschsprung's disease. J Clin Invest. 2015;125: 4483–96.
20. Theocharidis G, Drymoussi Z, Kao AP, Barber AH, Lee DA, Braun KM, Connelly JT. Type VI Collagen Regulates Dermal Matrix Assembly and Fibroblast Motility. J Invest Dermatol. 2016;136:74–83.
21. Ishikawa Y, Vranka J, Wirz J, Nagata K, Bachinger HP. The rough endoplasmic reticulum-resident FKS06-binding protein FKBP65 is a molecular chaperone that interacts with collagens. J Biol Chem. 2008;283:31584–90.
22. Staab-Weijnitz CA, Fernandez IE, Knuppel L, Maul J, Heinzelmann K, Juan-Guardela BM, Hennen E, Preissler G, Winter H, Neurohr C, et al. FK506-Binding Protein 10, a Potential Novel Drug Target for Idiopathic Pulmonary Fibrosis. Am J Respir Crit Care Med. 2015;192:455–67.
23. Knüppel L, Ishikawa Y, Aichler M, Heinzelmann K, Hatz R, Behr J, Walch A, Bachinger HP, Eickelberg O, Staab-Weijnitz CA. A Novel Antifibrotic Mechanism of Nintedanib and Pirfenidone. Inhibition of Collagen Fibril Assembly. Am J Respir Cell Mol Biol. 2017;57:77–90.
24. Undyala VV, Dembo M, Cembrola K, Perrin BJ, Huttenlocher A, Elce JS, Greer PA, Wang YL, Beningo KA. The calpain small subunit regulates cell-substrate mechanical interactions during fibroblast migration. J Cell Sci. 2008;121:3581–8.
25. Mitra SK, Hanson DA, Schlaepfer DD. Focal adhesion kinase: in command and control of cell motility. Nat Rev Mol Cell Biol. 2005;6:56–68.
26. Roskoski R Jr. ERK1/2 MAP kinases: structure, function, and regulation. Pharmacol Res. 2012;66:105–43.
27. Twal WO, Czirok A, Hegedus B, Knaak C, Chintalapudi MR, Okagawa H, Sugi Y, Argraves WS. Fibulin-1 suppression of fibronectin-regulated cell adhesion and motility. J Cell Sci. 2001;114:4587–98.
28. Canty EG, Kadler KE. Procollagen trafficking, processing and fibrillogenesis. J Cell Sci. 2005;118:1341–53.
29. Timpl R, Engel J: Type VI Collagen. In *Biology of extracellular matrix: Structure and function of collagen types*. Edited by Mayne R, Burgeson RE. Orlando: Academic Press; 1987: 105-143, 317 p.
30. Engvall E, Hessle H, Klier G. Molecular assembly, secretion, and matrix deposition of type VI collagen. J Cell Biol. 1986;102:703–10.
31. Argraves WS, Tran H, Burgess WH, Dickerson K. Fibulin is an extracellular matrix and plasma glycoprotein with repeated domain structure. J Cell Biol. 1990;111:3155–64.
32. Liang X, Chai B, Duan R, Zhou Y, Huang X, Li Q. Inhibition of FKBP10 Attenuates Hypertrophic Scarring through Suppressing Fibroblast Activity and Extracellular Matrix Deposition. J Invest Dermatol. 2017;137:2326–35.
33. Osornio-Vargas AR, Kalter VG, Badgett A, Hernandez-Rodriguez N, Aguilar-Delfin I, Brody AR. Early-passage rat lung fibroblasts do not migrate in vitro to transforming growth factor-beta. Am J Respir Cell Mol Biol. 1993;8:468–71.
34. Oberringer M, Meins C, Bubel M, Pohlemann T. In vitro wounding: effects of hypoxia and transforming growth factor beta1 on proliferation, migration and myofibroblastic differentiation in an endothelial cell-fibroblast co-culture model. J Mol Histol. 2008;39:37–47.
35. Poon R, Nik SA, Ahn J, Slade L, Alman BA. Beta-catenin and transforming growth factor beta have distinct roles regulating fibroblast cell motility and the induction of collagen lattice contraction. BMC Cell Biol. 2009;10:38.
36. Pechkovsky DV, Scaffidi AK, Hackett TL, Ballard J, Shaheen F, Thompson PJ, Thannickal VJ, Knight DA. Transforming growth factor beta1 induces alphavbeta3 integrin expression in human lung fibroblasts via a beta3 integrin-, c-Src-, and p38 MAPK-dependent pathway. J Biol Chem. 2008;283: 12898–908.
37. Le Clainche C, Carlier MF. Regulation of actin assembly associated with protrusion and adhesion in cell migration. Physiol Rev. 2008;88:489–513.
38. Carragher NO, Frame MC. Focal adhesion and actin dynamics: a place where kinases and proteases meet to promote invasion. Trends Cell Biol. 2004;14:241–9.
39. Carragher NO, Westhoff MA, Fincham VJ, Schaller MD, Frame MC. A novel role for FAK as a protease-targeting adaptor protein: Regulation by p42 ERK and Src. Current Biology. 2003;13:1442–50.
40. Hanks SK, Ryzhova L, Shin NY, Brabek J. Focal adhesion kinase signaling activities and their implications in the control of cell survival and motility. Front Biosci. 2003;8:d982–96.
41. Webb DJ, Donais K, Whitmore LA, Thomas SM, Turner CE, Parsons JT, Horwitz AF. FAK-Src signalling through paxillin, ERK and MLCK regulates adhesion disassembly. Nat Cell Biol. 2004;6:154–61.
42. Zhao X, Guan JL. Focal adhesion kinase and its signaling pathways in cell migration and angiogenesis. Adv Drug Deliv Rev. 2011;63:610–5.

43. Franco SJ, Rodgers MA, Perrin BJ, Han J, Bennin DA, Critchley DR, Huttenlocher A. Calpain-mediated proteolysis of talin regulates adhesion dynamics. Nat Cell Biol. 2004;6:977–83.
44. Chan KT, Bennin DA, Huttenlocher A. Regulation of adhesion dynamics by calpain-mediated proteolysis of focal adhesion kinase (FAK). J Biol Chem. 2010;285:11418–26.
45. Gvaramia D, Blaauboer ME, Hanemaaijer R, Everts V. Role of caveolin-1 in fibrotic diseases. Matrix Biol. 2013;32:307–15.
46. Nethe M, Hordijk PL. The role of ubiquitylation and degradation in RhoGTPase signalling. J Cell Sci. 2010;123:4011–8.
47. Uetrecht AC, Bear JE. Coronins: the return of the crown. Trends Cell Biol. 2006;16:421–6.
48. Friedl P, Zanker KS, Brocker EB. Cell migration strategies in 3-D extracellular matrix: differences in morphology, cell matrix interactions, and integrin function. Microsc Res Tech. 1998;43:369–78.
49. Mc Henry KT, Montesano R, Zhu S, Beshir AB, Tang HH, Yeung KC, Fenteany G. Raf kinase inhibitor protein positively regulates cell-substratum adhesion while negatively regulating cell-cell adhesion. J Cell Biochem. 2008;103:972–85.
50. Palecek SP, Loftus JC, Ginsberg MH, Lauffenburger DA, Horwitz AF. Integrin-ligand binding properties govern cell migration speed through cell-substratum adhesiveness. Nature. 1997;385:537–40.
51. Liu S, Xu SW, Blumbach K, Eastwood M, Denton CP, Eckes B, Krieg T, Abraham DJ, Leask A. Expression of integrin beta1 by fibroblasts is required for tissue repair in vivo. J Cell Sci. 2010;123:3674–82.
52. Fang KP, Zhang JL, Ren YH, Qian YB. Talin-1 correlates with reduced invasion and migration in human hepatocellular carcinoma cells. Asian Pac J Cancer Prev. 2014;15:2655–61.
53. Nuckolls GH, Romer LH, Burridge K. Microinjection of antibodies against talin inhibits the spreading and migration of fibroblasts. J Cell Sci. 1992; 102(Pt 4):753–62.
54. Albiges-Rizo C, Frachet P, Block MR. Down regulation of talin alters cell adhesion and the processing of the alpha 5 beta 1 integrin. J Cell Sci. 1995; 108(Pt 10):3317–29.
55. Wei X, Sun Y, Wu Y, Zhu J, Gao B, Yan H, Zhao Z, Zhou J, Jing Z. Downregulation of Talin-1 expression associates with increased proliferation and migration of vascular smooth muscle cells in aortic dissection. BMC Cardiovasc Disord. 2017;17:162.
56. Ilic D, Furuta Y, Kanazawa S, Takeda N, Sobue K, Nakatsuji N, Nomura S, Fujimoto J, Okada M, Yamamoto T. Reduced cell motility and enhanced focal adhesion contact formation in cells from FAK-deficient mice. Nature, 544. 1995;377:539.
57. Klinghoffer RA, Sachsenmaier C, Cooper JA, Soriano P. Src family kinases are required for integrin but not PDGFR signal transduction. EMBO J. 1999;18: 2459–71.
58. Westhoff MA, Serrels B, Fincham VJ, Frame MC, Carragher NO. SRC-mediated phosphorylation of focal adhesion kinase couples actin and adhesion dynamics to survival signaling. Mol Cell Biol. 2004;24:8113–33.
59. Asano S, Ito S, Takahashi K, Furuya K, Kondo M, Sokabe M, Hasegawa Y. Matrix stiffness regulates migration of human lung fibroblasts. Physiol Rep. 2017;5
60. Rosentreter A, Hofmann A, Xavier CP, Stumpf M, Noegel AA, Clemen CS. Coronin 3 involvement in F-actin-dependent processes at the cell cortex. Exp Cell Res. 2007;313:878–95.
61. Behrens J, Solga R, Ziemann A, Rastetter RH, Berwanger C, Herrmann H, Noegel AA, Clemen CS. Coronin 1C-free primary mouse fibroblasts exhibit robust rearrangements in the orientation of actin filaments, microtubules and intermediate filaments. Eur J Cell Biol. 2016;95:239–51.
62. Galvez BG, Matias-Roman S, Yanez-Mo M, Vicente-Manzanares M, Sanchez-Madrid F, Arroyo AG. Caveolae are a novel pathway for membrane-type 1 matrix metalloproteinase traffic in human endothelial cells. Mol Biol Cell. 2004;15:678–87.
63. Ge S, Pachter JS. Caveolin-1 knockdown by small interfering RNA suppresses responses to the chemokine monocyte chemoattractant protein-1 by human astrocytes. J Biol Chem. 2004;279:6688–95.
64. Grande-Garcia A, Echarri A, de Rooij J, Alderson NB, Waterman-Storer CM, Valdivielso JM, del Pozo MA. Caveolin-1 regulates cell polarization and directional migration through Src kinase and Rho GTPases. Journal of Cell Biology. 2007;177:683–94.
65. Charras G, Sahai E. Physical influences of the extracellular environment on cell migration. Nat Rev Mol Cell Biol. 2014;15:813–24.
66. Bonaldo P, Braghetta P, Zanetti M, Piccolo S, Volpin D, Bressan GM. Collagen VI deficiency induces early onset myopathy in the mouse: an animal model for Bethlem myopathy. Hum Mol Genet. 1998;7:2135–40.
67. Ishikawa Y, Mizuno K, Bachinger HP. Ziploc-ing the structure 2.0: Endoplasmic reticulum-resident peptidyl prolyl isomerases show different activities toward hydroxyproline. J Biol Chem. 2017;292:9273–82.
68. Ishikawa Y, Bachinger HP. A molecular ensemble in the rER for procollagen maturation. Biochim Biophys Acta. 1833;2013:2479–91.
69. Ducros E, Berthaut A, Mirshahi P, Lemarchand S, Soria J, Legeais JM, Mirshahi M. Expression of extracellular matrix proteins fibulin-1 and fibulin-2 by human corneal fibroblasts. Curr Eye Res. 2007;32:481–90.
70. Colombatti A, Bonaldo P. Biosynthesis of chick type VI collagen. II. Processing and secretion in fibroblasts and smooth muscle cells. J Biol Chem. 1987;262:14461–6.
71. Mak KM, Sehgal P, Harris CK. Type VI Collagen: Its Biology and Value as a Biomarker of Hepatic Fibrosis. Austin Biomarkers & Diagnosis. 2014;1:9.
72. Everts V, Korper W, Niehof A, Jansen I, Beertsen W. Type VI collagen is phagocytosed by fibroblasts and digested in the lysosomal apparatus: involvement of collagenase, serine proteinases and lysosomal enzymes. Matrix Biol. 1995;14:665–76.
73. Kutys ML, Doyle AD, Yamada KM. Regulation of cell adhesion and migration by cell-derived matrices. Exp Cell Res. 2013;319:2434–9.
74. Duran I, Martin JH, Weis MA, Krejci P, Konik P, Li B, Alanay Y, Lietman C, Lee B, Eyre D, et al. A Chaperone Complex Formed by HSP47, FKBP65, and BiP Modulates Telopeptide Lysyl Hydroxylation of Type I Procollagen. J Bone Miner Res. 2017;32:1309–19.
75. Gjaltema RA, van der Stoel MM, Boersema M, Bank RA. Disentangling mechanisms involved in collagen pyridinoline cross-linking: The immunophilin FKBP65 is critical for dimerization of lysyl hydroxylase 2. Proc Natl Acad Sci U S A. 2016;113:7142–7.
76. Schwarze U, Cundy T, Pyott SM, Christiansen HE, Hegde MR, Bank RA, Pals G, Ankala A, Conneely K, Seaver L, et al. Mutations in FKBP10, which result in Bruck syndrome and recessive forms of osteogenesis imperfecta, inhibit the hydroxylation of telopeptide lysines in bone collagen. Hum Mol Genet. 2013;22:1–17.
77. Chung HJ, Steplewski A, Chung KY, Uitto J, Fertala A. Collagen fibril formation. A new target to limit fibrosis. Journal of Biological Chemistry. 2008;283:25879–86.
78. Fleischmajer R, Olsen BR, Timpl R, Perlish JS, Lovelace O. Collagen fibril formation during embryogenesis. Proc Natl Acad Sci U S A. 1983;80:3354–8.
79. Fleischmajer R, Timpl R, Tuderman L, Raisher L, Wiestner M, Perlish JS, Graves PN. Ultrastructural identification of extension aminopropeptides of type I and III collagens in human skin. Proc Natl Acad Sci U S A. 1981;78: 7360–4.
80. Romanic AM, Adachi E, Kadler KE, Hojima Y, Prockop DJ. Copolymerization of pNcollagen III and collagen I. pNcollagen III decreases the rate of incorporation of collagen I into fibrils, the amount of collagen I incorporated, and the diameter of the fibrils formed. J Biol Chem. 1991;266: 12703–9.

2.3 Novel Antifibrotic Mechanism of Nintedanib and Pirfenidone: Inhibition of Collagen Fibril Assembly

This publication directly compares the effects of nintedanib and pirfenidone on phLF, two recently approved IPF drugs with not fully elucidated mechanisms of actions. Within this publication the effects on collagen biosynthesis and maturation of both drugs in donor and IPF fibroblasts were analyzed. Fibrotic marker expression was reduced by both drugs, however nintedanib was more effective than pirfenidone in regards of used concentrations and efficacy. Additionally, we were able to reveal a new mechanism of action, the inhibition of collagen fibril formation by both drugs. Nintedanib and pirfenidone altered the appearance of collagen fibrils.

Contribution:
The author of this thesis contributed to conception and design of this study, to the experimental work, analysis and interpretation as well as drafting the manuscript and the intellectual content.

Knüppel L, Ishikawa Y, Aichler M, Heinzelmann K, Hatz R, Behr J, Walch A, Bächinger HP, Eickelberg O, Staab-Weijnitz CA. Novel Antifibrotic Mechanism of Nintedanib and Pirfenidone: Inhibition of Collagen Fibril Assembly. *American Journal of Respiratory Cell and Molecular Biology*, 2017. 57(1): p. 77-90.

The *American Journal of Respiratory Cell and Molecular Biology* is an official journal of the American Thoracic Society.

ORIGINAL RESEARCH

A Novel Antifibrotic Mechanism of Nintedanib and Pirfenidone
Inhibition of Collagen Fibril Assembly

Larissa Knüppel[1], Yoshihiro Ishikawa[2,3], Michaela Aichler[4], Katharina Heinzelmann[1], Rudolf Hatz[5,6], Jürgen Behr[6,7], Axel Walch[4], Hans Peter Bächinger[2,3], Oliver Eickelberg[1,8], and Claudia A. Staab-Weijnitz[1]

[1]Comprehensive Pneumology Center, and [4]Research Unit Analytical Pathology, Helmholtz-Zentrum München, Munich, Germany; [2]Department of Biochemistry and Molecular Biology, Oregon Health and Science University, Portland, Oregon; [3]Research Department, Shriners Hospital for Children, Portland, Oregon; [5]Thoraxchirurgisches Zentrum, Klinik für Allgemeine-, Viszeral-, Transplantations-, Gefäß- und Thoraxchirurgie, Klinikum Großhadern, and [7]Medizinische Klinik und Poliklinik V, Klinikum der Ludwig-Maximilians-Universität, Ludwig-Maximilians-Universität, Munich, Germany; [6]Asklepios Fachkliniken München-Gauting, Munich, Germany; and [8]Pulmonary and Critical Care Medicine University, Colorado Anschutz Medical Campus, Denver, Colorado

ORCID ID: 0000-0002-1211-7834 (C.A.S.-W.).

Abstract

Idiopathic pulmonary fibrosis (IPF) is characterized by excessive deposition of extracellular matrix, in particular, collagens. Two IPF therapeutics, nintedanib and pirfenidone, decelerate lung function decline, but their underlying mechanisms of action are poorly understood. In this study, we sought to analyze their effects on collagen synthesis and maturation at important regulatory levels. Primary human fibroblasts from patients with IPF and healthy donors were treated with nintedanib (0.01–1.0 μM) or pirfenidone (100-1,000 μM) in the absence or presence of transforming growth factor-β1. Effects on collagen, fibronectin, FKBP10, and HSP47 expression, and collagen I and III secretion, were analyzed by quantitative polymerase chain reaction and Western blot. The appearance of collagen fibrils was monitored by scanning electron microscopy, and the kinetics of collagen fibril assembly was assessed using a light-scattering approach. In IPF fibroblasts, nintedanib reduced the expression of collagen I and V, fibronectin, and FKBP10 and attenuated the secretion of collagen I and III. Pirfenidone also down-regulated collagen V but otherwise showed fewer and less pronounced effects. By and large, the effects were similar in donor fibroblasts. For both drugs, electron microscopy of IPF fibroblast cultures revealed fewer and thinner collagen fibrils compared with untreated controls. Finally, both drugs dose-dependently delayed fibril formation of purified collagen I. In summary, both drugs act on important regulatory levels in collagen synthesis and processing. Nintedanib was more effective in down-regulating profibrotic gene expression and collagen secretion. Importantly, both drugs inhibited collagen I fibril formation and caused a reduction in and an altered appearance of collagen fibril bundles, representing a completely novel mechanism of action for both drugs.

Keywords: idiopathic pulmonary fibrosis; extracellular matrix; nintedanib; pirfenidone

Clinical Relevance

Accumulation of extracellular matrix, mainly collagen, is a main feature of idiopathic pulmonary fibrosis (IPF). Nintedanib and pirfenidone, two recently approved therapeutics for IPF, decelerate disease progression, but their antifibrotic mechanisms of action are incompletely understood. To the best of our knowledge, this study provides the first evidence for the inhibition of collagen fibril formation as a major mechanism of action for nintedanib and pirfenidone and puts forward extracellular collagen self-assembly as a druggable target in IPF.

(Received in original form July 12, 2016; accepted in final form March 3, 2017)

This work was supported by the Helmholtz Association, the German Center for Lung Research, and the Shriners Hospital for Children (Grant No. 85100).

Author Contributions: Conception and design: L.K., Y.I., K.H., R.H., J.B., A.W., H.P.B., O.E., and C.A.S.-W.; experimental work, analysis, and interpretation: L.K., Y.I., M.A., H.P.B., and C.A.S.-W.; and drafting of the manuscript and revision for intellectual content: L.K., Y.I., M.A., H.P.B., O.E., and C.A.S.-W.

Correspondence and requests for reprints should be addressed to: Claudia A. Staab-Weijnitz, Ph.D., Comprehensive Pneumology Center, Ludwig-Maximilians-Universität and Helmholtz Zentrum München, Max-Lebsche-Platz 31, 81377 München, Germany. E-mail: staab-weijnitz@helmholtz-muenchen.de

This article has an online data supplement, which is accessible from this issue's table of content online at www.atsjournals.org

Am J Respir Cell Mol Biol Vol 57, Iss 1, pp 77–90, Jul 2017

Originally Published in Press as DOI: 10.1165/rcmb.2016-0217OC on March 3, 2017
Internet address: www.atsjournals.org

Idiopathic pulmonary fibrosis (IPF) is a progressive and fatal interstitial lung disease with a median survival of 3–5 years after diagnosis (1). The underlying pathogenic processes are poorly understood, but the aberrant fibrotic response is likely initiated by repeated microinjuries to the airway and the alveolar epithelium (2). This leads to the secretion of fibrotic mediators, including transforming growth factor β (TGF-β), which results in the accumulation of myofibroblasts in alveolar regions. Multiple progenitor cells may contribute to the myofibroblast population, but the most well-established source is the interstitial fibroblast (3). Myofibroblasts synthesize and deposit excessive amounts of extracellular matrix (ECM) proteins, such as collagen type I, III, and V, and fibronectin (4). The resulting accumulation of ECM in the alveolar region is the ultimate pathological feature of lung fibrosis, leading to progressive lung function decline (5).

A recent study highlights that collagens are the main components of newly synthesized ECM in lung fibrosis (6), but large-scale quantitative proteome approaches have also demonstrated that the ECM composition (the matrisome) is far more complex than previously assumed (7). In addition, the complexity of collagen biosynthesis and maturation is rarely taken into account in mechanistic studies of the evaluation of antifibrotic strategies. Collagen modification and folding in the rough endoplasmic reticulum (rER) requires several enzymes and molecular chaperones essential for post-translational modifications (PTMs) and the processing of procollagen into triple helices, where one of the rate-limiting steps is the *cis-trans* isomerization of proline residues catalyzed by rER resident peptidyl prolyl isomerases (8). Collagen triple helix formation is followed by its secretion, extracellular fibril formation, and fiber assembly (9). Two endoplasmic reticulum proteins participating in this multistep process are the collagen chaperones FK506-binding protein 10 (FKBP10, also called FKBP65) and heat-shock protein 47 (HSP47, also called SerpinH1) (9). Notably, both FKBP10 and HSP47 are up-regulated in bleomycin-induced lung fibrosis and in IPF (10, 11). Secretion of procollagen from HSP47-deficient fibroblasts is reduced compared with control cells (12) and similarly, knockdown of FKBP10 in IPF fibroblasts decreases collagen type I synthesis and secretion (10). In addition, PTMs such as hydroxylation of lysyl or prolyl residues, or glycosylation of hydroxylysines, are essential for proper stability, assembly, and secretion of procollagen, as well as for the final supramolecular structure of these molecules (13). For example, hydroxylation of proline residues on position three (3-Hyp) might play a role in inter-triple-helical interactions and probably assists in the assembly of supramolecular collagen and lateral fibril growth (14, 15).

Nintedanib and pirfenidone were approved recently for IPF therapy, because both drugs have been shown to slow down disease progression as measured by reduced lung function decline. Despite their widespread application in IPF in recent times, their mechanisms of action are poorly understood and remain to be fully elucidated (16, 17). Nintedanib, originally developed as an anticancer drug, is a receptor tyrosine kinase inhibitor of platelet-derived growth factor receptor, fibroblasts growth factor receptor, and vascular endothelial growth factor receptor, all of which play important roles in the pathogenesis of IPF (5). Pirfenidone is an antifibrotic, antiinflammatory, and antioxidant compound with beneficial effects in lung, hepatic, kidney, and cardiac fibrosis, but its direct targets are unknown (18, 19, 20). Several studies have investigated the effects of either nintedanib or pirfenidone on collagen type I expression or secretion in several cell types (10, 21–26). No study to date, however, has directly compared both drugs on the multiple stages of intracellular collagen synthesis and extracellular maturation in the relevant cell type (i.e., the primary human lung fibroblast).

Therefore, the aim of our study was to comprehensively assess and directly compare the effects of nintedanib and pirfenidone on the different steps of collagen synthesis and maturation in primary human lung fibroblasts (phLF) from patients with IPF and healthy donors. We analyzed the expression of various collagens and the collagen chaperones *FKBP10* and *HSP47*, as well as collagen secretion in IPF and healthy phLF. In addition, we examined the effects of both drugs on the levels of selected PTMs of collagen in IPF fibroblasts and on collagen fibril formation.

Materials and Methods

For more details on materials and methods, *see* the online supplement. Statistical analysis was performed in GraphPadPrism 7.02 (GraphPad Software, San Diego, CA).

MTT Cytotoxicity Assay

See the online supplement.

Human Lung Material and Culture of phLF

Primary human lung fibroblasts, isolated from human lung explant material of patients with IPF or healthy donors, were obtained from the BioArchive CPC-M for lung diseases at the Comprehensive Pneumology Center (CPC, Munich, Germany). All participants gave written informed consent, and the study was approved by the local ethics committee of the Ludwig-Maximilians University of Munich, Germany. Isolation of phLF was performed as described previously (10). For more details, *see* the online supplement.

Cotreatment of IPF and Donor phLF with TGF-β1 and Nintedanib or Pirfenidone

Cells were seeded at a density of 20,000–25,000 cells/cm^2, followed by starvation for 24 hours in starvation medium (Dulbecco's modified Eagle medium/F12, 0.5% fetal bovine serum, penicillin/streptomycin, 0.1 mM 2-phospho-L-ascorbic acid). Subsequently, cells were treated with or without TGF-β1 (2 ng/ml) (R&D Systems, Minneapolis, MN) and with nintedanib (0.01 μM, 0.1 μM, 1.0 μM) or pirfenidone (100 μM, 500 μM, 1,000 μM) (both Selleck, Houston, TX) for 48 hours in starvation medium. Nintedanib and pirfenidone were dissolved in dimethyl sulfoxide. The final dimethyl sulfoxide concentration in the medium was always 1%.

RNA Isolation and Real-Time Quantitative Reverse-Transcriptase Polymerase Chain Reaction Analysis

See the online supplement.

Protein Isolation and Western Blot Analysis

See the online supplement.

Quantification of Secreted Collagen

Collagen I and III were precipitated from cell culture supernatant of cultured IPF and donor phLF as described previously (10). For more details, *see* the online supplement.

Collagen Precipitation and Analysis of PTM

See the online supplement.

Scanning Electron Microscopy for Assessment of Fibrils in the ECM of phLF

IPF phLF were grown on glass slides, treated with nintedanib (1 μM) or pirfenidone (1,000 μM) in combination with TGF-β1 (2 ng/ml) for 48 hours and fixed with paraformaldehyde and glutaraldehyde, 3% each, in 0.1% sodium cacodylate buffer pH 7.4 (Electron Microscopy Sciences, Munich, Germany). The specimens were dehydrated in gradual ethanol and dried by the critical-point method, using CO_2 as the transitional fluid (Polaron Critical Point Dryer CPC E3000; Quorum Technologies, Ringmer, UK). Specimens were sputter coated with a thin layer of platinum by a sputtering device (Emitech K575; Quorum Technologies) and observed by scanning electron microscopy (JSM 6300F; JEOL, Eching, Germany). Fibril thickness was assessed by measuring the diameter of the smallest unit of fiber forming fibrils, using the length measurement tool of the open source software ImageJ 1.50i (W.S. Rasband, National Institutes of Health, Bethesda, MD).

Collagen I Fibril Formation Assay

This assay was performed essentially as described previously (27). For more details, *see* the online supplement.

Results

Applied Concentrations of Nintedanib and Pirfenidone Were Well Tolerated by IPF phLF

For *in vitro* experiments, we selected a range of nintedanib and pirfenidone concentrations similar to those used in published studies (22, 23, 25). Notably, for pirfenidone, in an effort to adhere to physiologically relevant concentrations, we used 1,000 μM as the highest concentration, although others have used pirfenidone in concentrations of up to 10 mM in similar experiments (21, 26, 28). Initially, we analyzed the effect of increasing doses of nintedanib (0.01–1 μM) and pirfenidone (100-1,000 μM) on the viability of IPF fibroblasts in an MTT assay. The used concentrations of nintedanib and pirfenidone were well tolerated for the treatment period of 48 hours (*see* Figure E1 in the online supplement).

Nintedanib Reduced the Expression and Secretion of ECM Components More Effectively Than Did Pirfenidone in phLF

Next, we assessed the effect of different concentrations of both drugs on the expression and secretion of collagen I (*COL1A1*), III (*COL3A1*), V (*COL5A1*), fibronectin 1 (*FN1*), and plasminogen activator inhibitor 1 (*PAI-1*) in lysates and cell culture supernatants from primary human IPF and donor fibroblasts. Nintedanib consistently down-regulated transcript and protein levels of basal and TGF-β1–induced collagen I in IPF phLF (Figures 1A, 1C, 1E, and 1G). Pirfenidone reduced TGF-β1–induced *COL1A1* transcripts only marginally (Figures 1A and 1C), and collagen I protein remained largely unchanged (Figures 1E and 1G). Similar tendencies were observed in phLF isolated from healthy donor lungs (Figures 1B, 1D, and 1F), with the exception of *COL1A1* transcript (Figure 1B) and levels of basal secreted collagen I (Figure 1H), which both, in contrast to IPF, appeared unaffected by nintedanib in donor fibroblasts.

Similarly, the expression of collagen III was consistently down-regulated by nintedanib in IPF fibroblasts on transcript and protein levels, whereas pirfenidone merely regulated *COL3A1* transcripts, an effect which again did not translate to protein level (Figures 2A, 2C, and 2E). Interestingly, in donor fibroblasts, nintedanib increased and pirfenidone decreased *COL3A1* transcription (Figures 2B and 2D), whereas the amount of secreted collagen III remained largely unchanged or even tended to anticorrelate with transcript levels (Figure 2F).

As for collagen V, TGF-β1–induced collagen V was significantly reduced in IPF fibroblasts by both drugs, an effect that was captured only partly at the transcript level (Figures 3A, 3C, and 3E); similar trends were observed in donor phLF (Figures 3B, 3D, and 3F).

Expression of *FN1* was consistently decreased by nintedanib on transcript and protein levels, in both IPF and donor fibroblasts (Figure E2). In contrast, pirfenidone reduced *FN1* mRNA, but not protein levels, in IPF fibroblasts (Figures E2A, E2C, and E2E) and had no significant effect in donor phLF (Figures E2B, E2D, and E2F). Interestingly, pirfenidone actually showed a trend to increase FN1 protein levels in both IPF and donor phLF (Figures E2E and E2F). Expression of *PAI-1*, a classic TGF-β–induced gene, was reduced significantly by nintedanib in IPF and donor fibroblasts, with a more pronounced effect in the absence of TGF-β1 (Figure E3). Pirfenidone did not affect *PAI-1* expression.

In summary, in comparison with nintedanib, pirfenidone showed fewer effects on collagen expression and secretion and *FN1* and *PAI-1* expression. Notably, exceeding the effective concentration of nintedanib at by least 500 times, a concentration of 500 to 1,000 μM pirfenidone was necessary to achieve significant effects (e.g., on collagen I, III, and V and *FN1* expression) in TGF-β1–treated IPF fibroblasts (Figures 1A, 2A, 3E, and E2A).

Nintedanib, but Not Pirfenidone, Reduces the Expression of the Collagen Chaperone FKBP10 in IPF Fibroblasts

Next, we investigated the effects of nintedanib and pirfenidone on the expression of *FKBP10* and *HSP47*, two collagen I chaperones. Nintedanib moderately, but significantly, down-regulated protein levels of FKBP10 in mock- as well as in TGF-β1–treated IPF fibroblasts (Figure 4E). This effect was already visible on the transcript level for TGF-β–treated samples (Figures 4A and 4C). In contrast, pirfenidone did not influence *FKBP10* expression in IPF fibroblasts (Figures 4A, 4C, and 4E). Interestingly, clearly different results were obtained with donor fibroblasts here, where nintedanib failed to regulate *FKBP10* expression, and pirfenidone down-regulated *FKBP10* transcript but up-regulated FKBP10 protein levels (Figures 4B, 4D, and 4F). Regarding the expression of the major collagen I chaperone HSP47, neither drug reduced HSP47 protein levels in phLF (Figures 5E and 5F), even if both therapeutics decreased basal *HSP47* mRNA (Figures 5A–5D).

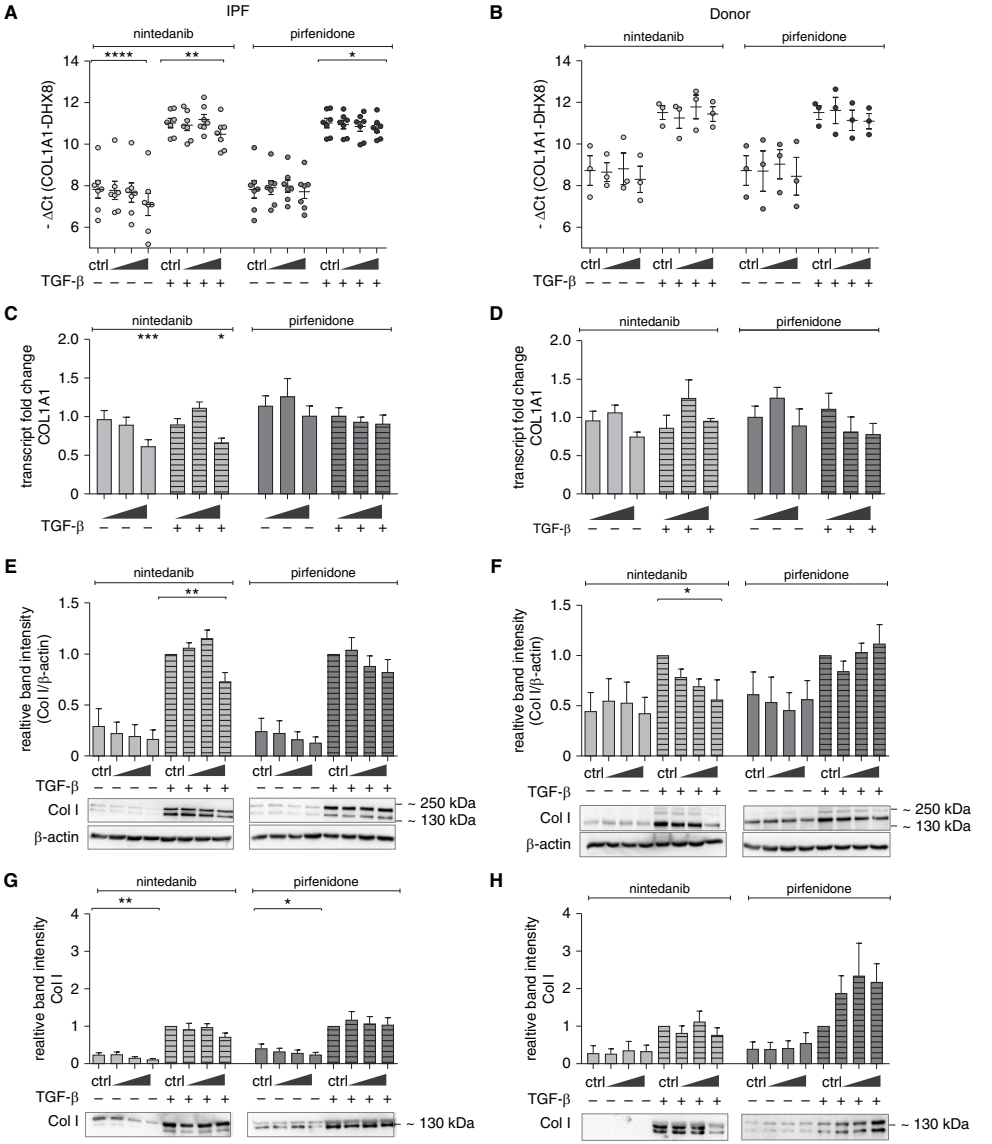

Figure 1. Nintedanib decreases collagen I expression and secretion more potently than does pirfenidone in idiopathic pulmonary fibrosis (IPF) fibroblasts. (*A–D*) Quantitative RT-PCR analysis of primary human lung fibroblasts (phLF) isolated from (*A* and *C*) patients with IPF or (*B* and *D*) healthy donors treated for 48 hours with increasing concentrations of nintedanib (0.01, 0.1, and 1 μM) or pirfenidone (100, 500, and 1,000 μM) in the absence or presence of transforming growth factor β (TGF-β) 1 (2 ng/ml). Transcript levels of *COL1A1* are shown as −ΔCt values (*A* and *B*) as well as transcript fold changes (*C* and *D*) to show the effect normalized to control (ctrl). DEAH (Asp-Glu-Ala-His) box polypeptide 8 (*DHX8*) was used as endogenous control. Data are based on

Selected Post-Translational Modifications of Collagen I Are Not Affected by Nintedanib or Pirfenidone

PTMs have a major impact on essential collagen properties such as the three-dimensional structure, thermodynamic stability, and biological functions (13, 14, 15), but, to date, whether antifibrotic drugs affect the PTMs of collagen secreted by IPF fibroblasts has not been assessed. Here, we tested whether nintedanib and pirfenidone affected the levels of selected PTMs of collagen I. More specifically, we compared the levels of prolyl-3-hydroxylation of the A1 site (Pro-986) and the A3 site (Pro-707) of the collagen α1 chain (15), prolyl-3-hydroxylation of the A3 site (Pro-707) of the collagen α2 chain and, finally, the glycosylation site of hydroxylysine (Lys-174) of collagen type I. Neither drug appeared to affect the levels of the assessed PTMs (Figure E4).

Nintedanib and Pirfenidone Affect Collagen Fibril Formation in IPF Fibroblasts

Scanning electron microscopy was used to assess the number, morphology, and thickness of extracellular fibrils formed in cultures of TGF-β1–treated IPF fibroblasts in the absence and presence of nintedanib or pirfenidone. Extracellular collagen fibers were identified as unbranched and dense bundles of thread-like–looking twisted fibrils of variable length, which were oriented randomly, and with a maximal diameter of 1 μm (Figure 6A) (29, 31). Cell cultures that had been treated with 1.0 μM nintedanib or 1.0 mM pirfenidone displayed a markedly reduced number of fibers and changes in overall fiber structure. In the presence of both drugs, fibers were shorter overall and showed a more frayed appearance than in control samples, and the fibril thickness was significantly reduced in nintedanib- and pirfenidone-treated samples compared with control fibrils (Figure 6B).

Nintedanib and Pirfenidone Inhibit Spontaneous Collagen I Fibril Formation

It seemed unlikely that the effects on collagen fibril formation observed by scanning electron microscopy could be accounted for by the effects of both drugs on collagen synthesis and secretion only, in particular in the case of pirfenidone. Therefore, we investigated the direct effect of both drugs on spontaneous collagen I fibril formation in a light-scattering approach. This assay is a well-established method of studying the formation of collagen fibrils in a solution of purified soluble collagen I. It relies on the principle that collagen I, dissolved initially in dilute acid, spontaneously forms fibrils on neutralization in a self-driven process. The resulting fibrils are similar to those formed *in vivo*, and the process can be visualized by dynamic light scattering at 313 nm (30, 31). We found that both therapeutics were able to considerably delay fibril formation of purified collagen I already at micromolar concentrations in a dose-dependent manner (Figure 7 and Table 1).

Discussion

In this study, we demonstrated that nintedanib and pirfenidone affect collagen synthesis and maturation on several regulatory levels, including the inhibition of collagen gene expression, collagen secretion, and, most importantly, fibril formation. In terms of intracellular regulation of the synthesis of ECM components and collagen secretion, nintedanib was clearly more effective, because it (*1*) exerted its effects at substantially lower concentrations (up to 1,000-fold) than did pirfenidone, (*2*) affected the expression and secretion of more ECM and ECM-related genes (i.e., fibronectin, FKBP10, and collagen I), and (*3*) showed more consistent effects on transcript and protein levels. With few exceptions, these effects were mostly similar in IPF and donor fibroblasts. Importantly, both drugs strongly inhibited extracellular fibril formation, and assessment of spontaneous fibril assembly using purified collagen I indicated that both drugs directly inhibited this process with comparable efficiency.

Both nintedanib and pirfenidone inhibited TGF-β–induced transcription of *COL1A1*, *COL3A1*, and *FN1*. In agreement, previous reports by others have shown that nintedanib and pirfenidone counteract TGF-β signaling and down-regulate these TGF-β target genes (23, 24, 32). Although pirfenidone showed these effects only in the presence of exogenously added TGF-β1, nintedanib also affected basal levels of *COL1A1* in IPF fibroblasts and basal levels of another TGF-β target gene, *PAI-1*, in both IPF and donor fibroblasts (Figures 1A and E3). The platelet-derived growth factor receptor (PDGFR) and the fibroblast growth factor receptor are known targets of the receptor tyrosine kinase inhibitor nintedanib, and this might reflect the inhibition of autocrine platelet-derived growth factor or fibroblast growth factor signaling, which has been shown to regulate collagen gene expression (5, 33, 34) via both the ERK and the PI3K/Akt signaling pathways (35). In agreement, phosphorylation of Akt was decreased in

Figure 1. (Continued). seven (IPF) or three (donor) completely independent experiments and are presented as mean ± SEM. Statistical significance between control and different concentrations of nintedanib or pirfenidone is indicated by *horizontal brackets* and *asterisks* for −ΔCt values and by *asterisks* only for fold changes relative to 1. (*E* and *F*) Western blot analysis of phLF isolated from (*E*) patients with IPF or (*F*) donors treated for 48 hours with increasing concentrations of nintedanib (0.01, 0.1, and 1 μM) or pirfenidone (100, 500, and 1,000 μM) in the absence or presence of TGF-β1 (2 ng/ml). Densitometric analysis and representative blots show the effect of nintedanib and pirfenidone on collagen I (Col I) protein expression relative to β-actin as loading control. Data are based on eight (IPF) or three (donor) completely independent experiments and are presented as mean ± SEM. Statistical significance between control and different concentrations of nintedanib or pirfenidone is indicated by *horizontal brackets* and *asterisks*. (*G* and *H*) Western blot analysis of secreted Col I precipitated from cell culture supernatant of (*G*) IPF or (*H*) donor fibroblasts treated for 48 hours with increasing concentrations of nintedanib (0.01, 0.1, and 1 μM) or pirfenidone (100, 500, and 1,000 μM) in the absence or presence of TGF-β1 (2 ng/ml). Densitometric analysis and representative blots show the effects of nintedanib and pirfenidone on secreted Col I after 48 hours. Data are based on seven (IPF) or three (donor) completely independent experiments and are given as mean ± SEM. Statistical significance between control and different concentrations of nintedanib or pirfenidone is indicated by *horizontal brackets* and *asterisks*. Statistical analysis was performed by one-way analysis of variance (post-test, Bonferroni's multiple comparison test: comparison against control). $^{*}P < 0.1$, $^{**}P < 0.01$, $^{***}P < 0.001$, $^{****}P < 0.0001$. The well-known effect of TGF-β1 on these transcripts and proteins was significant, but it is not specified in the interest of clarity.

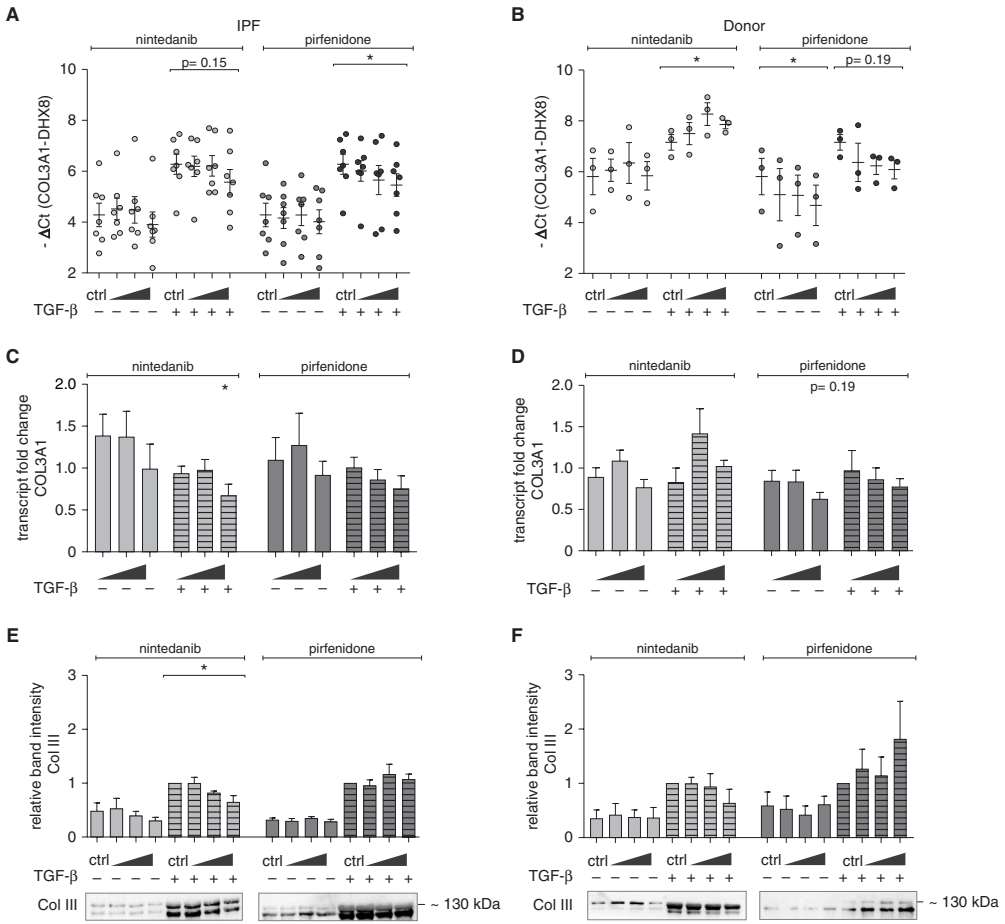

Figure 2. *COL3A1* transcription is decreased by nintedanib in IPF fibroblasts and increased in donor fibroblasts, whereas collagen III (Col III) secretion is decreased in both. (*A–D*) Quantitative RT-PCR analysis of phLF isolated from (*A* and *C*) patients with IPF or (*B* and *D*) healthy donors treated for 48 hours with increasing concentrations of nintedanib (0.01, 0.1, and 1 μM) or pirfenidone (100, 500, and 1,000 μM) in the absence or presence of TGF-β1 (2 ng/ml). Transcript levels of *COL3A1* are shown as −ΔCt values (*A* and *B*) as well as transcript fold changes (*C* and *D*) to show the effect normalized to control. *DHX8* was used as endogenous control. Data are based on seven (IPF) or three (donor) completely independent experiments and are given as mean ± SEM. Statistical significance between control and different concentrations of nintedanib or pirfenidone is indicated by *horizontal brackets* and *asterisks* for −ΔCt values and by *asterisks* only for fold changes relative to 1. The well-known effect of TGF-β1 on these transcripts was significant, but it is not specified in the interest of clarity. (*E* and *F*) Western blot analysis of secreted Col III precipitated from cell culture supernatant of (*E*) IPF or (*F*) donor fibroblasts after treatment of phLF isolated from patients with IPF treated for 48 hours with increasing concentrations of nintedanib (0.01, 0.1, and 1 μM) or pirfenidone (100, 500, and 1,000 μM) in the absence or presence of TGF-β1 (2 ng/ml). Densitometric analysis and representative blots show the effects of nintedanib and pirfenidone on secreted Col III after 48 hours. Data are based on seven (IPF) or three (donor) completely independent experiments and are given as mean ± SEM. Statistical significance between control and different concentrations of nintedanib or pirfenidone is indicated by *horizontal brackets* and *asterisks*. Statistical analysis was performed by one-way analysis of variance (posttest, Bonferroni's multiple comparison test: comparison against control). *$P < 0.1$.

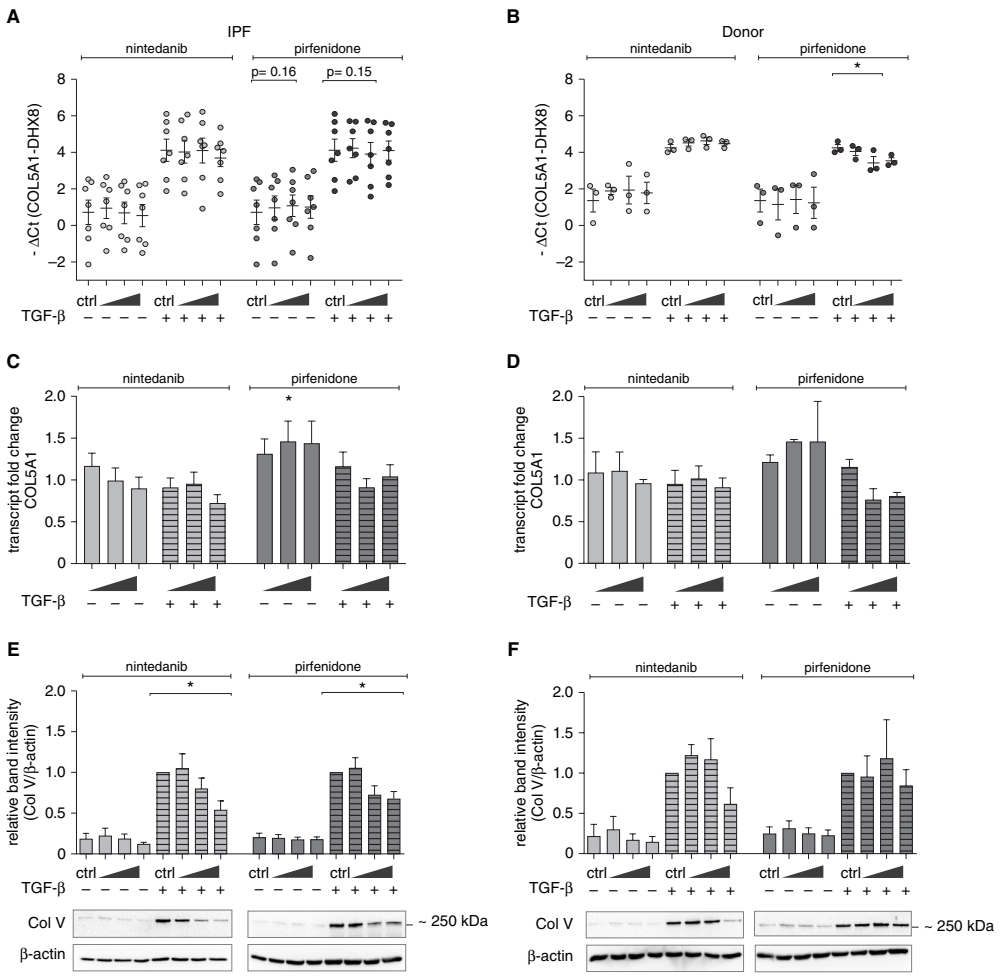

Figure 3. Nintedanib and pirfenidone down-regulate collagen V (Col V). (*A–D*) Quantitative RT-PCR analysis of phLF isolated from (*A* and *C*) patients with IPF or (*B* and *D*) healthy donors treated for 48 hours with increasing concentrations of nintedanib (0.01, 0.1, and 1 μM) or pirfenidone (100, 500, and 1,000 μM) in the absence or presence of TGF-β1 (2 ng/ml). Transcript levels of (*A* and *C*) IPF and (*B* and *D*) donor phLF of *COL5A1* are shown as −ΔCt values (*A* and *B*) as well as transcript fold changes (*C* and *D*) to show the effect normalized to control (ctrl). *DHX8* was used as endogenous control. Data are based on seven (IPF) or three (donor) completely independent experiments and are given as mean ± SEM. Statistical significance between control and different concentrations of nintedanib or pirfenidone is indicated by *horizontal brackets* and *asterisks* for −ΔCt values and by *asterisks* only for fold changes relative to 1. (*E* and *F*) Western blot analysis of phLF isolated from (*E*) patients with IPF or (*F*) healthy donors treated for 48 hours with increasing concentrations of nintedanib (0.01, 0.1, and 1 μM) or pirfenidone (100, 500, and 1,000 μM) in the absence or presence of TGF-β1 (2 ng/ml). Densitometric analysis and representative blots show the effect of nintedanib and pirfenidone on Col V protein expression relative to β-actin. Data are based on eight (IPF) or three (donor) completely independent experiments and are given as mean ± SEM. Statistical significance between control and different concentrations of nintedanib or pirfenidone is indicated by *horizontal brackets* and *asterisks*. Statistical analysis was performed by one-way analysis of variance (posttest, Bonferroni's multiple comparison test: comparison against control). *$P < 0.1$. The well-known effect of TGF-β1 on these transcripts and proteins was significant, but it is not specified in the interest of clarity.

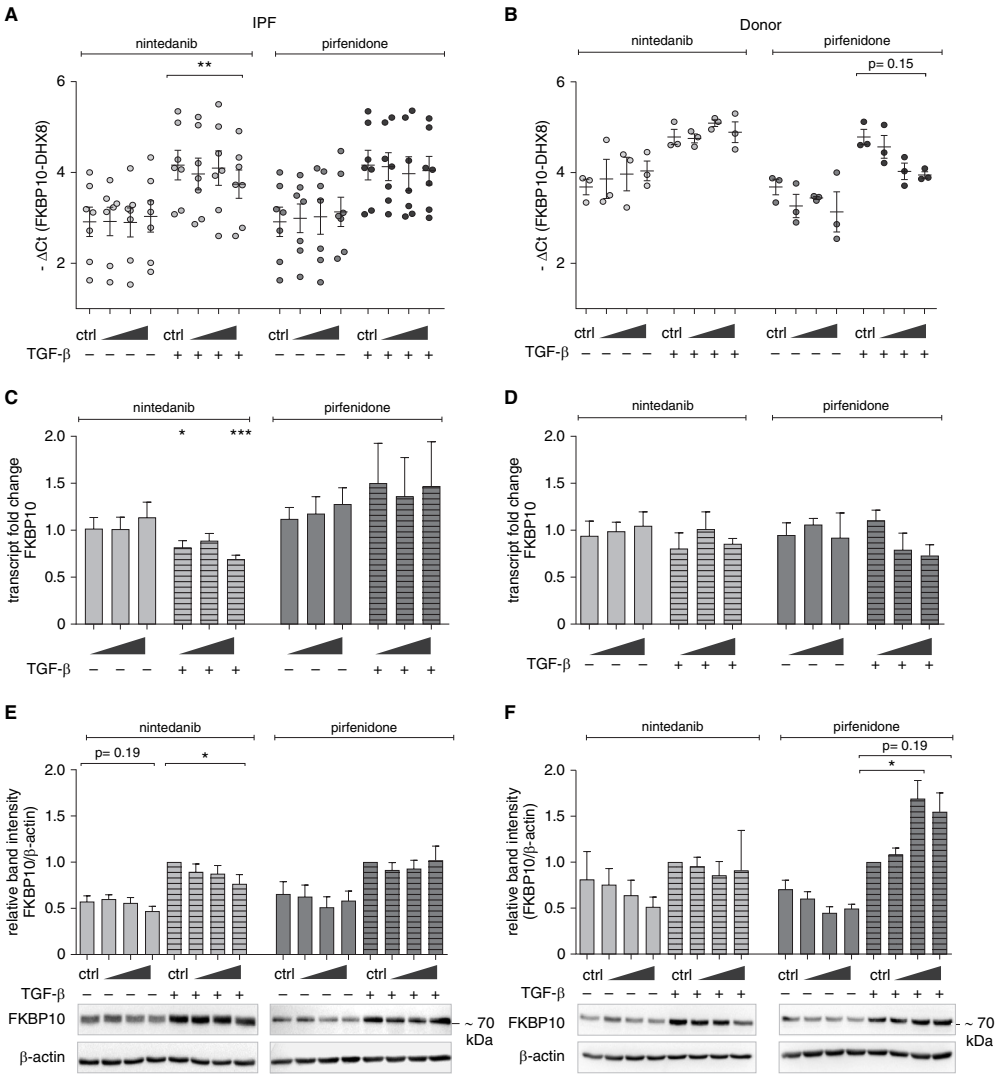

Figure 4. Expression of the collagen chaperone FKBP10 is consistently down-regulated by nintedanib in IPF but regulated more dynamically by pirfenidone in donor fibroblasts. (*A–D*) Quantitative RT-PCR analysis of phLF isolated from (*A* and *C*) patients with IPF or (*B* and *D*) healthy donors treated for 48 hours with increasing concentrations of nintedanib (0.01, 0.1, and 1 μM) or pirfenidone (100, 500, and 1,000 μM) in the absence or presence of TGF-β1 (2 ng/ml). Transcript levels of (*A* and *C*) IPF and (*B* and *D*) donor phLF of *FKBP10* are shown as −ΔCt values (*A* and *B*) as well as transcript fold changes (*C* and *D*) to show the effect normalized to control. *DHX8* was used as endogenous control. Data are based on seven (IPF) or three (donor) completely independent experiments and are given as mean ± SEM. Statistical significance between control and different concentrations of nintedanib or pirfenidone is indicated by *horizontal brackets* and *asterisks* for −ΔCt values and by *asterisks* only for fold changes relative to 1. (*E* and *F*) Western blot analysis of phLF isolated from (*E*) patients with IPF or (*F*) healthy donors treated for 48 hours with increasing concentrations of nintedanib (0.01, 0.1, and 1 μM) or pirfenidone (100, 500, and 1,000 μM) in the absence or presence of TGF-β1

response to nintedanib in all our experiments (Figures E5A and E5B). In contrast, phosphorylation of ERK was not consistently changed, either in IPF or in donor fibroblasts (Figures E5C and E5D). In light of the time point studied (48 h after treatment start), this argues for a stronger and more sustained inhibition of the PI3K/Akt signaling pathway by nintedanib in our studies. Inhibition of PDGFR signaling, however, cannot explain all our *in vitro* results, because a previous study from our laboratory (34) found that small interfering RNA–mediated down-regulation of PDGFR-α actually increased levels of collagen V drastically in primary human lung fibroblasts, which is in contrast to what we observed in the presence of nintedanib.

It is striking that many of the observed effects translated to the protein level only in the presence of nintedanib, but not pirfenidone. For instance, both drugs inhibit TGF-β–induced *COL1A1*, *COL3A1*, and *FN1* transcription, whereas the levels of collagen I protein, secreted collagen III, and fibronectin protein were reduced only by nintedanib in IPF fibroblasts (Figures 1, 2, and E2). These results suggest that post-transcriptional regulation mechanisms are affected differently by the drugs and highlight the importance of analysis at the protein level in this context. Nevertheless, other studies have reported effects of pirfenidone on collagen I and/or fibronectin protein levels in normal phLF (26), alveolar epithelial cells (21), and nasal polyp fibroblasts (28). These discrepancies, however, may be the result of the use of substantially higher concentrations of pirfenidone in those studies (1.6–10 mM). Notably, during standard treatment with pirfenidone of patients with IPF (three daily doses of 801 mg pirfenidone), serum levels of pirfenidone do not exceed 100 μM (36), a concentration at which we did not observe any effect on phLF gene expression.

Both nintedanib and pirfenidone significantly down-regulated collagen V in IPF fibroblasts, and a similar trend was observed in donor fibroblasts (Figures 3E and 3F). To our knowledge, down-regulation of collagen V levels in response to nintedanib or pirfenidone has not been reported before. Type V collagen is a minor component of collagen type I fibrils that plays an important role in fibrogenesis and regulation of fiber size (37–39). In IPF lungs, collagen V is heavily overexpressed compared with that in normal lungs (38). Importantly, in the context of the observed effects on fibril thickness (Figure 6B), collagen V has been shown to be crucial for the initiation of collagen fibril assembly (39). Therefore, down-regulation of collagen V by both drugs likely contributes to the phenomenon of fewer and thinner fibrils in the extracellular space of primary human IPF fibroblasts described here (Figure 6). Interestingly, Hostettler and colleagues (25) found that matrix metalloprotease 2, an ECM metalloprotease that cleaves collagen V, is up-regulated, and its inhibitor, metalloproteinase inhibitor 2 (TIMP2), is down-regulated in response to nintedanib. This provides indirect evidence for increased extracellular degradation of collagen V, and, collectively, this suggests that nintedanib may decrease collagen V via both an intracellular and an extracellular mechanism.

To date, few studies have assessed the effects of nintedanib and pirfenidone on collagen secretion. Previously, using Sirius Red–based quantification of total collagen in cell culture supernatant, we showed that nintedanib, but not pirfenidone, dose dependently inhibited collagen secretion in IPF fibroblasts (10). Similarly, Hostettler and colleagues reported a reduction of total secreted collagens in IPF and control fibroblasts on nintedanib treatment (25). Because collagen I and III are the most abundant fibrillar collagens in the lung interstitium and both are known to be increased in IPF (40), we further characterized the inhibition of collagen secretion by both drugs, looking at these two specific collagen subtypes in this study. Clearly, nintedanib was more effective in inhibiting basal collagen I and TGF-β–induced collagen III secretion. Pirfenidone showed only weak inhibitory effects on basal collagen I secretion (Figure 1G), and, notably, no significant effects on collagen III secretion (Figure 2E). Given the observed inhibitory effect of nintedanib on total collagen secretion in our previous study (10), this suggests that nintedanib-induced down-regulation of collagen III secretion contributes more strongly to the decrease of total secreted collagen than does collagen I in IPF fibroblasts.

FKBP10 and HSP47 are rER-resident chaperones, critical for the proper folding of triple-helical procollagen (9, 12). Deficiency of both proteins leads to changes in the extracellular appearance of collagen fibrils as, for example, reduced collagen crosslinking (41, 42) or aberrant fibril formation (12). Both collagen chaperones are increased in animal models of bleomycin-induced lung fibrosis and in patients with IPF (7, 10, 11), and we showed recently that small interfering RNA–mediated down-regulation of FKBP10 attenuates the expression and secretion of collagen in pHLF (10). Interestingly, it had been reported in two independent studies that pirfenidone down-regulated the expression of HSP47 in A549 cells and human lung fibroblasts, which suggested that pirfenidone exerted its antifibrotic effects in part via the inhibition of intracellular collagen folding (21, 26). Therefore, we also assessed the regulation of HSP47 and FKBP10 by nintedanib and pirfenidone in IPF and donor fibroblasts. Notably, nintedanib marginally, but significantly, down-regulated TGF-β–induced FKBP10 expression on transcript and protein levels in IPF fibroblasts, whereas pirfenidone had no effect (Figures 4A, 4C, and 4E). Strikingly, a different pattern was observed here for donor fibroblasts: FKBP10 expression remained unaffected by nintedanib, but decreased at the transcript and increased at the protein level by pirfenidone (Figures 4B, 4D, and 4F). Regarding HSP47 expression, neither drug had an effect on

Figure 4. (Continued). (2 ng/ml). Densitometric analysis and representative blots show the effect of nintedanib and pirfenidone on FKBP10 protein expression relative to β-actin. Data are based on eight (IPF) or three (donor) completely independent experiments and are given as mean ± SEM. Statistical significance between control and different concentrations of nintedanib or pirfenidone is indicated by *horizontal brackets* and *asterisks*. Statistical analysis was performed by one-way analysis of variance (posttest, Bonferroni's multiple comparison test: comparison against control). $^{*}P < 0.1$, $^{**}P < 0.01$, $^{***}P < 0.001$. The well-known effect of TGF-β1 on these transcripts and proteins was significant, but it is not specified in the interest of clarity.

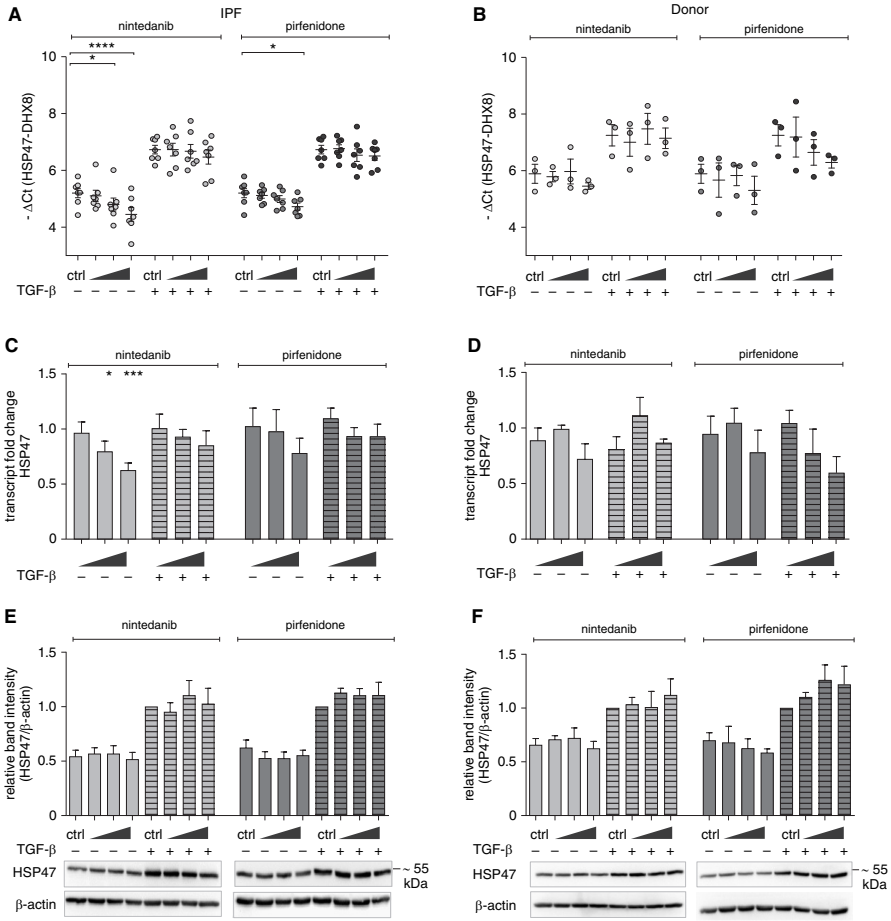

Figure 5. Expression of the major collagen I chaperone HSP47 is reduced only on the transcript level by both drugs in IPF fibroblasts. (*A–D*) Quantitative RT-PCR analysis of phLF isolated from (*A* and *C*) patients with IPF or (*B* and *D*) healthy donors treated for 48 hours with increasing concentrations of nintedanib (0.01, 0.1, and 1 μM) or pirfenidone (100, 500, and 1,000 μM) in the absence or presence of TGF-β1 (2 ng/ml). Transcript levels of (*A* and *C*) IPF and (*B* and *D*) donor phLF of *HSP47* are shown as −ΔCt values (*A* and *B*) as well as transcript fold changes (*C* and *D*) to show the effect normalized to control. *DHX8* was used as endogenous control. Data are based on seven (IPF) or three (donor) completely independent experiments and are given as mean ± SEM. Statistical significance between control and different concentrations of nintedanib or pirfenidone is indicated by *horizontal brackets* and *asterisks* for −ΔCt values and by *asterisks* only for fold changes relative to 1. (*E* and *F*) Western blot analysis of phLF isolated from (*E*) patients with IPF or (*F*) healthy donors treated for 48 hours with increasing concentrations of nintedanib (0.01, 0.1, and 1 μM) or pirfenidone (100, 500, and 1,000 μM) cotreated with or without TGF-β1 (2 ng/ml). Densitometric analysis and representative blots show the effect of nintedanib and pirfenidone on FKBP10 protein expression relative to β-actin. Data are based on eight (IPF) or three (donor) completely independent experiments and are given as mean ± SEM. Statistical significance between control and different concentrations of nintedanib or pirfenidone is indicated by *horizontal brackets* and *asterisks*. Statistical analysis was performed by one-way analysis of variance (posttest, Bonferroni's multiple comparison test: comparison against control). $^{*}P < 0.1$, $^{***}P < 0.001$, $^{****}P < 0.0001$. The well-known effect of TGF-β1 on these transcripts and proteins was significant, but it is not specified in the interest of clarity.

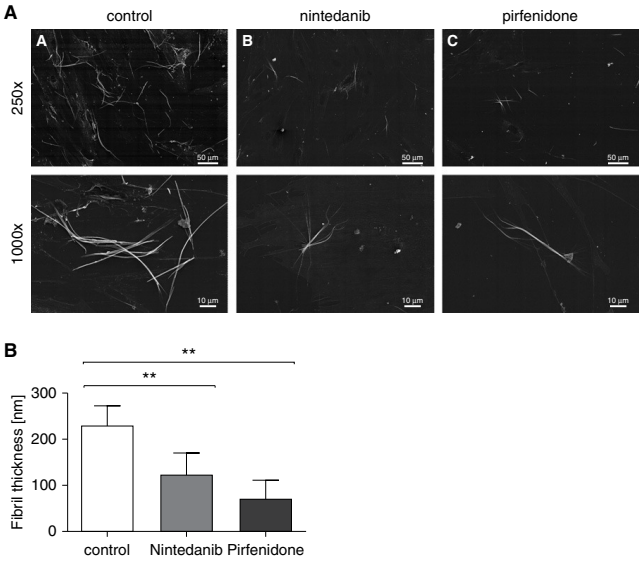

Figure 6. Nintedanib and pirfenidone decrease the number and thickness of collagen fibrils and alter their appearance. (*A*) Scanning electron microscopy of extracellular matrix fibrils deposited by phLF treated for 48 hours with nintedanib (1 μM, *middle panel*) or pirfenidone (1,000 μM, *right panel*) and TGF-β (2 ng/ml) showed fewer, thinner, and more frayed fiber bundles when compared with control (*left panel*). Magnification is indicated on the *left side* (*upper panel*: 250 ×; *lower panel*: 1000 ×). Results shown are representative images of three independent experiments with similar results. (*B*) Thickness of single fibrils was measured in scanning electron microscopy pictures in three experiments using independently derived IPF fibroblasts. Statistical analysis was performed by a paired *t* test. *Scale bars*, 50 μm in top panels of *A–C*, and 10 μm in bottom panels of *A–C*. $^{**}P < 0.01$.

protein levels (Figures 5E and 5F), even if both drugs showed effects on the transcript level (Figures 5A and 5C). Again, this is in contrast to previously reported results, but may be due to higher pirfenidone concentrations used in those studies (21, 26).

Importantly, we found much fewer, thinner, and aberrantly structured collagen fibrils in the extracellular space of IPF fibroblasts treated with nintedanib or pirfenidone (Figure 6). This was particularly unexpected for pirfenidone, because we had observed only minor effects on collagen synthesis and secretion. As pointed out earlier in the text, a partial explanation for this result may be the observed down-regulation of type V collagen, which, even if it represents a minor constituent of collagen fibrils, appears to be crucial for collagen fibrogenesis (39). Because deficiency of 3-Hyp has been shown to have major effects on lateral fibril growth (15), we also assessed hydroxylation of three 3-Hyp sites in collagen I, a comparatively rare collagen PTM, next to a lysyl glycosylation site in collagen I. We did not observe any effect of nintedanib or pirfenidone on these PTMs of collagen I (Figure E4). However, there are clearly many more collagen PTMs to consider and, in light of the recently reported profibrotic properties of ECM of patients with IPF (43), a broader PTM fingerprinting of collagens in the context of fibrotic disease would undoubtedly be warranted.

Extracellular collagen fibril formation is mainly an entropy-driven self-assembly process (31). The so-called collagen D-stagger is formed by specific interactions of the residues along the triple-helical molecules with regularly staggered ends. After cleavage of the propeptides, the collagen molecules become competent for fibril formation. We took advantage of the fact that this process can be studied in a straightforward manner using purified pepsin-digested collagen (27) and found that low micromolar concentrations of both drugs inhibited collagen I fibril formation with comparable efficiencies in a dose-dependent manner (Figure 7). Even if the exact molecular mechanisms remain obscure, it can be speculated that pirfenidone and nintedanib directly bind to collagen triple helices and mask or alter interaction sites caused by changes in hydrophobicity or charges on the surface of the triple helix. Moreover, considering that higher concentrations of pirfenidone than of nintedanib were necessary to achieve the same amplitude of effect, nintedanib likely displays a stronger affinity to collagen than does pirfenidone. Finally, because pepsin-digested solubilized collagen is used in our cell-free system, it can be concluded that the direct drug–collagen interaction takes place in the collagenous region of collagen and not in the telopeptides and propeptides, which are typically removed by pepsin digestion.

Interestingly, inhibition of collagen I self-assembly has been proposed as a strategy for antifibrotic therapy, but this concept has received little attention in the field of lung fibrosis thus far (44). Instead, efforts have been undertaken to evaluate the inhibition of collagen crosslinking by the enzyme lysyl oxidase-like 2, notably a step subsequent to spontaneous fibril formation that stabilizes existing fibrils (31, 45). Recently, however, a phase II study with a monoclonal anti–lysyl oxidase-like 2 antibody was terminated because of a lack of efficacy (46). Here we show, to our knowledge for the first time, that nintedanib and pirfenidone down-regulate collagen V, a minor collagen important for the initiation of extracellular fibrillogenesis, and directly inhibit collagen fibril formation. This suggests that both therapeutics exert their antifibrotic actions at least in part via the inhibition of collagen fibril formation, which provides additional support for the concept of inhibition of collagen self-assembly as a promising antifibrotic strategy. This is a particularly interesting finding for pirfenidone, in which the well-known antifibrotic effects *in vivo* to date stay in

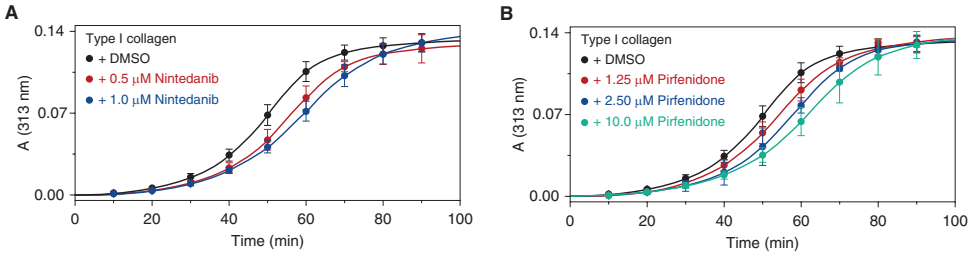

Figure 7. Spontaneous collagen fibril formation is inhibited by both drugs in a dose-dependent manner. A collagen type I stock solution in 50 mM acetic acid was diluted to a final concentration of 0.1 μM into a 0.1 M $NaHCO_3$ buffer (pH 7.8) containing 0.15 M NaCl and 1 mM $CaCl_2$ and heated up to 34°C, followed by monitoring of absorbance (light scattering) at 313 nm. (*A*) Nintedanib (*red*, 0.5 μM [$n = 2$]; *blue*, 1.0 μM [$n = 5$]) and (*B*) pirfenidone (*red*, 1.25 μM [$n = 3$]; *blue*, 2.50 μM [$n = 2$]; *green*, 10.0 μM [$n = 3$]) on collagen type I fibril formation in comparison to dimethyl sulfoxide control (*black* [$n = 4$]) are shown. The resulting half-time values for fibril formation are given in Table 1.

sharp contrast to concentrations in the millimolar range required to observe effects on fibrotic marker expression (19–21, 26, 36). Notably, we believe our study is the first to offer evidence for an antifibrotic effect of pirfenidone *in vitro*, which occurs at a micromolar concentration. For nintedanib, which affects the intracellular collagen pathway more strongly and in physiologically relevant concentrations, the reduced fibril formation is probably a combined result of intracellular and extracellular events. Our findings furthermore emphasize that collagen V plays a hitherto underestimated role in fibrogenesis.

We observed only few differences between IPF and donor fibroblasts regarding the effects of nintedanib and pirfenidone on the expression of the studied targets. The most striking difference was observed in the regulation of the collagen chaperone FKBP10, the expression of which was consistently down-regulated by nintedanib in IPF fibroblasts without evidence for down-regulation in donor fibroblasts. Even more surprisingly, pirfenidone, which did not affect FKBP10 expression in IPF fibroblasts, decreased FKBP10 transcript and increased FKBP10 protein levels in donor fibroblasts. Another difference was that nintedanib had a stronger negative effect on *COL1A1*, *COL3A1*, and *HSP47* transcription in IPF fibroblasts than in donor fibroblasts; at the same time, however, protein levels were unchanged or regulated similarly. Finally, both drugs down-regulated basal collagen I secretion only in IPF fibroblasts and not in donor fibroblasts. Apart from these differences, by and large, the tendencies of the effects of nintedanib and pirfenidone between IPF and donor fibroblasts on fibrotic markers, collagen chaperones, and collagen secretion were similar. Notably, in a previous study, we also observed that the effects on collagen synthesis and secretion were similar in IPF and normal control fibroblasts, and we ultimately pooled those results for data presentation (10). This is also in agreement with the findings of two previously published studies (25, 47). Lehtonen and colleagues (47) examined the effect of nintedanib and pirfenidone on fibroblast and myofibroblast properties and also observed only marginal differences between cells from control and IPF lungs. Hostettler and colleagues (25) studied collagen secretion by nintedanib in phLF and IPF fibroblasts and found that collagen secretion was down-regulated to the same extent in both cell types.

In conclusion, our findings provide an overview and a direct comparison of the effects of the Food and Drug Administration/European Medicines Agency-approved IPF drugs nintedanib and pirfenidone on different stages of expression and maturation of collagen in primary human lung fibroblast derived from patients with IPF as well as from healthy donors. Nintedanib clearly was more efficient than pirfenidone in inhibiting profibrotic gene expression and collagen secretion, both in terms of the required effective concentration as well as in the number, consistency, and

Table 1. Half-Time Values for Fibril Formation (Fibril $Formation_{50}$)

Concentration of Indicated Drug (*μM*)	Fibril $Formation_{50}$ (*min*)	*P* Value*
0 (DMSO control)	49.6 ± 2.1	
Nintedanib		
0.5	55.6 ± 2.1	n.d.
1.0	59.1 ± 2.0	0.000218†
Pirfenidone		
1.25	54.2 ± 4.7	0.133
2.5	57.3 ± 4.6	n.d.
10	61.6 ± 3.1	0.00165‡

Definition of abbreviation: n.d., not determined ($n = 2$).
Nintedanib and pirfenidone increase half-time values for fibril formation (fibril $formation_{50}$) dose dependently. Half-time values for fibril formation (fibril $formation_{50}$) are defined as the time at which the absorbance reaches half the value of the total absorbance change. Data are derived from graphs shown in Figure 7 and are presented as mean ± SD.
*Statistical analysis was performed on half-time values relative to DMSO control using one-way analysis of variance.
†$P < 0.001$.
‡$P < 0.01$.

magnitude of its effects in independently derived IPF fibroblast lines. Finally, nintedanib and pirfenidone inhibited collagen fibril self-assembly, which represents a novel antifibrotic mechanism of action for both drugs. We suggest two independent potential mechanisms for this observation, namely, down-regulation of collagen V and inhibition of extracellular fibril formation by direct interaction of the drugs with triple-helical collagen. ■

Author disclosures are available with the text of this article at www.atsjournals.org.

References

1. Kim DS, Collard HR, King TE Jr. Classification and natural history of the idiopathic interstitial pneumonias. *Proc Am Thorac Soc* 2006;3: 285–292.
2. Coward WR, Saini G, Jenkins G. The pathogenesis of idiopathic pulmonary fibrosis. *Ther Adv Respir Dis* 2010;4:367–388.
3. Rock JR, Barkauskas CE, Cronce MJ, Xue Y, Harris JR, Liang J, Noble PW, Hogan BL. Multiple stromal populations contribute to pulmonary fibrosis without evidence for epithelial to mesenchymal transition. *Proc Natl Acad Sci USA* 2011;108:E1475–E1483.
4. Fernandez IE, Eickelberg O. The impact of TGF-β on lung fibrosis: from targeting to biomarkers. *Proc Am Thorac Soc* 2012;9:111–116.
5. Wollin L, Wex E, Pautsch A, Schnapp G, Hostettler KE, Stowasser S, Kolb M. Mode of action of nintedanib in the treatment of idiopathic pulmonary fibrosis. *Eur Respir J* 2015;45:1434–1445.
6. Decaris ML, Gatmaitan M, FlorCruz S, Luo F, Li K, Holmes WE, Hellerstein MK, Turner SM, Emson CL. Proteomic analysis of altered extracellular matrix turnover in bleomycin-induced pulmonary fibrosis. *Mol Cell Proteomics* 2014;13:1741–1752.
7. Schiller HB, Fernandez IE, Burgstaller G, Schaab C, Scheltema RA, Schwarzmayr T, Strom TM, Eickelberg O, Mann M. Time- and compartment-resolved proteome profiling of the extracellular niche in lung injury and repair. *Mol Syst Biol* 2015;11:819.
8. Ishikawa Y, Bachinger HP. A molecular ensemble in the rER for procollagen maturation. *Biochim Biophys Acta* 2013;1833: 2479–2491.
9. Ishikawa Y, Boudko S, Bachinger HP. Ziploc-ing the structure: triple helix formation is coordinated by rough endoplasmic reticulum resident PPIases. *Biochim Biophys Acta* 2015;1850:1983–1993.
10. Staab-Weijnitz CA, Fernandez IE, Knüppel L, Maul J, Heinzelmann K, Juan-Guardela BM, Hennen E, Preissler G, Winter H, Neurohr C, *et al*. FK506-binding protein 10, a potential novel drug target for idiopathic pulmonary fibrosis. *Am J Respir Crit Care Med* 2015;192: 455–467.
11. Razzaque MS, Nazneen A, Taguchi T. Immunolocalization of collagen and collagen-binding heat shock protein 47 in fibrotic lung diseases. *Mod Pathol* 1998;11:1183–1188.
12. Ishida Y, Kubota H, Yamamoto A, Kitamura A, Bächinger HP, Nagata K. Type I collagen in Hsp47-null cells is aggregated in endoplasmic reticulum and deficient in N-propeptide processing and fibrillogenesis. *Mol Biol Cell* 2006;17:2346–2355.
13. Hudson DM, Eyre DR. Collagen prolyl 3-hydroxylation: a major role for a minor post-translational modification? *Connect Tissue Res* 2013; 54:245–251.
14. Weis MA, Hudson DM, Kim L, Scott M, Wu JJ, Eyre DR. Location of 3-hydroxyproline residues in collagen types I, II, III, and V/XI implies a role in fibril supramolecular assembly. *J Biol Chem* 2010;285: 2580–2590.
15. Pokidysheva E, Zientek KD, Ishikawa Y, Mizuno K, Vranka JA, Montgomery NT, Keene DR, Kawaguchi T, Okuyama K, Bächinger HP. Posttranslational modifications in type I collagen from different tissues extracted from wild type and prolyl 3-hydroxylase 1 null mice. *J Biol Chem* 2013;288:24742–24752.
16. Blackwell TS, Tager AM, Borok Z, Moore BB, Schwartz DA, Anstrom KJ, Bar-Joseph Z, Bitterman P, Blackburn MR, Bradford W, *et al*. Future directions in idiopathic pulmonary fibrosis research. An NHLBI workshop report. *Am J Respir Crit Care Med* 2014;189:214–222.
17. Richeldi L, du Bois RM, Raghu G, Azuma A, Brown KK, Costabel U, Cottin V, Flaherty KR, Hansell DM, Inoue Y, *et al*.; INPULSIS Trial Investigators. Efficacy and safety of nintedanib in idiopathic pulmonary fibrosis. *N Engl J Med* 2014;370:2071–2082.
18. Datta A, Scotton CJ, Chambers RC. Novel therapeutic approaches for pulmonary fibrosis. *Br J Pharmacol* 2011;163:141–172.
19. Schaefer CJ, Ruhrmund DW, Pan L, Seiwert SD, Kossen K. Antifibrotic activities of pirfenidone in animal models. *Eur Respir Rev* 2011;20:85–97.
20. Chambers RC, Mercer PF. Mechanisms of alveolar epithelial injury, repair, and fibrosis. *Ann Am Thorac Soc* 2015;12:S16–S20.
21. Hisatomi K, Mukae H, Sakamoto N, Ishimatsu Y, Kakugawa T, Hara S, Fujita H, Nakamichi S, Oku H, Urata Y, *et al*. Pirfenidone inhibits TGF-β1-induced over-expression of collagen type I and heat shock protein 47 in A549 cells. *BMC Pulm Med* 2012;12:24.
22. Di Sario A, Bendia E, Svegliati Baroni G, Ridolfi F, Casini A, Ceni E, Saccomanno S, Marzioni M, Trozzi L, Sterpetti P, *et al*. Effect of pirfenidone on rat hepatic stellate cell proliferation and collagen production. *J Hepatol* 2002;37:584–591.
23. Huang J, Beyer C, Palumbo-Zerr K, Zhang Y, Ramming A, Distler A, Gelse K, Distler O, Schett G, Wollin L, *et al*. Nintedanib inhibits fibroblast activation and ameliorates fibrosis in preclinical models of systemic sclerosis. *Ann Rheum Dis* 2016;75:883–890.
24. Rangarajan S, Kurundkar A, Kurundkar D, Bernard K, Sanders YY, Ding Q, Antony VB, Zhang J, Zmijewski J, Thannickal VJ. Novel mechanisms for the anti-fibrotic action of nintedanib. *Am J Respir Cell Mol Biol* 2016;54:51–59.
25. Hostettler KE, Zhong J, Papakonstantinou E, Karakiulakis G, Tamm M, Seidel P, Sun Q, Mandal J, Lardinois D, Lambers C, *et al*. Anti-fibrotic effects of nintedanib in lung fibroblasts derived from patients with idiopathic pulmonary fibrosis. *Respir Res* 2014;15:157.
26. Nakayama S, Mukae H, Sakamoto N, Kakugawa T, Yoshioka S, Soda H, Oku H, Urata Y, Kondo T, Kubota H, *et al*. Pirfenidone inhibits the expression of HSP47 in TGF-β1-stimulated human lung fibroblasts. *Life Sci* 2008;82:210–217.
27. Ishikawa Y, Bächinger HP. A substrate preference for the rough endoplasmic reticulum resident protein FKBP22 during collagen biosynthesis. *J Biol Chem* 2014;289:18189–18201.
28. Shin JM, Park JH, Park IH, Lee HM. Pirfenidone inhibits transforming growth factor β1-induced extracellular matrix production in nasal polyp-derived fibroblasts. *Am J Rhinol Allergy* 2015;29:408–413.
29. Hashizume H, Hitomi J, Ushiki T. Growth of collagen fibrils produced by human osteosarcoma cells: high-resolution scanning electron microscopy. *Arch Histol Cytol* 1999;62:327–335.
30. Williams BR, Gelman RA, Poppke DC, Piez KA. Collagen fibril formation. Optimal *in vitro* conditions and preliminary kinetic results. *J Biol Chem* 1978;253:6578–6585.
31. Kadler KE, Holmes DF, Trotter JA, Chapman JA. Collagen fibril formation. *Biochem J* 1996;316:1–11.
32. Lin X, Yu M, Wu K, Yuan H, Zhong H. Effects of pirfenidone on proliferation, migration, and collagen contraction of human Tenon's fibroblasts *in vitro*. *Invest Ophthalmol Vis Sci* 2009;50:3763–3770.
33. Pierce GF, Mustoe TA, Altrock BW, Deuel TF, Thomason A. Role of platelet-derived growth factor in wound healing. *J Cell Biochem* 1991;45:319–326.
34. Heinzelmann K, Noskovičová N, Merl-Pham J, Preissler G, Winter H, Lindner M, Hatz R, Hauck SM, Behr J, Eickelberg O. Surface proteome analysis identifies platelet derived growth factor receptor-α as a critical mediator of transforming growth factor-β-induced collagen secretion. *Int J Biochem Cell Biol* 2016;74:44–59.
35. Tourkina E, Richard M, Gööz P, Bonner M, Pannu J, Harley R, Bernatchez PN, Sessa WC, Silver RM, Hoffman S. Antifibrotic properties of caveolin-1 scaffolding domain *in vitro* and *in vivo*. *Am J Physiol Lung Cell Mol Physiol* 2008;294:L843–L861.
36. Wollin L, Schuett J, Ostermann A. The effect of nintedanib compared to pirfenidone on serum-stimulated proliferation of human primary lung fibroblasts at clinically relevant concentrations. *Am J Respir Crit Care Med* 2015;191:A4940.

37. Parra ER, Teodoro WR, Velosa AP, de Oliveira CC, Yoshinari NH, Capelozzi VL. Interstitial and vascular type V collagen morphologic disorganization in usual interstitial pneumonia. J *Histochem Cytochem* 2006;54:1315–1325.
38. Vittal R, Mickler EA, Fisher AJ, Zhang C, Rothhaar K, Gu H, Brown KM, Emtiazdjoo A, Lott JM, Frye SB, *et al*. Type V collagen induced tolerance suppresses collagen deposition, TGF-β and associated transcripts in pulmonary fibrosis. *PLoS One* 2013;8:e76451.
39. Wenstrup RJ, Florer JB, Brunskill EW, Bell SM, Chervoneva I, Birk DE. Type V collagen controls the initiation of collagen fibril assembly. *J Biol Chem* 2004;279:53331–53337.
40. Dancer RC, Wood AM, Thickett DR. Metalloproteinases in idiopathic pulmonary fibrosis. *Eur Respir J* 2011;38:1461–1467.
41. Lindert U, Weis MA, Rai J, Seeliger F, Hausser I, Leeb T, Eyre D, Rohrbach M, Giunta C. Molecular Consequences of the SERPINH1/HSP47 mutation in the Dachshund natural model of osteogenesis imperfecta. *J Biol Chem* 2015;290:17679–17689.
42. Barnes AM, Cabral WA, Weis M, Makareeva E, Mertz EL, Leikin S, Eyre D, Trujillo C, Marini JC. Absence of FKBP10 in recessive type XI osteogenesis imperfecta leads to diminished collagen cross-linking and reduced collagen deposition in extracellular matrix. *Hum Mutat* 2012; 33:1589–1598.
43. Parker MW, Rossi D, Peterson M, Smith K, Sikström K, White ES, Connett JE, Henke CA, Larsson O, Bitterman PB. Fibrotic extracellular matrix activates a profibrotic positive feedback loop. *J Clin Invest* 2014;124: 1622–1635.
44. Chung HJ, Steplewski A, Chung KY, Uitto J, Fertala A. Collagen fibril formation. A new target to limit fibrosis. *J Biol Chem* 2008;283:25879–25886.
45. Cox TR, Bird D, Baker AM, Barker HE, Ho MW, Lang G, Erler JT. LOX-mediated collagen crosslinking is responsible for fibrosis-enhanced metastasis. *Cancer Res* 2013;73:1721–1732.
46. Gilead. Gilead terminates phase 2 study of simtuzumab in patients with idiopathic pulmonary fibrosis. Foster City, CA: Gilead Sciences, Inc.; January 5, 2016 [accessed 2016 Jul 12]. Available from: http://www.gilead.com/news/press-releases/2016/1/gilead-terminates-phase-2-study-of-simtuzumab-in-patients-with-idiopathic-pulmonary-fibrosis
47. Lehtonen ST, Veijola A, Karvonen H, Lappi-Blanco E, Sormunen R, Korpela S, Zagai U, Sköld MC, Kaarteenaho R. Pirfenidone and nintedanib modulate properties of fibroblasts and myofibroblasts in idiopathic pulmonary fibrosis. *Respir Res* 2016;17:14.

AJRCMB Articles in Press. Published on 03-March-2017 as 10.1165/rcmb.2016-0217OC

A NOVEL ANTIFIBROTIC MECHANISM OF NINTEDANIB AND PIRFENIDONE: INHIBITION OF COLLAGEN FIBRIL ASSEMBLY

Larissa Knüppel[1], Yoshihiro Ishikawa[2], Michaela Aichler[3], Katharina Heinzelmann[1], Rudolf Hatz[4,5], Jürgen Behr[5,6], Axel Walch[3], Hans Peter Bächinger[2], Oliver Eickelberg[1,7] and Claudia A. Staab-Weijnitz[1]

ONLINE DATA SUPPLEMENT

Material and Methods

Material:

Primers were purchased by MWG Eurofins (Ebersberg, Germany) and are listed in Supplementary Table E1. Used primary antibodies are given in Supplementary Table E2. Secondary HRP-linked antibodies were purchased from GE Healthcare Life Sciences (Freiburg, Germany).

Statistical analysis

Statistical analysis was performed in GraphPad Prism 7.02 (GraphPad Software, San Diego, CA). For quantification of transcript and protein, results are given as mean ± SEM of independent experiments with fibroblasts derived from at least four different IPF patients. Paired t-test was used for statistical analysis of fiber thickness and one way ANOVA (post test: Bonferroni`s multiple comparison test: comparison against control) was used for statistical analysis for all other experiments. Significance is indicated as follows: *$p<0.1$, **$p<0.01$, ***$p<0.001$, ****$p<0.0001$.

MTT Cytotoxicity Assay

To assess cytotoxicity of nintedanib and pirfenidone, 20.000 cells/cm^2 IPF fibroblasts were seeded in 24-well plates in absence and presence of TGF-β1 (R&D Systems, Minneapolis,

AJRCMB Articles in Press. Published on 03-March-2017 as 10.1165/rcmb.2016-0217OC

MN) (2ng/mL) in combination with nintedanib (0.01 μM, 0.1 μM, 1.0 μM) or pirfenidone (100 μM, 500 μM, 1000 μM) (both Selleck, Houston, TX) for 48h in starvation medium. Nintedanib and pirfenidone were dissolved in DMSO. The final DMSO concentration in the medium was always 1%.

After 48h thiazolyl-blue-tetrazolium-bromide (Sigma-Aldrich) in PBS was added to each well (final: 0.5mg/mL) and incubated at 37°C, 5% CO_2 for 30 min. The supernatant was aspirated and crystals were dissolved in 0.5 mL isopropanol/0.1% Triton X-100 for 30 min at room temperature on a shaker. Absorbance (570 nm) was measured using the Sunrise multiplate reader (Tecan; Männedorf, Switzerland).

Isolation and culture of primary human lung IPF and donor fibroblasts (phLF)

Lung specimens from IPF patients and healthy donors were dissected into pieces of 1-2 cm^2 followed by collagenase I (1 mg/mL) (Biochrom, Berlin, Germany) digestion at 37°C for 2 hours, filtration through nylon filters with a pore size of 70 μm (BD Falcon,Bedford, USA) and centrifugation at 400 *g* at 4°C for 5 minutes. Cells were resuspended in DMEM/F-12 medium (Life Technologies; Carlsbad, CA, USA) supplemented with 20% fetal bovine serum (Pan Biotech, Aidenbach, Germany) and penicillin/streptomycin (Life Technologies, Carlsbad, CA, USA) and seeded onto 10 cm cell culture dishes. For expansion, phLF were cultured in DMEM/F12 (Life Technologies) supplemented with 20% FBS (Pan Biotech) and penicillin/streptomycin (Life Technologies). Cells were routinely split when reaching a confluency of 80-90%. For this study, phLF from six different IPF patients were used in passages 5-8.

RNA isolation and Real-Time quantitative Reverse-Transcriptase PCR (qRT-PCR) Analysis

Isolation of RNA from cultured cells was performed by using the peqGOLD RNA isolation kit (Macherey-Nagel, Düren, Germany). Subsequently, RNA was reverse-transcribed

according to the manufacturer`s protocol (Life Technologies) in a 40 µL reaction using M-MLV reverse transcriptase and random hexamers. For quantitative real-time PCR (qRT-PCR) SYBR Green PCR master mix (Roche Applied Science, Mannheim, Germany) and primer mixtures given in Table 1 were used (95°C for 5 min, followed by 45 cycles of 95°C for 5 sec, 59°C for 5 sec and 72°C for 10 sec). Relative transcript abundance of a gene is expressed as -ΔCp values (-ΔCp = $Cp^{reference}$ - Cp^{target}) or as Fold Change derived from the relevant ΔΔCp values, using $2^{-(\Delta\Delta Cp)}$. As endogenous control, DHX8 was used for standardization of relative mRNA expression.

Protein Isolation and Western Blot Analysis

To extract proteins from cultured cells, cells were scraped into Radio-Immunoprecipitation Assay (RIPA) buffer (50 mM Tris HCl pH 7.4, 150 mM NaCl, 1% Triton X100, 0.5% sodium deoxycholate, 1 mM EDTA, 0.1% SDS) containing a protease inhibitor and a phosphatase inhibitor cocktail (both Roche), incubated and centrifuged for 15 min at 13.000 rpm at 4°C. The supernatant was used to determine protein concentration via Pierce BCA Protein Assay (Thermo Fisher Scientific, Waltham, USA). After denaturation of the samples with Laemmli buffer (65 mM Tris-HCl pH 6.8, 10% glycerol, 2% SDS, 0.01% bromophenolblue, 100 mM DTT), proteins were resolved by SDS-PAGE and transferred to polyvinylidene difluoride (PVDF) membranes. The membrane was blocked for 1 hour at room temperature with 5% milk in TBS-T (0.1% Tween 20, TBS) to prevent nonspecific binding. Then, the membrane was shortly rinsed and washed (three times for 5 min) in TBS-T followed by incubation with primary antibody (Table 2) overnight at 4°C. After washing (three times for 5 min) and incubation with the secondary antibody for 1 hour at room temperature, the proteins were visualized with either SuperSignal™ West Dura Extended Duration Substrate or SuperSignal™ West Femto Maximum Sensitivity Substrate (both Thermo Fisher Scientific)

AJRCMB Articles in Press. Published on 03-March-2017 as 10.1165/rcmb.2016-0217OC

and analyzed by the ChemiDocXRS+ imaging system (Bio-Rad, Munich, Germany). Band quantification was performed in Image Lab (version 3.0, Bio-Rad, Hercules, CA).

Quantification of secreted collagen

Precipitation of collagen I and III was carried out as follows: 0.2 g/mL solid $(NH_4)_2SO_4$ was added to the supernatant and the solution was incubated on ice for 30 min. After centrifugation at 20.000 *g* for 30 min at 4°C, the pellet was dissolved in 1/10 of the original volume of 0.1 M acetic acid containing 0.1 mg/mL pepsin (Thermo Fisher Scientific) and incubated on ice overnight at 4°C. Subsequently, 5 M NaCl was added to a final concentration of 0.7 M, incubated on ice for 30 min followed by centrifugation at 20.000 g for 30 min at 4°C. The pellet containing collagen type I and III was resuspended in 0.1 M acetic acid and analyzed by Western blot.

Collagen precipitation for post-translational modification analysis

IPF fibroblasts were seeded at a density of 20.000 – 25.000 cells/cm^2 and cultured in DMEM/F12 (20% FBS, 0.1 mM 2-phospho-L-ascorbic acid, penicillin/streptomycin). When cells had reached a confluency of 80% serum-free DMEM/F12 medium (0.1 mM 2-phospho-L-ascorbic acid) was added containing TGF-β1 (2 ng/mL) and nintedanib (1 μM) or pirfenidone (1000 μM) or DMSO for control and incubated for 24h followed by collection of the medium. DMEM/F12 (20% FBS, 0.1 mM 2-phospho-L-ascorbic acid, penicillin/streptomycin) containing TGF-β1 (2 ng/mL) was added for 24h, followed by alternating cycles of serum-free media supplemented with TGF-β1 and nintedanib or pirfenidone or DMSO and media containing 20% FBS and TGF-β1. Serum-free cell culture supernatants were collected (20mL in each collection cycle) until 100 mL were obtained.

Precipitation of collagens from cell culture supernatant was in principle carried out in a scale-up version as described previously (1). 0.2 g/mL solid $(NH_4)_2SO_4$ was added to the supernatant and the solution was incubated on ice for 30 min. After centrifugation at 20.000 *g*

for 30 min at 4°C, the pellet was dissolved in 1/6 of the original volume of 0.1 M acetic acid containing 0.1 mg/mL pepsin (Thermo Fisher Scientific) and incubated on ice overnight at 4°C (Input). Subsequently, 5 M NaCl was added to a final concentration of 0.7 M, incubated on ice for 30 min followed by centrifugation at 20.000 g for 30 min at 4°C. After collection of the supernatant, the pellet was resuspended in 0.1 M acetic acid (0.7 M fraction). 5 M NaCl was added to the supernatant to a final concentration of 1.2 M and incubated on ice for 30 min, followed by centrifugation at 20.000 g for 30 min at 4°C. The supernatant was collected and the pellet was resuspended in 0.1 M acetic acid (1.2 M fraction). Again, 5 M NaCl was added to a final concentration of 2.5 M, incubated on ice for 30 min followed by centrifugation at 20.000 g for 30 min at 4°C. The pellet was resuspended in 0.1 M acetic acid (2.5 M fraction). The different fractions were resolved by SDS-PAGE (Input: 60 µL, 0.7 M fraction 20 µL, 1.2 M - 2.5 M fractions 80 µL) and visualized by Coomassie staining, followed by band excision, collagen digestion, mass spectrometry (MS) and amino acid analysis

Collagen Digestion and MS Analysis

SDS-PAGE bands were subjected to in-gel digestion with trypsin. Digest conditions were 13 ng/µl Promega trypsin in 100 mM ammonium bicarbonate at 37°C for 18h. Identification of tryptic peptides was performed on a Q-TOF Micro mass spectrometer (Waters, Billerica, MA) equipped with an electrospray ionization source. Data were collected with the MassLynx (version 4.1) data acquisition software (Waters) and processed using Mascot Distiller (Matrix Software, London, UK). High performance liquid chromatography was performed with a nanoACQUITY (Waters) system using a 75 µm x 100-mm 3-µm Atlantis dC18 column as the analytical column and a 180 µm x 20-mm 5-µm Symmetry C18 column as the trapping column. Chromatography mobile phases consisted of solvents A (0.1% formic acid and 99.9% water (v/v)) and B (0.1% formic acid and 99.9% acetonitrile (v/v)). Peptide samples were

AJRCMB Articles in Press. Published on 03-March-2017 as 10.1165/rcmb.2016-0217OC

loaded onto the trapping column and equilibrated for 2 min in 99% solvent A followed by a 120-min gradient to 60% solvent A at a constant flow rate of 1 µl/min. Analysis was performed in survey scan mode. Tryptic peptides were identified from MS/MS spectra by a Mascot search against the National Center for Biotechnology Information (NCBI) nr database (peptide tolerance 1.0 Da, MS/MS tolerance 1.0 Da)

Amino Acid Analysis

Acid Hydrolysis was performed in 6 x 50-mm Pyrex culture tubes placed in Pico Tag reaction vessels fitted with a sealable cap (Eldex Laboratories, Inc., Napa, CA). Samples were placed in culture tubes, dried in a SpeedVac (GMI, Inc. Albertsville, MN). Acid hydrolysis was performed in a reaction vessel that contained 500 µL of 6 M HCl (Pierce). The vessel was then purged with argon and the samples were hydrolyzed under vacuum at 110 °C for 24 h. The acid hydrolyzed samples were then dried under vacuum and reconstituted in 100 mL of 0.02 M HCl containing an internal standard (100 µM norvaline; Sigma). Analysis was performed by ion exchange chromatography with postcolumn ninhydrin derivatization and visible detection (440 nm/570 nm) with a Hitachi L-8800A amino acid analyzer (Hitachi High Technologies America, Inc., San Jose, CA) running the EZChrom Elite software (Scientific Software, Inc., Pleasanton, CA).

Base hydrolysis was performed in a reaction vessel that contained 100 µL of 4M NaOH per sample. The vessel was then purged with argon and the samples were allowed to hydrolyze under vacuum at 110 °C for 24 h. The base hydrolyzed samples were then dried under vacuum and reconstituted in 100 µL of 0.1M pH 9.5 borate buffer. 50 µL of 10 mM 4-fluoro-7-nitrobenzofurazan (NBD-F) in acetonitrile was added and the solution was incubated at room temperature for 6 hours. 100 µL of 0.2 M pH 2.0 tartarate buffer was added to the solution to quench the reaction. Analysis was performed by liquid chromatography on a 2695

HPLC (Waters, Inc. Milford, MA) with a Model 121 fluorometer detector (Ex. 460 Em. 530 Gilson Middleton, WI) running the MassLynx software

Collagen I fibril formation assay

A stock solution of collagen type I in 50 mM acetic acid was diluted to a final concentration of 0.1 μM into 0.1 M sodium bicarbonate buffer (pH 7.8) containing 0.15 M sodium chloride and 1 mM calcium chloride. Nintedanib (0.5 μM, 1 μM), pirfenidone (1.25 μM, 2.5 μM, 10 μM) or the same volume of DMSO (control) was added to the solution to obtain 0.5% final DMSO concentration. The solution was heated up to 34°C and the absorbance (light scattering) was recorded at 313 nm as a function of time.

Table E1. Primer table for qRT-PCR. Primers were synthesized by MWG Eurofins (Ebersberg, Germany).

Target	**Species**	**Forward primer** (5′-3′)	**Reverse primer** (5′-3′)
COL1A1	human	TACAGAACGGCCTCAGGTACCA	ACAGATCACGTGATCGCACAAC
COL3A1	human	ATCAACACCGATGAGATTAT	AGTATTCTCCACTCTTGAGTTC
COL5A1	human	CTTCAAGGTTTACTGCAAC	CCCTTCGGACTTCTTG
FN1	human	CCGACCAGAAGTTTGGGTTCT	CAATGCGGTACATGACCCCT
FKBP10	human	CGACACCAGCTACAGTAAG	TAATCTTCCTTCTCTCTCCA
SERPINH1	human	ATGTTCTTCAAGCCACAC	TCGTCGTCGTAGTAGTTGTA
PAI-1	human	GACATCCTGGAACTGCCCTA	GGTCATGTTGCCTTTCCAGT
DHX8	human	TGACCCAGAGAAGTGGGAGA	ATCTCAAGGTCCTCATCTTCTTCA

AJRCMB Articles in Press. Published on 03-March-2017 as 10.1165/rcmb.2016-0217OC

Table E2. Primary antibodies. Primary antibodies which were used for Western Blot analysis. Secondary HRP-linked antibodies were purchased from GE Healthcare Life Sciences (Freiburg, Germany).

Target	**Antibody**	**Provider**
ACTB	HRP-conjugated anti-ACTB antibody	Sigma Aldrich, Louis, MO, USA
AKT	rabbit polyclonal anti AKT antibody	Cell Signaling, Boston, USA
Collagen type I	rabbit polyclonal anti-Collagen I antibody	Rockland, Gilbertsville, PA, USA
Collagen type III	rabbit polyclonal anti-Collagen III antibody	Rockland, Gilbertsville, PA, USA
Collagen type V	rabbit polyclonal anti-Collagen V antibody	Santa Cruz, Dallas, TX, USA
ERK1	mouse monoclonal anti-ERK1 antibody	BD Biosciences, New Jersey, USA
Fibronectin	rabbit polyclonal anti-Fibronectin antibody	Santa Cruz, Dallas, TX, USA
FKBP10	rabbit polyclonal anti-FKBP10 antibody	ATLAS, Stockholm, Sweden
HSP47	mouse monoclonal anti-HSP47 antibody	Enzo Life Sciences, Inc., USA
p-AKT	rabbit monoclonal anti-pAKT (Ser473) antibody	Cell Signaling, Boston, USA
p-ERK	rabbit monoclonal anti-pERK1/2 (Thr202/Thr204)	Cell Signaling, Boston, USA

Figure E1: Effect of nintedanib and pirfenidone on the viability of phLF from IPF patients

Effect of increasing concentrations of nintedanib (0.01 μM, 0.1 μM, 1μM) and pirfenidone (100 μM, 500 μM, 1000 μM) on the viability of phLF of IPF patients after 48h treatment in combination with and without TGF-β1 (2 ng/mL), as measured by MTT assay. n=2.

Figure E2: Nintedanib reduces FN1 expression similarly in IPF and donor fibroblasts

(**A-D**) Quantitative reverse transcriptase-polymerase chain reaction analysis of phLF isolated from (**A, C)** IPF patients or (**B, D**) healthy donors treated for 48h with increasing concentrations of nintedanib (0.01, 0.1, 1 μM) or pirfenidone (100, 500, 1000 μM) in absence or presence of TGF-β1 (2 ng/mL). Transcript levels of FN1 are shown as -ΔCt values (**A, B**) as well as as transcript fold changes (**C, D**) to show the effect normalized to control. DEAH (Asp-Glu-Ala-His) Box Polypeptide 8 (DHX8) was used as endogenous control. Data are based on 7 (IPF) or 3 (donor) completely independent experiments and are given as mean ± SEM. Statistical significance between control and different concentrations of nintedanib or pirfenidone is indicated by horizontal brackets and asterisks for -ΔCt values and asterisks only for fold changes relative to 1.

(**E, F**) Western Blot analysis of phLF isolated from (**E**) IPF patients or (**F**) healthy donors treated for 48h with increasing concentrations of nintedanib (0.01, 0.1, 1 μM) or pirfenidone (100, 500, 1000 μM) in absence or presence of TGF-β1 (2 ng/mL). Densitometric analysis and representative blots show the effect of nintedanib and pirfenidone on FN1 protein expression relative to β-actin (ACTB). Data are based on 8 (IPF) or 3 (donor) completely independent experiments and are given as mean ± SEM. Statistical significance between control and different concentrations of nintedanib or pirfenidone is indicated by horizontal brackets and asterisks.

AJRCMB Articles in Press. Published on 03-March-2017 as 10.1165/rcmb.2016-0217OC

Statistical analysis was performed by One-Way ANOVA (post test: Bonferroni`s multiple comparison test: comparison against control). (*p<0.1, **p<0.01, ***p<0.001, ****p<0.0001). The well-known effect of TGF-β1 on these transcripts and proteins was significant, but is not specified in the interest of clarity. ctrl = control; TGF-β1 = transforming growth factor β1.

Figure E3: *PAI-1* transcripts are downregulated by nintedanib in IPF and donor fibroblasts

(**A-D**) Quantitative reverse transcriptase-polymerase chain reaction analysis of phLF isolated from (**A, C**) IPF patients or (**B, D**) healthy donors treated for 48h with increasing concentrations of nintedanib (0.01, 0.1, 1 μM) or pirfenidone (100, 500, 1000 μM) in absence or presence of TGF-β1 (2 ng/mL). Transcript levels of PAI1 are shown as -ΔCt values (**A, B**) as well as as transcript fold changes (**C, D**) to show the effect normalized to control. DEAH (Asp-Glu-Ala-His) Box Polypeptide 8 (DHX8) was used as endogenous control. Data are based on 7 (IPF) or 3 (donor) completely independent experiments and are given as mean ± SEM. Statistical significance between control and different concentrations of nintedanib or pirfenidone is indicated by horizontal brackets and asterisks for -ΔCt values and asterisks only for fold changes relative to 1. The well-known effect of TGF-β1 on these transcripts was significant, but is not specified in the interest of clarity. ctrl = control; TGF-β1 = transforming growth factor β1. Statistical analysis was performed by One-Way ANOVA (post test: Bonferroni`s multiple comparison test: comparison against control). (*p<0.1, **p<0.01, ***p<0.001, ****p<0.0001). The well-known effect of TGF-β1 on these transcripts and proteins was significant, but is not specified in the interest of clarity. ctrl = control; TGF-β1 = transforming growth factor β1.

Figure E4: Selected PTMs are neither affected by nintedanib nor by pirfenidone

SDS gel electrophoresis of different fractions of collagens precipitated out of 100 mL cell culture media of primary human IPF fibroblasts treated with nintedanib (1 μM) or pirfenidone (1000 μM) in combination with TGF-β1 (2 ng/mL) (A). SDS gel bands (indicated by red boxes) corresponding to the α1-chain of type I collagen (upper red boxes) and the α2-chain of type I collagen (lower red boxes) of the 0.7 M and the 1.2 M fraction were extracted and trypsin digested (A). MS/MS data of the A1 site (Pro-986) of α1-chain of type I (B), A3 site (Pro-707) of α1-chain of type I collagen (C), A3 site (Pro-707) of α2-chain of type I collagen (D) and glycosylation site of hydroxylysine (Lys-174) (E) of control, nintedanib- and pirfenidone-treated samples show no qualitative difference in intensity of prolyl-3-hydroxylation or glycosylation at these sites.

Figure E5: After 48 h, the RTK inhibitor nintedanib consistently inhibits PDGFR/AKT signaling in IPF and donor fibroblasts but not FGFR/ERK signaling

(**A-D**) Western Blot analysis of phLF isolated from (**A, C**) IPF patients or (**B, D**) healthy donors treated for 48h with increasing concentrations of nintedanib (0.01, 0.1, 1 μM) in absence or presence of TGF-β1 (2 ng/mL). (**A, B**) Densitometric analysis and representative blots show the effect of nintedanib and pirfenidone on AKT phosphorylation relative to total AKT levels. (**C, D**) Densitometric analysis and representative blots show the effect of nintedanib and pirfenidone on ERK phosphorylation relative to total ERK levels. Data are based on 8 (IPF) or 3 (donor) completely independent experiments and are given as mean ± SEM. Statistical significance between control and different concentrations of nintedanib or pirfenidone is indicated by horizontal brackets and asterisks. Statistical analysis was performed by One-Way ANOVA (post test: Bonferroni`s multiple comparison test: comparison against control). (*p<0.1, **p<0.01, ***p<0.001, ****p<0.0001).

AJRCMB Articles in Press. Published on 03-March-2017 as 10.1165/rcmb.2016-0217OC

REFERENCES

1. Staab-Weijnitz CA, Fernandez IE, Knüppel L, Maul J, Heinzelmann K, Juan-Guardela BM, Hennen E, Preissler G, Winter H, Neurohr C, Hatz R, Lindner M, Behr J, Kaminski N, Eickelberg O. FK506-Binding Protein 10, a Potential Novel Drug Target for Idiopathic Pulmonary Fibrosis. *Am J Respir Crit Care Med* 2015; 192: 455-467.

Figure S1

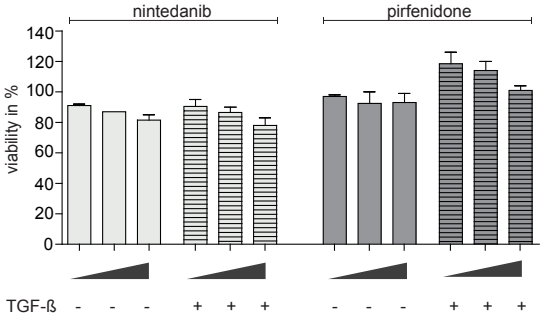

Figure S2 AJRCMB Articles in Press. Published on 03-March-2017 as 10.1165/rcmb.2016-0217OC

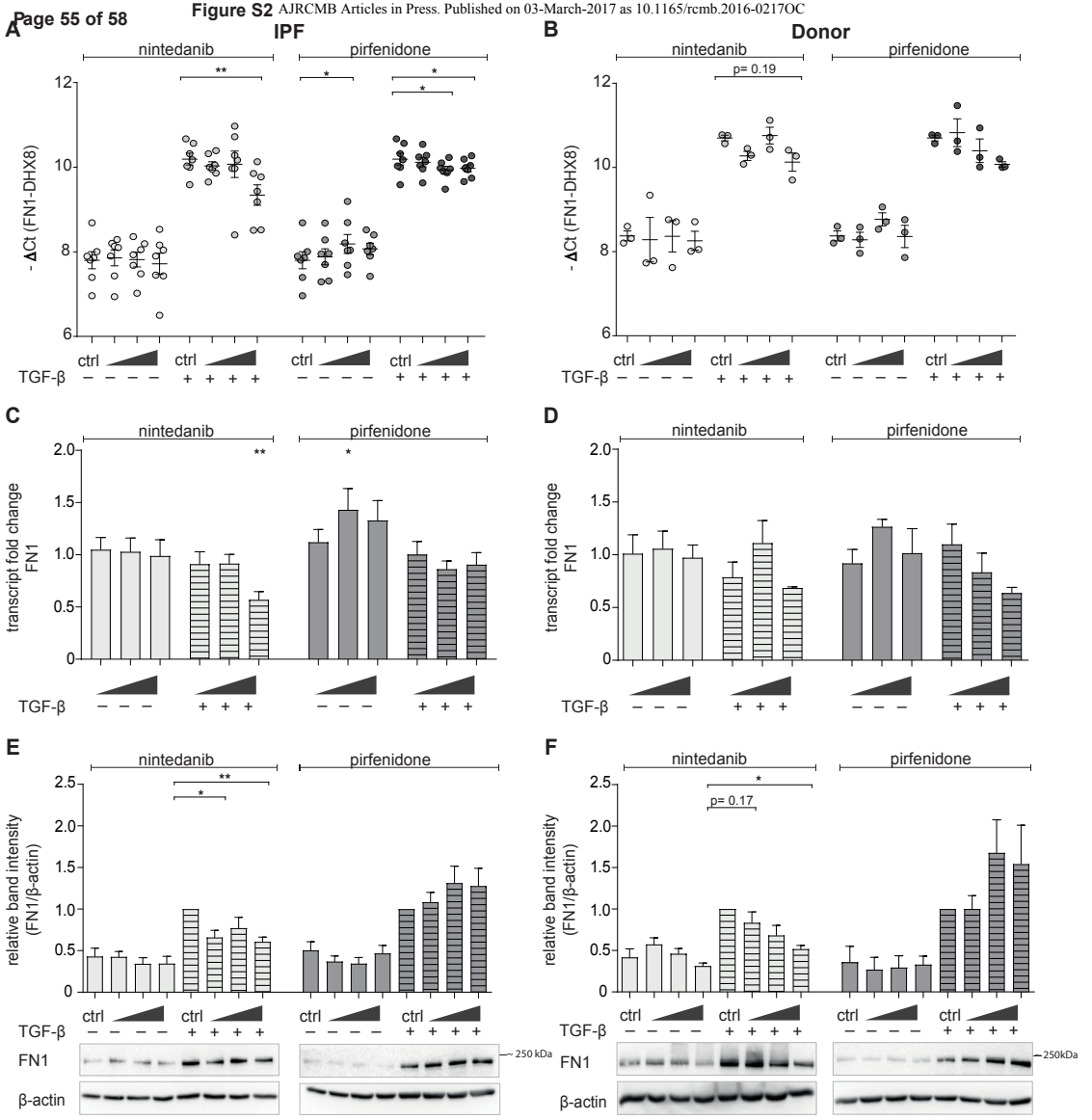

AJRCMB Articles in Press. Published on 03-March-2017 as 10.1165/rcmb.2016-0217OC

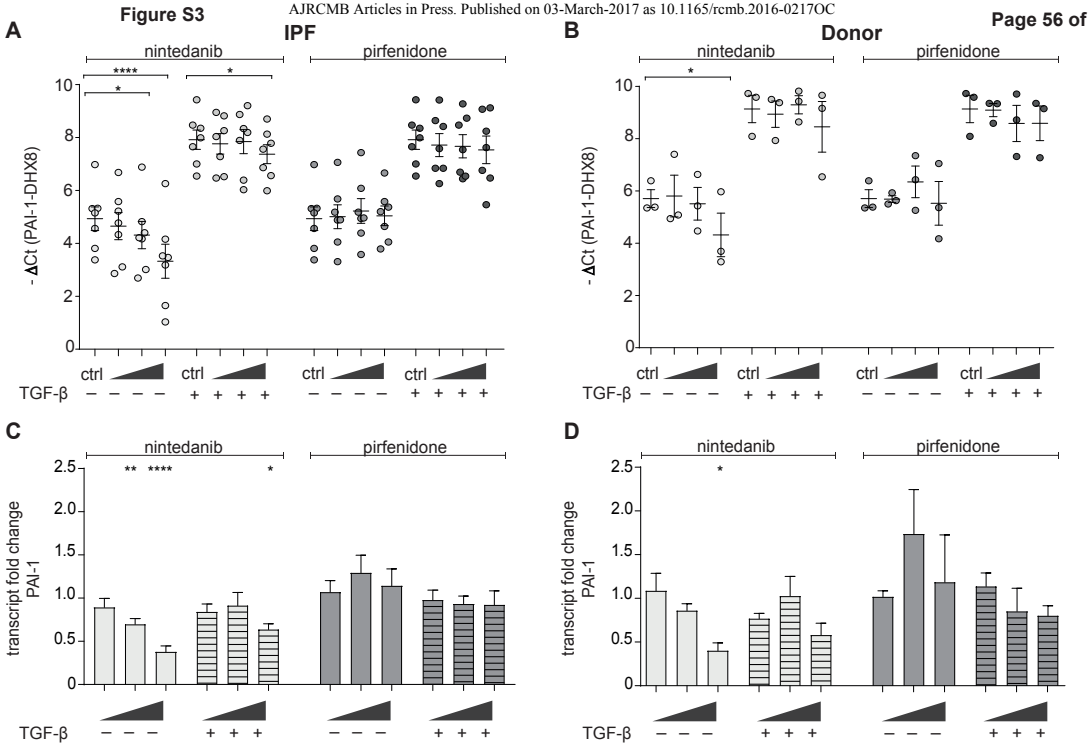

AJRCMB Articles in Press. Published on 03-March-2017 as 10.1165/rcmb.2016-0217OC

Figure S4

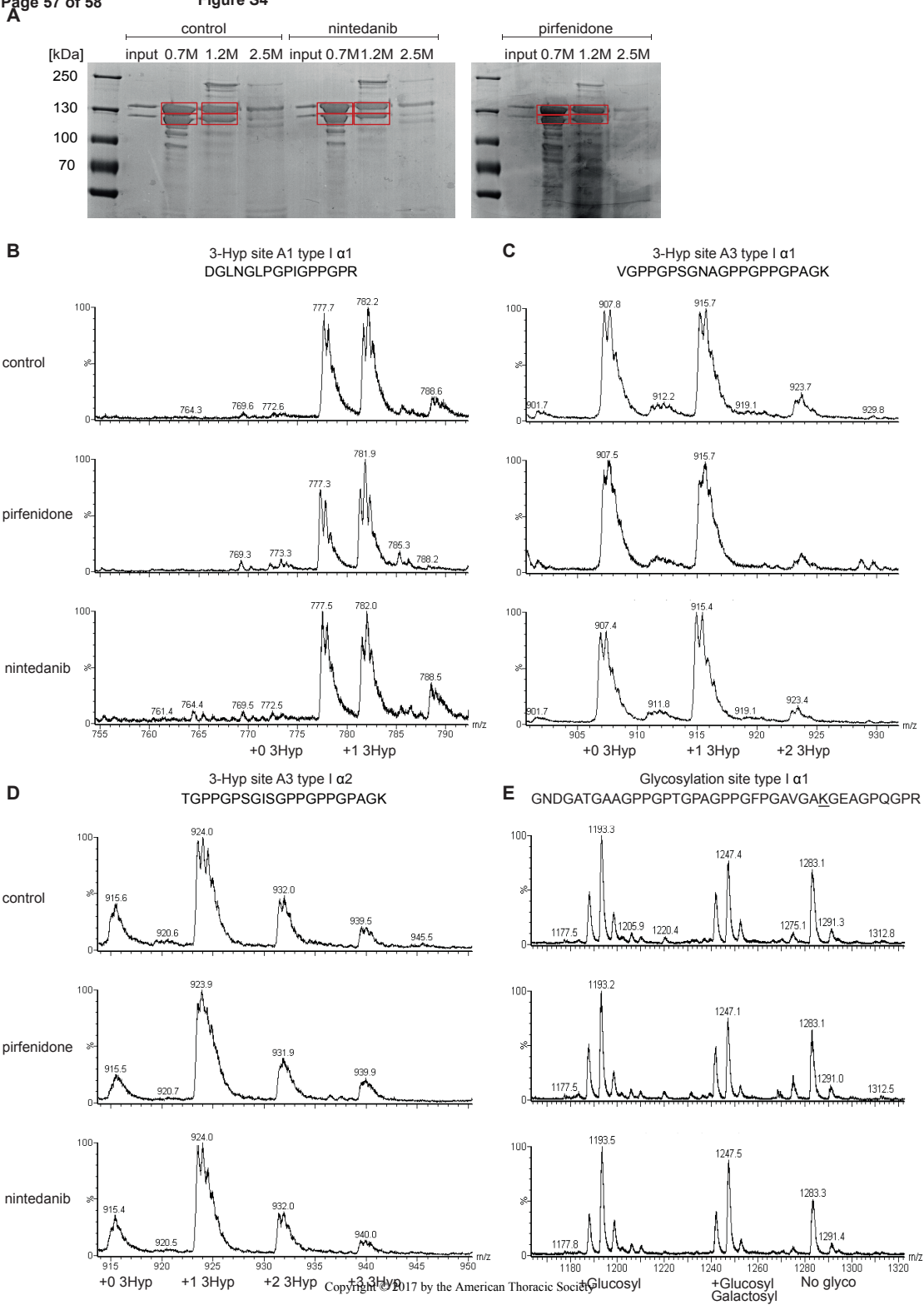

Figure S5

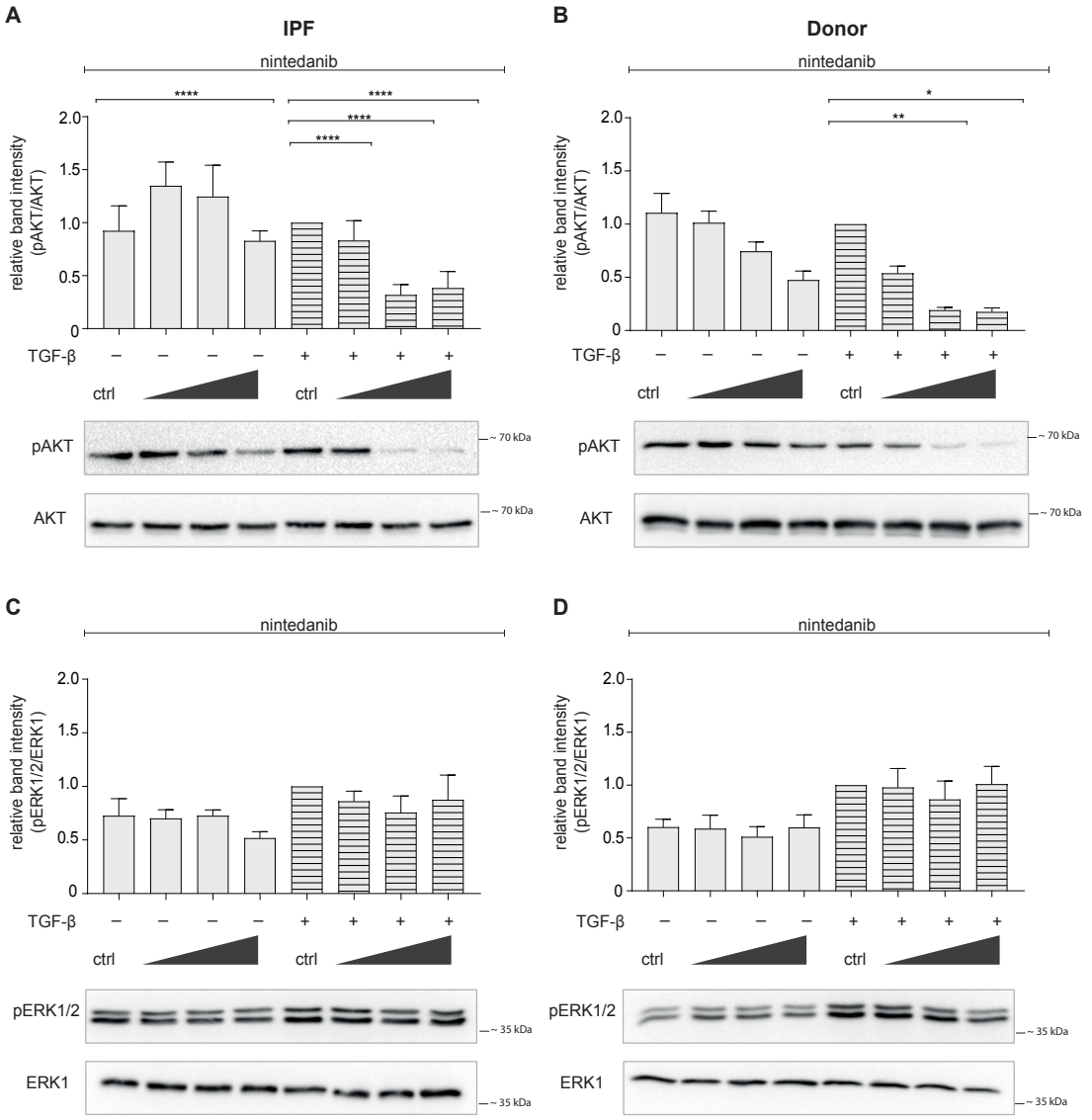

3. Discussion[1]

Collagens play a major role in IPF disease progression, due to excessive accumulation of collagens as well as other ECM proteins which results in the distortion of the normal lung architecture (Wilson and Wynn, 2009; Fernandez and Eickelberg, 2012; Decaris *et al.*, 2014).

Currently, IPF is an irreversible, highly progressive disease and lung fibrosis cannot be resolved. To date, pirfenidone and nintedanib are the only therapeutics that have consistently proven effectiveness in reduction of lung function decline and deceleration of disease progression. Considering that IPF used to be an untreatable disease, their approval constituted a breakthrough for IPF therapy; however, both drugs merely slow down, but do not stop disease progression. Therefore, there is a big need for drugs that can stop the disease progression not just only to slow it down. A promising approach may be the interference with the synthesis and deposition of collagens, given that this would counteract the irreversible distortion of the lung architecture.

Recently we proposed FKBP10, upregulated in IPF and in bleomycin-induced lung fibrosis, as a potential novel drug target in IPF (Staab-Weijnitz *et al.*, 2015) (*cf.* Chapter 2.1). This ER resident protein is mainly expressed by (myo)fibroblasts and its deficiency lead to reduced expression of fibrotic markers including collagen I, collagen V, FN and α-SMA. Most interestingly, collagen secretion of phLF was attenuated in the absence of FKBP10. This effect was comparable to the effect of micromolar concentrations of nintedanib on collagen secretion and even greater than millimolar concentrations of pirfenidone (Staab-Weijnitz *et al.*, 2015) (*cf.* Chapter 2.1).

As mentioned earlier, the immunophilin FKBP10 is a member of FK506 binding proteins that can be inhibited by the binding of FK506 to their PPIase domain. In the case of FKBP10, one of its four PPIase domains can be inhibited by FK506 (Coss *et al.*, 1995; Ishikawa *et al.*, 2008).

Several publications describe the antifibrotic effects of the immunosuppressive drug FK506 in lung fibrosis. Treatment of IPF patients with FK506 in combination with a steroid prevented acute exacerbation (Horita *et al.*, 2011). Furthermore, Nagano and

[1] Parts are based on the discussions in [Staab-Weijnitz *et al.*, 2015; Knüppel *et al.* 2017; Knüppel *et al.*, 2018]

colleagues reported an inhibition of TGF-β-induced collagen synthesis in human lung fibroblasts and a suppression of bleomycin-induced TGF-β receptor I expression upon FK506 treatment. TGF-β receptor I is indispensable for TGF-β signaling which is initiated by TGF-β binding to constitutively active TGF-β receptor II that in turn activates TGF-β receptor I (Derynck and Feng, 1997; Nagano *et al.*, 2006). This result was confirmed in human foreskin fibroblasts where FK506 treatment suppressed the expression of TGF-β receptor I and II, inhibited fibroblast proliferation and TGF-β-induced collagen I expression (Lan *et al.*, 2014). Studies in keloid fibroblasts reported the same effects as Lan and colleagues and in addition an effect on TGF-β-induced fibroblast migration (Wu *et al.*, 2012).
It is tempting to speculate that FK506 exerts its antifibrotic effects via inhibition of FKBP10, however unpublished data from our laboratory revealed that FK506 did not influence collagen secretion *in vitro*. Furthermore, FK506 is only able to inhibit one the four FKBD in FKBP10 (Zeng *et al.*, 1998). Based on that, it is unlikely that the inhibition of FKBP10 by FK506 might be responsible for the antifibrotic effects observed for FK506. The observed antifibrotic effects might be rather translated by another FKBP.

The characteristic aberrant wound healing response in IPF includes aberrant fibroblast adhesion and migration. Data from our laboratory showed that FKBP10 deficiency in phLF significantly decreased fibroblast adhesion and migration capacity, which agrees with observations upon FKBP10 loss in skin myofibroblasts (Knüppel *et al.*, 2018; Liang *et al.*, 2017). Key molecules implicated in these processes, like talin-1, calpain-4, integrin-β1, coronin-1C and fibulin-1, were mostly upregulated in our study. The increase in these molecules directs to a mechanism of the cell to compensate the inhibitory effect of FKBP10 loss on adhesion and migration capacity. Moreover, the activation of major signaling molecules including FAK, Src and ERK was not affected by FKBP10 loss, which further provided a hint for another probably extracellular mechanism besides intracellular regulation of fibroblast migration (Knüppel *et al.*, 2018) (*cf.* Chapter 2.2).
In a recent publication it was shown that siRNA mediated knockdown of α-SMA in phLF reduced cell migration, whereas FAK activation was not changed (Asano *et al.*, 2017). FKBP10 deficiency reduces α-SMA, collagen I and FN, molecules implicated in cell migration (Lafrenie and Yamada, 1996; Gabbiani, 2003; Staab-Weijnitz *et al.*, 2015; Zhao

et al., 2016; Asano *et al.*, 2017), and cell migration is affected by the density of adhesion ligands, by the composition and stiffness (Charras and Sahai, 2014; Burgess *et al.*, 2016). Another collagen implicated in cell migration is collagen VI, one of the major ECM proteins that mediate cell attachment (Aumailley *et al.*, 1989). Collagen VI is an important regulator in wound healing and it plays a role in the 3D meshwork organization of collagen fibers as well as in the 3D organization of FN (Everts *et al.*, 1995; Naugle *et al.*, 2006; Mak, 2014). In recent studies, mutations in *COL6A2* or blocking the collagen VI assembly by an antibody resulted in inhibited wound closing capacity in tendon fibroblasts (Sardone *et al.*, 2016). Interestingly, collagen VI expression was reduced by FKBP10 deficiency; coating culture dishes type VI collagen could compensate the inhibitory effect of FKBP10 loss on phLF migration more efficiently than coating with type I (Knüppel *et al.*, 2018) (*cf.* Chapter 2.2). The major role of collagen VI in ECM organization and the dependency of cell migration on the topography of the ECM put forward the assumption that FKBP10 regulates phLF migration mainly through collagen VI. The fact that other ECM proteins, including FN, collagen V (Staab-Weijnitz *et al.*, 2015) (*cf.* Chapter 2.1) and collagen III (unpublished data from our laboratory) are also reduced upon FKBP10 knockdown, might indicate that the ECM topography is changed due to FKBP10 deficiency which alters migration and adhesion behavior of the cell and further emphasizes FKBP10 as a promising novel drug target in IPF and important regulator of ECM remodeling.

To date, nintedanib and pirfenidone are used for IPF treatment. Both drugs decelerate disease progression as measured by reduced lung function decline, but their mechanism of action is not entirely elucidated (Blackwell *et al.*, 2014; Richeldi *et al.*, 2014).
Our studies showed that nintedanib and pirfenidone treatment of phLF lead to a reduced amount and an altered appearance of collagen fibril bundles compared to controls. The presence of both drugs reduced the thickness of formed collagen fibrils significantly. Interestingly, nintedanib and pirfenidone decreased collagen V expression, which is increased in IPF. Collagen V is an important factor for the initiation of collagen fibril assembly as a component of collagen I fibrils and a regulator of fiber size (Wenstrup *et al.*, 2004; Parra *et al.*, 2006; Vittal *et al.*, 2013; Knüppel *et al.*, 2017). Additionally, both drugs inhibit collagen I fibril assembly in a dose-dependent manner (Knüppel *et al.*, 2017) (*cf.* Chapter 2.3). These findings present the extracellular inhibition of collagen fibril assembly as a so far unknown mechanism of action of both drugs executed firstly

by the downregulation of collagen V which possibly contributes to the altered appearance of collagen fibrils. Secondly, both drugs might directly interact with triple helical collagen. This interaction of nintedanib and pirfenidone with the collagen triple helix probably masks or alters interaction sites that induced changes in the hydrophobicity or the charges on the triple helical surface (Knüppel *et al.*, 2017) (*cf.* Chapter 2.3).

Overall, the direct comparison of nintedanib and pirfenidone in our studies revealed nintedanib as more effective in regard of the used concentrations, extent and number of targeted fibrotic markers; for example, nintedanib downregulated mRNA and protein levels of collagen I, III and FN in IPF phLF, compared to the negligible effects of pirfenidone (Knüppel *et al.*, 2017) (*cf.* Chapter 2.3). Nintedanib also decreases the expression of FKBP10, a PPIase and collagen chaperone (Ishikawa *et al.*, 2008; Knüppel *et al.*, 2017) (*cf.* Chapter 2.3).

3.1 Targeting Collagen Biosynthesis and Maturation as Therapeutic Strategy in IPF

3.1.1 Targeting intracellular events of collagen biosynthesis

3.1.1.1 Prolyl- and lysyl hydroxylases

Already in the past, several studies have been undertaken to target the collagen biosynthesis and maturation pathway. As already described above, in the ER, collagen is post-translationally modified by enzymes like prolyl- or lysyl hydroxylases. For instance the inhibition of prolyl hydroxylation by e.g. pyridine-2,5-dicarboxylate results in decreased thermal stability of the triple helix and thus to incorrect folding followed by proteolytic degradation (Kagan, 2000). Studies in bleomycin-induced lung fibrosis in mice and in cultured lung fibroblasts showed that treatment with pyridine-2,5-dicarboxylate diminished TGF-β-stimulated collagen production indicating prolyl hydroxylase inhibition as promising drug target in pulmonary fibrosis (Luo *et al.*, 2015).

Collagen lysyl hydroxylation is executed by three different lysyl hydroxylases, LH1, LH2 and LH3 encoded by *PLOD1*, *PLOD2* and *PLOD3* genes. Lysyl hydroxylation in the helical regions is completed by LH1 and LH3 (Takaluoma *et al.*, 2007); LH2 is responsible for lysine hydroxylation in the telopeptide region of collagen (Uzawa *et al.*, 1999; van der Slot

et al., 2003; van der Slot *et al.*, 2004). Telopeptide lysyl hydroxylations are from great importance given that they are needed for pyridinoline crosslink formation by lysyl oxidase (LO) enzymes in the extracellular space (Reiser *et al.*, 1992; Smith-Mungo and Kagan, 1998; Yamauchi and Sricholpech, 2012).

The inhibition of LHs was proposed as antifibrotic strategy; the compound minoxidil was shown to inhibit LHs mRNA as follows: LH1>>LH2b>LH3 (Zuurmond *et al.*, 2005). Overall, there was no reduction of the total amount of pyridinoline cross links when minoxidil was administered, dismissing the compound as antifibrotic drug (Zuurmond *et al.*, 2005). Nevertheless, the potential of LH2 as a possible therapeutic target is reinforced by experiments of Gistelinck *et al.*, revealing that homozygous PLOD2 nonsense mutation in zebrafish resulted in decreased telopeptide hydroxylation, crosslinking and less organized collagen I fibrils (Gistelinck *et al.*, 2016). Interestingly, mutations in LH2 and FKBP10 lead to Bruck syndrome type 1 and 2, respectively, a disease phenotypically related to OI (Gjaltema *et al.*, 2016). Missense mutations of FKBP10 resulting in its loss are found in OI and cause instable collagen trimers and reduced telopeptide lysyl hydroxylation by LH2 (Schwarze *et al.*, 2013). Gjaltema and colleagues reported that FKBP10 is critical for LH2 activity and therefore indirectly affects pyridinoline crosslinking of collagen (Gjaltema *et al.*, 2016). Overall, this highlights intracellular FKBP10 activity as indispensable for extracellular collagen processing and ultimately for collagen fibril formation and stabilization.

3.1.1.2 Collagen Chaperones HSP47 and FKBP10

HSP47 is a collagen-specific chaperone with known binding affinity for collagen I-V (Natsume *et al.*, 1994; Hagiwara *et al.*, 2007; Ishikawa and Bächinger, 2013; Ishikawa *et al.*, 2015). Furthermore, HSP47 interacts with FKBP10 in the ER and both molecules cooperate during post translational maturation of procollagen I (Duran *et al.*, 2015; Ishikawa *et al.*, 2017). Ishikawa *et al.* suggested that FKBP10 might protect HSP47 from aggregation and that their interaction increases their stability. Mutations of HSP47 in humans result in a protein level decrease of both HSP47 and FKBP10 in the cell (Duran *et al.*, 2015; Ishikawa *et al.*, 2017). In a collagen III *in vitro* refolding assay, the addition of both proteins accelerated the reaction and yielded in increased amount folded product (Ishikawa *et al.*, 2017). Based on these results the authors concluded that HSP47 might act as a center molecule directing other collagen binding proteins to their site of action. The binding of FKBP10 at this hub might increase collagen folding (Ishikawa *et al.*, 2017).

Mutation in both *SERPINH1 (HSP47)* and *FKBP10* cause a similar phenotype in OI (Alanay *et al.*, 2010; Christiansen *et al.*, 2010; Marini *et al.*, 2014). Additionally, HSP47 and FKBP10 are increased in bleomycin-induced lung fibrosis and in IPF patient samples (Razzaque *et al.*, 1998; Razzaque *et al.*, 1998; Schiller *et al.*, 2015; Staab-Weijnitz *et al.*, 2015) and deficiency of both is associated with reduced collagen secretion and crosslinking or deficient fibrillogenesis (Ishida *et al.*, 2006; Barnes *et al.*, 2012; Lindert *et al.*, 2015; Staab-Weijnitz *et al.*, 2015). In IPF the major expressed collagens are collagen I and III and HSP47 and FKBP10 are both known to influence their maturation (Laurent, 1986; Taguchi and Razzaque, 2007; Ishikawa *et al.*, 2008; Ishikawa *et al.*, 2017). *In vivo* studies on the inhibition of HSP47 did reduce collagen production and progression of fibrotic lesions (Razzaque and Taguchi, 1997; Sunamoto *et al.*, 1998).
Different approaches have been used in the recent years to inhibit HSP47. For example, antisense oligonucleotides (ASOs) against HSP47 in different models of fibrosis significantly neutralized morphological changes by reducing collagen accumulation (Hagiwara *et al.*, 2007; Hagiwara *et al.*, 2007) and counteracted the increased expression of HSP47, collagen I, III and α-SMA (Nishino *et al.*, 2003).

Taken together, *FKBP10*, *PLOD2* and *SERPINH1* are indispensable for the stability and post-translational modifications of procollagen I (Schwarze *et al.*, 2013), and therefore suitable therapeutic targets in fibrosis. However, it is tempting to speculate that FKBP10 deficiency alone might already results in dysfunctional HSP47 and LH2. As mentioned earlier, FKBP10 might be needed for hindering HSP47 aggregation and LH2 activation.

3.1.2 Targeting extracellular events of collagen biosynthesis

3.1.2.1 Propeptide Proteinases

After the secretion of procollagen, C- and N- terminal propeptide cleavage is executed by BMP-1 (bone morphogenetic protein 1) and ADAMTS (a disintegrin and metalloproteinase with thrombospondin motifs), respectively. The cleavage that generates the telopeptides occurs in the extracellular space and initiates the entropy-driven collagen self-assembly into fibrils (Kadler *et al.*, 1996; Kagan and Li, 2003; Muiznieks and Keeley, 2013).

Due to the importance of BMP-1 and ADAMTS in collagen maturation, studies have been undertaken to analyze the effects of their loss. Nonetheless, knockout of ADAMTS did

not affect collagen I processing indicating the implication of other metalloproteases that could compensate the lack of ADAMTS (Li *et al.*, 2001).
BMP-1, on the other hand has been targeted by several inhibitors to limit fibrosis (Ovens *et al.*, 2000; Fish *et al.*, 2007). However, besides procollagen I there are also other, non-collagen fibril formation-related substrates that get processed by BMP-1, which makes it inhibition unfavorable. (Imamura *et al.*, 1998; Amano *et al.*, 2000; Scott *et al.*, 2000)
Therefore, Chung and colleagues blocked the telopeptide regions of collagen with a specific antibody leading to the impairment of extracellular fibril formation and thereby reduced the amount of collagen by hindering C-terminal propeptide cleavage by BMP-1 and consequently collagen fibril formation (Kadler *et al.*, 1987; Chung *et al.*, 2008).
Hence, impeding telopeptide regions of collagen and thereby fibril self-assembly might be a better approach than the direct inhibition of C- and N-terminal proteinases.

3.1.2.2 Lysyl oxidases

The lysyl oxidase (LO) family compromises five paralogues, including the enzymes lysyl oxidase (LOX) and LOX like 1-4 (LOXL1-4). LO are secreted into the extracellular space and LOX and LOXL1 are proteolytically activated by proteinases like BMP-1 (Kagan, 2000). Aberrant regulation of LO is associated with IPF and liver fibrosis (Kagan, 1994; Barry-Hamilton *et al.*, 2010; Chien *et al.*, 2014; Aumiller *et al.*, 2017). It is argued that inhibition of LO would be a useful therapy in fibrosis given that collagen molecules without crosslinks are more prone to proteolytic degradation, as already mentioned above (Vater *et al.*, 1979). Well known inhibitors of LO include β-aminopropionitrile (BAPN) (Tang *et al.*, 1983) and β-bromoethylamine (Liu *et al.*, 1997).

BAPN is a non-specific inhibitor of LO activity and was reported to protect hamsters from bleomycin-induced lung fibrosis and to be beneficial in liver and cardiac fibrosis (Riley *et al.*, 1982; Liu *et al.*, 2016; Martinez-Martinez *et al.*, 2016). In recent studies, Tjin and colleagues tested BAPN and compound A which is specifically inhibiting LOXL2. In contrast to compound A, BAPN inhibited TGF-β-induced collagen remodeling (Tjin *et al.*, 2017). Analysis of LO family protein expression revealed an increase of LOXL1 and LOXL2 in IPF lung tissue in comparison to healthy controls which correlated with an increase in the organization of fibrillar collagen and in TGF-β stimulated NHLF cells, LOXL4 was the most upregulated LO, suggesting that inhibiting a single LO enzyme may

not be sufficient for efficient therapy (Aumiller *et al.*, 2017; Tjin *et al.*, 2017). This is supported by a clinical study on simtuzumab, a humanized monoclonal antibody against LOXL2, which was recently terminated in phase II due to lack of efficacy (Gilead Sciences, 2016).

In addition to the LO family, transglutaminase 2 (TG2) plays an important role in collagen I and FN crosslinking (Verderio *et al.*, 2004). TG2 is upregulated in IPF, liver- and kidney fibrosis (Grenard *et al.*, 2001; Shweke *et al.*, 2008; Olsen *et al.*, 2011; Philp *et al.*, 2017). Inhibition of TG2 in bleomycin-induced lung fibrosis during the post-inflammatory fibrotic phase resulted in a reduction of whole lung collagen (Philp *et al.*, 2017) explainable by a decrease of TG2 mediated collagen crosslinking and thereby an increase of collagen degradation (Olsen *et al.*, 2011). Furthermore, *in vitro* TG2 knockdown in primary human fibroblasts led to less adhesive and migratory properties (Olsen *et al.*, 2011; Philp *et al.*, 2017).

Although the inhibition of crosslinking enzymes showed beneficial effects in models of fibrosis, the process of crosslinking occurs way after collagen fibril formation and, as recently published, a non-specific inhibition of several crosslinking enzymes is required for positive results (Aumiller *et al.*, 2017; Tjin *et al.*, 2017). Therefore, interfering with steps before collagen fibril formation might be more promising and would ultimately hamper the supramolecular assembly of collagen as well.

3.1.2.3 Small Leucine Rich Proteoglycans

Furthermore, small leucine-rich proteoglycans like decorin are also important in collagen fibril formation and with it the structure of collagen matrix and function (Kalamajski and Oldberg, 2010). Decorin binds to collagen I, II, III, VI and TGF-β1 (Reed and Iozzo, 2002). More than one decade ago decorin was already proposed as potential target to limit lung fibrosis (Kolb *et al.*, 2001; Kolb *et al.*, 2001). Decorin is a TGF-β inhibitor and is known to delay collagen fibril formation (Neame *et al.*, 2000; Kolb *et al.*, 2001; Kolb *et al.*, 2001). Overexpression of decorin was able to reduce TGF-β-induced lung fibrosis *in vivo* (Kolb *et al.*, 2001). The antifibrotic effect of decorin was not only observed in the lung, but also in the model of carbon tetrachloride induced liver fibrosis in mice, where the addition of decorin reduced the expression of fibrotic markers and prevented from fibrosis (Ma *et al.*, 2014). The antifibrotic effects of decorin might be executed on the one hand by the

inhibition of TGF-β, however on the other hand by the ability of decorin to inhibit collagen.

3.2 Conclusions and Future Directions

In conclusion, the presented manuscripts within this thesis in the context of the current literature, underline that targeting FKBP10 may be a promising strategy to prevent IPF disease progression. FKBP10 deficiency not only results in the inhibition of intracellular collagen triple helix formation and secretion but can also be anticipated to inhibit extracellular collagen fibril formation and stabilization. The last point is strengthened by the fact that both approved IPF therapeutics, effective in the treatment of IPF, inhibit collagen fibril formation. Additionally, our results indicate FKBP10 as an intracellular regulator of ECM remodeling. These findings put forward the targeting of collagen synthesis and maturation as promising antifibrotic strategy, which is reinforced by the fact that collagen is the main newly synthesized protein in fibrotic ECM (Decaris *et al.*, 2014).

In the past, several inhibitors against intra- and extracellular molecules participating in collagen biosynthesis and maturation have been developed and tested, however FKBP10 inhibition alone might be already very effective in the reduction of fibrotic features: Firstly, FKBP10 knockdown reduced collagen I expression and secretion as well as the expression of other fibrotic markers including collagen V, collagen VI, FN, α-SMA (Ghosh and Vaughan, 2012; Staab-Weijnitz *et al.*, 2015) (*cf.* Chapter 2.1) and collagen III (preliminary data from our laboratory). As mentioned before, *in vivo* collagen fibril formation is inhibited in absence of e.g. FN or collagen V (Kadler *et al.*, 2008).
Additionally, FKBP10 loss also reduced the expression of *Pai-1*, a serine protease inhibitor implicated in a signaling cascade resulting in MMP activation and finally in collagen degradation (Ghosh and Vaughan, 2012; Staab-Weijnitz *et al.*, 2015). Besides the regulation of ECM protein expression by FKBP10, the reduction of Pai-1 is also of importance as described by Gharee-Kermani and colleagues. Mice, deficient of Pai-1 were protected from accumulation of collagen after bleomycin-induced lung fibrosis (Gharaee-Kermani *et al.*, 2008). Furthermore, the recent hypothesis of Ishikawa and colleagues that FKBP10 might be needed to prevent HSP47 aggregation is another sign for the wide range of antifibrotic effects of FKBP10 deficiency (Ishikawa *et al.*, 2017).

Secondly, FKBP10 deficiency decreased phLF migration, an important feature of IPF, by downregulation of collagen VI and to lesser extent by collagen I (*cf.* Chapter 2.2), likely due to the need of FKBP10 for collagen VI triple helix formation, like it is needed for collagen I and III (Ishikawa *et al.*, 2008; Ishikawa and Bächinger, 2013; Ishikawa *et al.*, 2015; Ishikawa *et al.*, 2017). Given that ECM proteins including collagen I, V and FN expression is changed upon FKBP10 loss might point to an overall change of ECM topography and thereby reduces adhesive and migratory behavior of phLF (Knüppel *et al.*, 2018) (*cf.* Chapter 2.2).

Interestingly, loss of FKBP10 through missense mutation in another collagen related disorder, OI, resulted in unstable collagen with reduced extracellular crosslinking due to decreased lysyl hydroxylation in the telopeptide region of collagen, indicating FKBP10 as indirect modulator of lysyl hydroxylation of telopeptides through LH2 activity regulation, and thereby the extend of extracellular crosslinks (Barnes *et al.*, 2012; Schwarze *et al.*, 2013; Gjaltema *et al.*, 2016; Chen *et al.*, 2017; Duran *et al.*, 2017). Besides LH2 activity, FKBP10 might also indirectly influence LH1 activity as well. P3H4 (Sc65) forms a complex with P3H3 and cyclophilin B in the ER, affecting LH1 activity and P3H4 loss resulted in altered lysine hydroxylation and cross linking (Heard *et al.*, 2016). Unpublished data from our laboratory show that FKBP10 deficiency led to reduced mRNA levels of P3H4 in phLF, indicating FKBP10 as an potential indirect modulator of lysine hydroxylation of helical regions by LH1 and an modulator of telopeptide regions by LH2 (Uzawa *et al.*, 1999; van der Slot *et al.*, 2003; van der Slot *et al.*, 2004; Takaluoma *et al.*, 2007). Interestingly, nintedanib treatment of phLF reduced P3H4 mRNA and protein levels as well (preliminary data from our laboratory).

The extent of post translational modifications like lysyl hydroxylation of collagen determines fibril formation, extracellular intermolecular collagen crosslinking and thereby the stability of mature collagen molecules (Yamauchi and Shiiba, 2008).

Extracellular intermolecular crosslinking of collagen fibrils by LO and TG2 is a step after collagen fibril formation and crosslinked fibrillar collagen is more resistant to proteasomal degradation (Prockop and Kivirikko, 1995; Robins, 2007; Manka *et al.*, 2012; Panwar *et al.*, 2013). Clinical studies in phase II on a monoclonal antibody against LOXL2 were terminated due to inefficacy (Gilead Sciences, 2016).

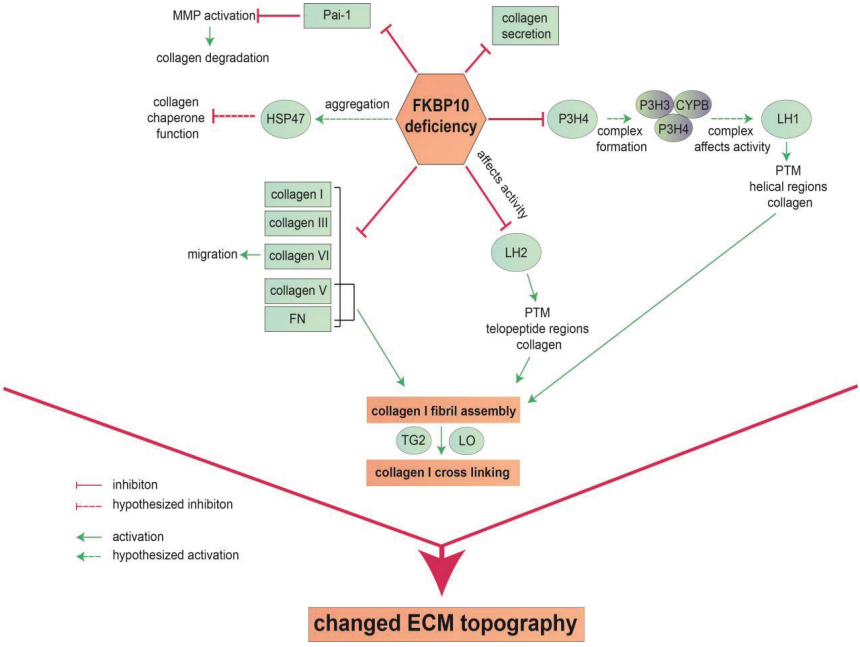

Figure 5. Effects of FKBP10 deficiency. FKBP10 deficiency leads to several antifibrotic effects based on altered collagen or fibrotic marker expression. FKBP10 loss reduces collagen secretion and collagen I, III, V, FN expression. Collagen V and FN in turn are needed for extracellular collagen I fibril formation *in vivo*. FKBP10 downregulates collagen VI expression which in turn leads to reduced cell migration. FKBP10 might be needed to prevent HSP47 aggregation, which is needed for collagen triple helix formation, like FKBP10. P3H4 forms a complex with P3H3 and Cyclophilin B (CYPB) influencing LH1 activity. LH1 is needed for the generation of PTM in the helical regions of collagen. FKBP10 is a known modulator of LH2 activity. LH2 is responsible for PTMs in the telopeptide regions of collagen I, which are important in collagen fibril formation. Missing PTMs result in aberrant collagen fibril formation, followed by impaired collagen crosslinking and ultimately in an altered ECM topography. (Source: Larissa Knüppel)

Therefore, either inhibition of intracellular collagen maturation, e.g. in the ER or inhibition of extracellular collagen fibril assembly might be a more promising strategy to fight IPF disease progression than targeting the subsequent extracellular intermolecular collagen crosslinking. In the past, inhibition of collagen fibril formation as potential antifibrotic strategy has been already proposed and is now strengthened by the fact that both approved IPF therapeutics also act on these levels (Chung, *et al.*, 2008; Knüppel *et al.*, 2017) (*cf.* Chapter 2.3).

Future work will include the analysis of the effect of FKBP10 loss on prolyl- and lysyl hydroxylases in phLF, to get additional insights into the functions of FKBP10 as a regulator of intracellular ECM remodeling. To date, there is limited information about how changes in PTMs of collagen influence the disease progression of IPF.

Our study was limited by the fact that, for functional analysis, we did not go beyond cell culture experiments. Nevertheless, at the same time it is a strength of this study that experiments were performed in the relevant cell type, phLF including such derived from IPF patients, and with physiological relevant concentrations of TGF-β1 and 2-phosphoascorbate.
Moreover, the effect of FKBP10 deficiency was just analyzed in a 2D environment. However, the generation of cell derived matrices was established (results not shown), which can be used to study migration and adhesion behavior in a 3D environment in future studies

The main limitation of our study was that effect of FKBP10 deficiency was not studied *in vivo*. Given that FKBP10 knock out mice are embryonically lethal (Lietman *et al.*, 2014), we were reliant on the establishment of a collaboration to receive conditional knockout mice of FKBP10 from Brendan Lee (Texas). Additionally, a fibroblast specific Col1A2-Cre-driver was not commercially available for a long period of time.

Therefore, in the future the effects of FKBP10 deficiency of our *in vitro* studies will be compared with *in vivo* experiments of FKBP10 conditional knockout mice in a model of bleomycin-induced lung fibrosis.

The potential of FKBP10 as a drug target in IPF indicates the need for the development of effective inhibitors against FKBP10, which can be either small molecules or ASOs. The inhibition of FKBP10 might not interfere with normal tissue repair as FKBP10 is mainly expressed during embryonal development whereas it is little expressed in adult tissues but reactivated after lung injury (Zeng *et al.*, 1998; Patterson *et al.*, 2005; Ishikawa *et al.*, 2008). However, the development and *in silico* screening of small molecule inhibitors against FKBP10 might be a challenge since it`s structure is not fully elucidated so far. Therefore, the design of FKBP10 ASOs might have higher potential to succeed. Promising results have already been achieved in bleomycin-induced lung fibrosis in rats with the administration of ASOs specific for HSP47, a collagen chaperone like FKBP10,

due to the reduction of fibrotic lesions and suppressed collagen accumulation (Hagiwara *et al.*, 2007).

In conclusion, our findings suggest direct interference with collagen biosynthesis and maturation as a promising therapeutic strategy to fight IPF, with emphasis on targeting FKBP10. As depicted in figure 5, FKBP10 deficiency results in a wide range of ECM changing effects that might lead to an overall altered ECM topography and might be thereby beneficial to prevent IPF disease progression.

4. References

Adamali, H. I. and T. M. Maher (2012). "Current and novel drug therapies for idiopathic pulmonary fibrosis." Drug Des Devel Ther **6**: 261-272.

Alanay, Y., H. Avaygan, N. Camacho, G. E. Utine, K. Boduroglu, D. Aktas, M. Alikasifoglu, E. Tuncbilek, D. Orhan, F. T. Bakar, B. Zabel, A. Superti-Furga, L. Bruckner-Tuderman, C. J. Curry, S. Pyott, P. H. Byers, D. R. Eyre, D. Baldridge, B. Lee, A. E. Merrill, E. C. Davis, D. H. Cohn, N. Akarsu and D. Krakow (2010). "Mutations in the gene encoding the RER protein FKBP65 cause autosomal-recessive osteogenesis imperfecta." Am J Hum Genet **86**(4): 551-559.

Allen, R. J., J. Porte, R. Braybrooke, C. Flores, T. E. Fingerlin, J. M. Oldham, B. Guillen-Guio, S. F. Ma, T. Okamoto, A. E. John, M. Obeidat, I. V. Yang, A. Henry, R. B. Hubbard, V. Navaratnam, G. Saini, N. Thompson, H. L. Booth, S. P. Hart, M. R. Hill, N. Hirani, T. M. Maher, R. J. McAnulty, A. B. Millar, P. L. Molyneaux, H. Parfrey, D. M. Rassl, M. K. B. Whyte, W. A. Fahy, R. P. Marshall, E. Oballa, Y. Bosse, D. C. Nickle, D. D. Sin, W. Timens, N. Shrine, I. Sayers, I. P. Hall, I. Noth, D. A. Schwartz, M. D. Tobin, L. V. Wain and R. G. Jenkins (2017). "Genetic variants associated with susceptibility to idiopathic pulmonary fibrosis in people of European ancestry: a genome-wide association study." Lancet Respir Med **5**(11): 869-880.

Amano, S., I. C. Scott, K. Takahara, M. Koch, M. F. Champliaud, D. R. Gerecke, D. R. Keene, D. L. Hudson, T. Nishiyama, S. Lee, D. S. Greenspan and R. E. Burgeson (2000). "Bone morphogenetic protein 1 is an extracellular processing enzyme of the laminin 5 gamma 2 chain." J Biol Chem **275**(30): 22728-22735.

Arora, P. D., M. F. Manolson, G. P. Downey, J. Sodek and C. A. McCulloch (2000). "A novel model system for characterization of phagosomal maturation, acidification, and intracellular collagen degradation in fibroblasts." J Biol Chem **275**(45): 35432-35441.

Asano, S., S. Ito, K. Takahashi, K. Furuya, M. Kondo, M. Sokabe and Y. Hasegawa (2017). "Matrix stiffness regulates migration of human lung fibroblasts." Physiol Rep **5**(9).

Aumailley, M., K. Mann, H. von der Mark and R. Timpl (1989). "Cell attachment properties of collagen type VI and Arg-Gly-Asp dependent binding to its alpha 2(VI) and alpha 3(VI) chains." Exp Cell Res **181**(2): 463-474.

Aumiller, V., B. Strobel, M. Romeike, M. Schuler, B. E. Stierstorfer and S. Kreuz (2017). "Comparative analysis of lysyl oxidase (like) family members in pulmonary fibrosis." Sci Rep **7**(1): 149.

Bächinger, H. P., P. Bruckner, R. Timpl, D. J. Prockop and J. Engel (1980). "Folding mechanism of the triple helix in type-III collagen and type-III pN-collagen. Role of disulfide bridges and peptide bond isomerization." Eur J Biochem **106**(2): 619-632.

Bächinger, H. P., N. P. Morris and J. M. Davis (1993). "Thermal stability and folding of the collagen triple helix and the effects of mutations in osteogenesis imperfecta on the triple helix of type I collagen." Am J Med Genet **45**(2): 152-162.

Barnes, A. M., W. A. Cabral, M. Weis, E. Makareeva, E. L. Mertz, S. Leikin, D. Eyre, C. Trujillo and J. C. Marini (2012). "Absence of FKBP10 in recessive type XI osteogenesis imperfecta leads to diminished collagen cross-linking and reduced collagen deposition in extracellular matrix." Hum Mutat **33**(11): 1589-1598.

Barry-Hamilton, V., R. Spangler, D. Marshall, S. McCauley, H. M. Rodriguez, M. Oyasu, A. Mikels, M. Vaysberg, H. Ghermazien, C. Wai, C. A. Garcia, A. C. Velayo, B. Jorgensen, D. Biermann, D. Tsai, J. Green, S. Zaffryar-Eilot, A. Holzer, S. Ogg, D. Thai, G. Neufeld, P. Van Vlasselaer and V. Smith (2010). "Allosteric inhibition of lysyl oxidase-like-2 impedes the development of a pathologic microenvironment." Nat Med **16**(9): 1009-1017.

Bhattacharyya, P., D. Acharya and S. Roychowdhury (2007). "Role of Matrix Metalloproteinases in the Pathophysiology of Idiopathic Pulmonary Fibrosis." Lung India **24**: 61-65.

Birk, D. E., J. M. Fitch, J. P. Babiarz and T. F. Linsenmayer (1988). "Collagen type I and type V are present in the same fibril in the avian corneal stroma." J Cell Biol **106**(3): 999-1008.

Blackwell, T. S., A. M. Tager, Z. Borok, B. B. Moore, D. A. Schwartz, K. J. Anstrom, Z. Bar-Joseph, P. Bitterman, M. R. Blackburn, W. Bradford, K. K. Brown, H. A. Chapman, H. R. Collard, G. P. Cosgrove, R. Deterding, R. Doyle, K. R. Flaherty, C. K. Garcia, J. S. Hagood, C. A. Henke, E. Herzog, C. M. Hogaboam, J. C. Horowitz, T. E. King, Jr., J. E. Loyd, W. E. Lawson, C. B. Marsh, P. W. Noble, I. Noth, D. Sheppard, J. Olsson, L. A. Ortiz, T. G. O'Riordan, T. D. Oury, G. Raghu, J. Roman, P. J. Sime, T. H. Sisson, D. Tschumperlin, S. M. Violette, T. E. Weaver, R. G. Wells, E. S. White, N. Kaminski, F. J. Martinez, T. A. Wynn, V. J. Thannickal and J. P. Eu (2014). "Future directions in idiopathic pulmonary fibrosis research. An NHLBI workshop report." Am J Respir Crit Care Med **189**(2): 214-222.

Booth, A. J., R. Hadley, A. M. Cornett, A. A. Dreffs, S. A. Matthes, J. L. Tsui, K. Weiss, J. C. Horowitz, V. F. Fiore, T. H. Barker, B. B. Moore, F. J. Martinez, L. E. Niklason and E. S. White (2012). "Acellular normal and fibrotic human lung matrices as a culture system for in vitro investigation." Am J Respir Crit Care Med **186**(9): 866-876.

Burgess, J. K., T. Mauad, G. Tjin, J. C. Karlsson and G. Westergren-Thorsson (2016). "The extracellular matrix - the under-recognized element in lung disease?" J Pathol **240**(4): 397-409.

Canty, E. G. and K. E. Kadler (2005). "Procollagen trafficking, processing and fibrillogenesis." J Cell Sci **118**(Pt 7): 1341-1353.

Carragher, N. O. and M. C. Frame (2004). "Focal adhesion and actin dynamics: a place where kinases and proteases meet to promote invasion." Trends Cell Biol **14**(5): 241-249.

Chang, Y. Z., L. Yang and C. Q. Yang (2008). "Migration of hepatic stellate cells in fibrotic microenvironment of diseased liver model." Hepatobiliary Pancreat Dis Int **7**(4): 401-405.

Charras, G. and E. Sahai (2014). "Physical influences of the extracellular environment on cell migration." Nat Rev Mol Cell Biol **15**(12): 813-824.

Chen, C. Z. and M. Raghunath (2009). "Focus on collagen: in vitro systems to study fibrogenesis and antifibrosis state of the art." Fibrogenesis Tissue Repair **2**: 7.

Chen, Y., M. Terajima, P. Banerjee, H. Guo, X. Liu, J. Yu, M. Yamauchi and J. M. Kurie (2017). "FKBP65-dependent peptidyl-prolyl isomerase activity potentiates the lysyl hydroxylase 2-driven collagen cross-link switch." Sci Rep **7**: 46021.

Chien, J. W., T. J. Richards, K. F. Gibson, Y. Zhang, K. O. Lindell, L. Shao, S. K. Lyman, J. I. Adamkewicz, V. Smith, N. Kaminski and T. O'Riordan (2014). "Serum lysyl oxidase-like 2 levels and idiopathic pulmonary fibrosis disease progression." Eur Respir J **43**(5): 1430-1438.

Christiansen, H. E., U. Schwarze, S. M. Pyott, A. AlSwaid, M. Al Balwi, S. Alrasheed, M. G. Pepin, M. A. Weis, D. R. Eyre and P. H. Byers (2010). "Homozygosity for a missense mutation in SERPINH1, which encodes the collagen chaperone protein HSP47, results in severe recessive osteogenesis imperfecta." Am J Hum Genet **86**(3): 389-398.

Chung, H. J., A. Steplewski, K. Y. Chung, J. Uitto, A. Fertala (2008). "Collagen fibril formation - a new target to limit fibrosis." J Biol Chem **283**(38): 25879-25886.

Clarke, D. L., A. M. Carruthers, T. Mustelin and L. A. Murray (2013). "Matrix regulation of idiopathic pulmonary fibrosis: the role of enzymes." Fibrogenesis Tissue Repair **6**(1): 20.

Conte, E., E. Gili, E. Fagone, M. Fruciano, M. Iemmolo and C. Vancheri (2014). "Effect of pirfenidone on proliferation, TGF-beta-induced myofibroblast differentiation and fibrogenic activity of primary human lung fibroblasts." European Journal of Pharmaceutical Sciences **58**: 13-19.

Correale, M., A. Totaro, D. Lacedonia, D. Montrone, M. Di Biase, M. P. Barbaro Foschino and N. D. Brunetti (2013). "Novelty in treatment of pulmonary fibrosis: pulmonary hypertension drugs and others." Cardiovasc Hematol Agents Med Chem **11**(3): 169-178.

Coss, M. C., D. Winterstein, R. C. Sowder, 2nd and S. L. Simek (1995). "Molecular cloning, DNA sequence analysis, and biochemical characterization of a novel 65-kDa FK506-binding protein (FKBP65)." J Biol Chem **270**(49): 29336-29341.

Dancer, R. C., A. M. Wood and D. R. Thickett (2011). "Metalloproteinases in idiopathic pulmonary fibrosis." Eur Respir J **38**(6): 1461-1467.

Datta, A., C. J. Scotton and R. C. Chambers (2011). "Novel therapeutic approaches for pulmonary fibrosis." British Journal of Pharmacology **163**(1): 141-172.

Davis, E. C., T. J. Broekelmann, Y. Ozawa and R. P. Mecham (1998). "Identification of tropoelastin as a ligand for the 65-kD FK506-binding protein, FKBP65, in the secretory pathway." J Cell Biol **140**(2): 295-303.

Decaris, M. L., M. Gatmaitan, S. FlorCruz, F. Luo, K. Li, W. E. Holmes, M. K. Hellerstein, S. M. Turner and C. L. Emson (2014). "Proteomic analysis of altered extracellular matrix turnover in bleomycin-induced pulmonary fibrosis." Molecular & Cellular Proteomics **13**(7): 1741-1752.

Derynck, R. and X. H. Feng (1997). "TGF-beta receptor signaling." Biochim Biophys Acta **1333**(2): F105-150.

Duran, I., J. H. Martin, M. A. Weis, P. Krejci, P. Konik, B. Li, Y. Alanay, C. Lietman, B. Lee, D. Eyre, D. H. Cohn and D. Krakow (2017). "A Chaperone Complex Formed by HSP47, FKBP65, and BiP Modulates Telopeptide Lysyl Hydroxylation of Type I Procollagen." J Bone Miner Res **32**(6): 1309-1319.

Duran, I., L. Nevarez, A. Sarukhanov, S. Wu, K. Lee, P. Krejci, M. Weis, D. Eyre, D. Krakow and D. H. Cohn (2015). "HSP47 and FKBP65 cooperate in the synthesis of type I procollagen." Human Molecular Genetics **24**(7): 1918-1928.

Everts, V., W. Korper, A. Niehof, I. Jansen and W. Beertsen (1995). "Type VI collagen is phagocytosed by fibroblasts and digested in the lysosomal apparatus: involvement of collagenase, serine proteinases and lysosomal enzymes." Matrix Biol **14**(8): 665-676.

Everts, V., E. van der Zee, L. Creemers and W. Beertsen (1996). "Phagocytosis and intracellular digestion of collagen, its role in turnover and remodelling." Histochem J **28**(4): 229-245.

Fernandez, I. E. and O. Eickelberg (2012). "The impact of TGF-beta on lung fibrosis: from targeting to biomarkers." Proceedings of the American Thoracic Society **9**(3): 111-116.

Fernandez, I. E. and O. Eickelberg (2012). "New cellular and molecular mechanisms of lung injury and fibrosis in idiopathic pulmonary fibrosis." Lancet **380**(9842): 680-688.

Fingerlin, T. E., E. Murphy, W. Zhang, A. L. Peljto, K. K. Brown, M. P. Steele, J. E. Loyd, G. P. Cosgrove, D. Lynch, S. Groshong, H. R. Collard, P. J. Wolters, W. Z. Bradford, K. Kossen, S. D. Seiwert, R. M. du Bois, C. K. Garcia, M. S. Devine, G. Gudmundsson, H. J. Isaksson, N. Kaminski, Y. Zhang, K. F. Gibson, L. H. Lancaster, J. D. Cogan, W. R. Mason, T. M. Maher, P. L. Molyneaux, A. U. Wells, M. F. Moffatt, M. Selman, A. Pardo, D. S. Kim, J. D. Crapo, B. J. Make, E. A. Regan, D. S. Walek, J. J. Daniel, Y. Kamatani, D. Zelenika, K. Smith, D. McKean, B. S. Pedersen, J. Talbert, R. N. Kidd, C. R. Markin, K. B. Beckman, M. Lathrop, M. I. Schwarz and D. A. Schwartz (2013). "Genome-wide association study identifies multiple susceptibility loci for pulmonary fibrosis." Nat Genet **45**(6): 613-620.

Fish, P. V., G. A. Allan, S. Bailey, J. Blagg, R. Butt, M. G. Collis, D. Greiling, K. James, J. Kendall, A. McElroy, D. McCleverty, C. Reed, R. Webster and G. A. Whitlock (2007). "Potent and selective nonpeptidic inhibitors of procollagen C-proteinase." J Med Chem **50**(15): 3442-3456.

Fujimoto, H., T. Kobayashi and A. Azuma (2015). "Idiopathic Pulmonary Fibrosis: Treatment and Prognosis." Clin Med Insights Circ Respir Pulm Med **9**(Suppl 1): 179-185.

Gabbiani, G. (2003). "The myofibroblast in wound healing and fibrocontractive diseases." J Pathol **200**(4): 500-503.

Gharaee-Kermani, M., B. Hu, S. H. Phan and M. R. Gyetko (2008). "The role of urokinase in idiopathic pulmonary fibrosis and implication for therapy." Expert Opin Investig Drugs **17**(6): 905-916.

Ghosh, A. K. and D. E. Vaughan (2012). "PAI-1 in tissue fibrosis." J Cell Physiol **227**(2): 493-507.

Giannandrea, M. and W. C. Parks (2014). "Diverse functions of matrix metalloproteinases during fibrosis." Dis Model Mech **7**(2): 193-203.

Gilead Sciences, I. (2016). "Gilead Terminates Phase 2 Study of Simtuzumab in Patients With Idiopathic Pulmonary Fibrosis " Retrieved March 11, 2016, from

http://www.gilead.com/news/press-releases/2016/1/gilead-terminates-phase-2-study-of-simtuzumab-in-patients-with-idiopathic-pulmonary-fibrosis.

Gistelinck, C., P. E. Witten, A. Huysseune, S. Symoens, F. Malfait, D. Larionova, P. Simoens, M. Dierick, L. Van Hoorebeke, A. De Paepe, R. Y. Kwon, M. Weis, D. R. Eyre, A. Willaert and P. J. Coucke (2016). "Loss of Type I Collagen Telopeptide Lysyl Hydroxylation Causes Musculoskeletal Abnormalities in a Zebrafish Model of Bruck Syndrome." J Bone Miner Res **31**(11): 1930-1942.

Gjaltema, R. A., M. M. van der Stoel, M. Boersema and R. A. Bank (2016). "Disentangling mechanisms involved in collagen pyridinoline cross-linking: The immunophilin FKBP65 is critical for dimerization of lysyl hydroxylase 2." Proc Natl Acad Sci U S A **113**(26): 7142-7147.

Grenard, P., S. Bresson-Hadni, S. El Alaoui, M. Chevallier, D. A. Vuitton and S. Ricard-Blum (2001). "Transglutaminase-mediated cross-linking is involved in the stabilization of extracellular matrix in human liver fibrosis." J Hepatol **35**(3): 367-375.

Hagiwara, S., H. Iwasaka, S. Matsumoto and T. Noguchi (2007). "Antisense oligonucleotide inhibition of heat shock protein (HSP) 47 improves bleomycin-induced pulmonary fibrosis in rats." Respir Res **8**: 37.

Hagiwara, S., H. Iwasaka, S. Matsumoto and T. Noguchi (2007). "An antisense oligonucleotide to HSP47 inhibits paraquat-induced pulmonary fibrosis in rats." Toxicology **236**(3): 199-207.

Heard, M. E., R. Besio, M. Weis, J. Rai, D. M. Hudson, M. Dimori, S. M. Zimmerman, J. A. Kamykowski, W. R. Hogue, F. L. Swain, M. S. Burdine, S. G. Mackintosh, A. J. Tackett, L. J. Suva, D. R. Eyre and R. Morello (2016). "Sc65-Null Mice Provide Evidence for a Novel Endoplasmic Reticulum Complex Regulating Collagen Lysyl Hydroxylation." PLoS Genet **12**(4): e1006002.

Hinz, B., S. H. Phan, V. J. Thannickal, A. Galli, M. L. Bochaton-Piallat and G. Gabbiani (2007). "The myofibroblast: one function, multiple origins." Am J Pathol **170**(6): 1807-1816.

Horita, N., M. Akahane, Y. Okada, Y. Kobayashi, T. Arai, I. Amano, T. Takezawa, M. To and Y. To (2011). "Tacrolimus and steroid treatment for acute exacerbation of idiopathic pulmonary fibrosis." Intern Med **50**(3): 189-195.

Hostettler, K. E., J. Zhong, E. Papakonstantinou, G. Karakiulakis, M. Tamm, P. Seidel, Q. Sun, J. Mandal, D. Lardinois, C. Lambers and M. Roth (2014). "Anti-fibrotic effects of

nintedanib in lung fibroblasts derived from patients with idiopathic pulmonary fibrosis." Respiratory Research **15**: 157.

Hudson, D. M. and D. R. Eyre (2013). "Collagen prolyl 3-hydroxylation: a major role for a minor post-translational modification?" Connective Tissue Research **54**(4-5): 245-251.

Hulmes, D. J. (2002). "Building collagen molecules, fibrils, and suprafibrillar structures." J Struct Biol **137**(1-2): 2-10.

Imamura, Y., B. M. Steiglitz and D. S. Greenspan (1998). "Bone morphogenetic protein-1 processes the NH2-terminal propeptide, and a furin-like proprotein convertase processes the COOH-terminal propeptide of pro-alpha1(V) collagen." J Biol Chem **273**(42): 27511-27517.

Inase, N., M. Sawada, Y. Ohtani, S. Miyake, S. Isogai, H. Sakashita, Y. Miyazaki and Y. Yoshizawa (2003). "Cyclosporin A followed by the treatment of acute exacerbation of idiopathic pulmonary fibrosis with corticosteroid." Intern Med **42**(7): 565-570.

Ishida, Y., H. Kubota, A. Yamamoto, A. Kitamura, H. P. Bächinger and K. Nagata (2006). "Type I collagen in Hsp47-null cells is aggregated in endoplasmic reticulum and deficient in N-propeptide processing and fibrillogenesis." Molecular Biology of the Cell **17**(5): 2346-2355.

Ishikawa, Y. and H. P. Bächinger (2013). "A molecular ensemble in the rER for procollagen maturation." Biochim Biophys Acta **1833**(11): 2479-2491.

Ishikawa, Y., S. Boudko and H. P. Bächinger (2015). "Ziploc-ing the structure: Triple helix formation is coordinated by rough endoplasmic reticulum resident PPIases." Biochimica et Biophysica Acta **1850**(10): 1983-1993.

Ishikawa, Y., P. Holden and H. P. Bächinger (2017). "Heat shock protein 47 and 65-kDa FK506-binding protein weakly but synergistically interact during collagen folding in the endoplasmic reticulum." J Biol Chem **292**(42): 17216-17224.

Ishikawa, Y., J. Vranka, J. Wirz, K. Nagata and H. P. Bächinger (2008). "The rough endoplasmic reticulum-resident FK506-binding protein FKBP65 is a molecular chaperone that interacts with collagens." The Journal of Biological Chemistry **283**(46): 31584-31590.

Jorgensen, K. A., P. B. Koefoed-Nielsen and N. Karamperis (2003). "Calcineurin phosphatase activity and immunosuppression. A review on the role of calcineurin phosphatase activity and the immunosuppressive effect of cyclosporin A and tacrolimus." Scand J Immunol **57**(2): 93-98.

Kaarteenaho-Wiik, R., P. Paakko, R. Herva, J. Risteli and Y. Soini (2004). "Type I and III collagen protein precursors and mRNA in the developing human lung." J Pathol **203**(1): 567-574.

Kadler, K. E., A. Hill and E. G. Canty-Laird (2008). "Collagen fibrillogenesis: fibronectin, integrins, and minor collagens as organizers and nucleators." Curr Opin Cell Biol **20**(5): 495-501.

Kadler, K. E., Y. Hojima and D. J. Prockop (1987). "Assembly of collagen fibrils de novo by cleavage of the type I pC-collagen with procollagen C-proteinase. Assay of critical concentration demonstrates that collagen self-assembly is a classical example of an entropy-driven process." J Biol Chem **262**(32): 15696-15701.

Kadler, K. E., D. F. Holmes, J. A. Trotter and J. A. Chapman (1996). "Collagen fibril formation." Biochemical Journal **316 (Pt 1)**: 1-11.

Kagan, H. M. (1994). "Lysyl oxidase: mechanism, regulation and relationship to liver fibrosis." Pathol Res Pract **190**(9-10): 910-919.

Kagan, H. M. (2000). "Intra- and extracellular enzymes of collagen biosynthesis as biological and chemical targets in the control of fibrosis." Acta Trop **77**(1): 147-152.

Kagan, H. M. and W. Li (2003). "Lysyl oxidase: properties, specificity, and biological roles inside and outside of the cell." J Cell Biochem **88**(4): 660-672.

Kalamajski, S. and A. Oldberg (2010). "The role of small leucine-rich proteoglycans in collagen fibrillogenesis." Matrix Biol **29**(4): 248-253.

Kang, C. B., Y. Hong, S. Dhe-Paganon and H. S. Yoon (2008). "FKBP family proteins: immunophilins with versatile biological functions." Neurosignals **16**(4): 318-325.

Karsdal, M. A., M. J. Nielsen, J. M. Sand, K. Henriksen, F. Genovese, A. C. Bay-Jensen, V. Smith, J. I. Adamkewicz, C. Christiansen and D. J. Leeming (2013). "Extracellular matrix remodeling: the common denominator in connective tissue diseases. Possibilities for evaluation and current understanding of the matrix as more than a passive architecture, but a key player in tissue failure." Assay Drug Dev Technol **11**(2): 70-92.

Kim, D. S., H. R. Collard and T. E. King, Jr. (2006). "Classification and natural history of the idiopathic interstitial pneumonias." Proceedings of the American Thoracic Society **3**(4): 285-292.

King, T. E., Jr., A. Pardo and M. Selman (2011). "Idiopathic pulmonary fibrosis." Lancet **378**(9807): 1949-1961.

Knüppel, L., Y. Ishikawa, M. Aichler, K. Heinzelmann, R. Hatz, J. Behr, A. Walch, H. P. Bächinger, O. Eickelberg and C. A. Staab-Weijnitz (2017). "A Novel Antifibrotic Mechanism of Nintedanib and Pirfenidone. Inhibition of Collagen Fibril Assembly." Am J Respir Cell Mol Biol **57**(1): 77-90.

Knüppel, L., K. Heinzelmann, M. Lindner, R. Hatz, J. Behr, O. Eickelberg, C.A. Staab-Weijnitz (2018). "FKBP10 regulates fibroblast migration via synthesis of collagen VI." Respiratory Research **19**: 67.

Kolb, M., P. J. Margetts, T. Galt, P. J. Sime, Z. Xing, M. Schmidt and J. Gauldie (2001). "Transient transgene expression of decorin in the lung reduces the fibrotic response to bleomycin." Am J Respir Crit Care Med **163**(3 Pt 1): 770-777.

Kolb, M., P. J. Margetts, P. J. Sime and J. Gauldie (2001). "Proteoglycans decorin and biglycan differentially modulate TGF-beta-mediated fibrotic responses in the lung." Am J Physiol Lung Cell Mol Physiol **280**(6): L1327-1334.

Kreuter, M., F. Bonella, M. Wijsenbeek, T. M. Maher and P. Spagnolo (2015). "Pharmacological Treatment of Idiopathic Pulmonary Fibrosis: Current Approaches, Unsolved Issues, and Future Perspectives." Biomed Res Int **2015**: 329481.

Kreuter, M., S. Ehlers-Tenenbaum, K. Palmowski, J. Bruhwyler, U. Oltmanns, T. Muley, C. P. Heussel, A. Warth, M. Kolb and F. J. Herth (2016). "Impact of Comorbidities on Mortality in Patients with Idiopathic Pulmonary Fibrosis." PLoS One **11**(3): e0151425.

Lafrenie, R. M. and K. M. Yamada (1996). "Integrin-dependent signal transduction." J Cell Biochem **61**(4): 543-553.

Lan, C. C., A. H. Fang, P. H. Wu and C. S. Wu (2014). "Tacrolimus abrogates TGF-beta1-induced type I collagen production in normal human fibroblasts through suppressing p38MAPK signalling pathway: implications on treatment of chronic atopic dermatitis lesions." J Eur Acad Dermatol Venereol **28**(2): 204-215.

Lauer-Fields, J. L., D. Juska and G. B. Fields (2002). "Matrix metalloproteinases and collagen catabolism." Biopolymers **66**(1): 19-32.

Laurent, G. J. (1986). "Lung collagen: more than scaffolding." Thorax **41**(6): 418-428.

Leask, A. and D. J. Abraham (2004). "TGF-beta signaling and the fibrotic response." FASEB J **18**(7): 816-827.

Lee, W., J. Sodek and C. A. McCulloch (1996). "Role of integrins in regulation of collagen phagocytosis by human fibroblasts." J Cell Physiol **168**(3): 695-704.

Lehtonen, S. T., A. Veijola, H. Karvonen, E. Lappi-Blanco, R. Sormunen, S. Korpela, U. Zagai, M. C. Skold and R. Kaarteenaho (2016). "Pirfenidone and nintedanib modulate properties of fibroblasts and myofibroblasts in idiopathic pulmonary fibrosis." Respir Res **17**: 14.

Li, S. W., M. Arita, A. Fertala, Y. Bao, G. C. Kopen, T. K. Langsjo, M. M. Hyttinen, H. J. Helminen and D. J. Prockop (2001). "Transgenic mice with inactive alleles for procollagen N-proteinase (ADAMTS-2) develop fragile skin and male sterility." Biochem J **355**(Pt 2): 271-278.

Li, X., L. Zhu, B. Wang, M. Yuan and R. Zhu (2017). "Drugs and Targets in Fibrosis." Front Pharmacol **8**: 855.

Liang, X., B. Chai, R. Duan, Y. Zhou, X. Huang and Q. Li (2017). "Inhibition of FKBP10 Attenuates Hypertrophic Scarring through Suppressing Fibroblast Activity and Extracellular Matrix Deposition." J Invest Dermatol **137**(11): 2326-2335.

Lietman, C. D., A. Rajagopal, E. P. Homan, E. Munivez, M. M. Jiang, T. K. Bertin, Y. Chen, J. Hicks, M. Weis, D. Eyre, B. Lee and D. Krakow (2014). "Connective tissue alterations in Fkbp10-/- mice." Hum Mol Genet **23**(18): 4822-4831.

Lindert, U., M. A. Weis, J. Rai, F. Seeliger, I. Hausser, T. Leeb, D. Eyre, M. Rohrbach and C. Giunta (2015). "Molecular Consequences of the SERPINH1/HSP47 Mutation in the Dachshund Natural Model of Osteogenesis Imperfecta." Journal of Biological Chemistry **290**(29): 17679-17689.

Liu, G., K. Nellaiappan and H. M. Kagan (1997). "Irreversible inhibition of lysyl oxidase by homocysteine thiolactone and its selenium and oxygen analogues. Implications for homocystinuria." J Biol Chem **272**(51): 32370-32377.

Liu, S. B., N. Ikenaga, Z. W. Peng, D. Y. Sverdlov, A. Greenstein, V. Smith, D. Schuppan and Y. Popov (2016). "Lysyl oxidase activity contributes to collagen stabilization during liver fibrosis progression and limits spontaneous fibrosis reversal in mice." FASEB J **30**(4): 1599-1609.

Lu, K. P., G. Finn, T. H. Lee and L. K. Nicholson (2007). "Prolyl cis-trans isomerization as a molecular timer." Nat Chem Biol **3**(10): 619-629.

Luo, Y., W. Xu, H. Chen, D. Warburton, R. Dong, B. Qian, M. Selman, J. Gauldie, M. Kolb and W. Shi (2015). "A novel profibrotic mechanism mediated by TGFbeta-stimulated collagen prolyl hydroxylase expression in fibrotic lung mesenchymal cells." J Pathol **236**(3): 384-394.

Ma, R., S. He, X. Liang, H. Yu, Y. Liang and X. Cai (2014). "Decorin prevents the development of CCl(4)-induced liver fibrosis in mice." Chin Med J (Engl) **127**(6): 1100-1104.

Maher, T. M. (2010). "Pirfenidone in idiopathic pulmonary fibrosis." Drugs Today (Barc) **46**(7): 473-482.

Mak, K. M., Sehgal P, Harris, C K (2014). "Type VI Collagen: Its Biology and Value as a Biomarker of Hepatic Fibrosis." Austin Biomarkers & Diagnosis **1**(2): 9.

Manka, S. W., F. Carafoli, R. Visse, D. Bihan, N. Raynal, R. W. Farndale, G. Murphy, J. J. Enghild, E. Hohenester and H. Nagase (2012). "Structural insights into triple-helical collagen cleavage by matrix metalloproteinase 1." Proc Natl Acad Sci U S A **109**(31): 12461-12466.

Marini, J. C., A. Reich and S. M. Smith (2014). "Osteogenesis imperfecta due to mutations in non-collagenous genes: lessons in the biology of bone formation." Curr Opin Pediatr **26**(4): 500-507.

Martinez-Martinez, E., C. Rodriguez, M. Galan, M. Miana, R. Jurado-Lopez, M. V. Bartolome, M. Luaces, F. Islas, J. Martinez-Gonzalez, N. Lopez-Andres and V. Cachofeiro (2016). "The lysyl oxidase inhibitor (beta-aminopropionitrile) reduces leptin profibrotic effects and ameliorates cardiovascular remodeling in diet-induced obesity in rats." J Mol Cell Cardiol **92**: 96-104.

Mathai, S. K., I. V. Yang, M. I. Schwarz and D. A. Schwartz (2015). "Incorporating genetics into the identification and treatment of Idiopathic Pulmonary Fibrosis." BMC Med **13**: 191.

McKleroy, W., T. H. Lee and K. Atabai (2013). "Always cleave up your mess: targeting collagen degradation to treat tissue fibrosis." Am J Physiol Lung Cell Mol Physiol **304**(11): L709-721.

Mortality, G. B. D. and C. Causes of Death (2015). "Global, regional, and national age-sex specific all-cause and cause-specific mortality for 240 causes of death, 1990-2013: a systematic analysis for the Global Burden of Disease Study 2013." Lancet **385**(9963): 117-171.

Muiznieks, L. D. and F. W. Keeley (2013). "Molecular assembly and mechanical properties of the extracellular matrix: A fibrous protein perspective." Biochim Biophys Acta **1832**(7): 866-875.

Myllarniemi, M. and R. Kaarteenaho (2015). "Pharmacological treatment of idiopathic pulmonary fibrosis - preclinical and clinical studies of pirfenidone, nintedanib, and N-acetylcysteine." Eur Clin Respir J **2**.

Nagano, J., K. Iyonaga, K. Kawamura, A. Yamashita, H. Ichiyasu, T. Okamoto, M. Suga, Y. Sasaki and H. Kohrogi (2006). "Use of tacrolimus, a potent antifibrotic agent, in bleomycin-induced lung fibrosis." Eur Respir J **27**(3): 460-469.

Nagano, M., D. Hoshino, N. Koshikawa, T. Akizawa and M. Seiki (2012). "Turnover of focal adhesions and cancer cell migration." Int J Cell Biol **2012**: 310616.

Nakayama, S., H. Mukae, N. Sakamoto, T. Kakugawa, S. Yoshioka, H. Soda, H. Oku, Y. Urata, T. Kondo, H. Kubota, K. Nagata and S. Kohno (2008). "Pirfenidone inhibits the expression of HSP47 in TGF-beta1-stimulated human lung fibroblasts." Life Sciences **82**(3-4): 210-217.

Natsume, T., T. Koide, S. Yokota, K. Hirayoshi and K. Nagata (1994). "Interactions between collagen-binding stress protein HSP47 and collagen. Analysis of kinetic parameters by surface plasmon resonance biosensor." J Biol Chem **269**(49): 31224-31228.

Naugle, J. E., E. R. Olson, X. Zhang, S. E. Mase, C. F. Pilati, M. B. Maron, H. G. Folkesson, W. I. Horne, K. J. Doane and J. G. Meszaros (2006). "Type VI collagen induces cardiac myofibroblast differentiation: implications for postinfarction remodeling." Am J Physiol Heart Circ Physiol **290**(1): H323-330.

Navaratnam, V., D. L. Forrester and R. B. Hubbard (2016). Epidemiology. Idiopathic Pulmonary Fibrosis. U. Costabel, B. Crestani and A. U. Wells. Plymouth, UK, European Respiratory Society 1-16.

Neame, P. J., C. J. Kay, D. J. McQuillan, M. P. Beales and J. R. Hassell (2000). "Independent modulation of collagen fibrillogenesis by decorin and lumican." Cell Mol Life Sci **57**(5): 859-863.

Nishino, T., M. Miyazaki, K. Abe, A. Furusu, Y. Mishima, T. Harada, Y. Ozono, T. Koji and S. Kohno (2003). "Antisense oligonucleotides against collagen-binding stress protein HSP47 suppress peritoneal fibrosis in rats." Kidney Int **64**(3): 887-896.

Noth, I., Y. Zhang, S. F. Ma, C. Flores, M. Barber, Y. Huang, S. M. Broderick, M. S. Wade, P. Hysi, J. Scuirba, T. J. Richards, B. M. Juan-Guardela, R. Vij, M. K. Han, F. J. Martinez, K. Kossen, S. D. Seiwert, J. D. Christie, D. Nicolae, N. Kaminski and J. G. N. Garcia (2013).

"Genetic variants associated with idiopathic pulmonary fibrosis susceptibility and mortality: a genome-wide association study." Lancet Respir Med **1**(4): 309-317.

Olsen, K. C., R. E. Sapinoro, R. M. Kottmann, A. A. Kulkarni, S. E. Iismaa, G. V. Johnson, T. H. Thatcher, R. P. Phipps and P. J. Sime (2011). "Transglutaminase 2 and its role in pulmonary fibrosis." Am J Respir Crit Care Med **184**(6): 699-707.

Ovens, A., J. A. Joule and K. E. Kadler (2000). "Design and synthesis of acidic dipeptide hydroxamate inhibitors of procollagen C-proteinase." J Pept Sci **6**(9): 489-495.

Panwar, P., X. Du, V. Sharma, G. Lamour, M. Castro, H. Li and D. Bromme (2013). "Effects of cysteine proteases on the structural and mechanical properties of collagen fibers." J Biol Chem **288**(8): 5940-5950.

Parker, M. W., D. Rossi, M. Peterson, K. Smith, K. Sikstrom, E. S. White, J. E. Connett, C. A. Henke, O. Larsson and P. B. Bitterman (2014). "Fibrotic extracellular matrix activates a profibrotic positive feedback loop." J Clin Invest **124**(4): 1622-1635.

Parra, E. R., W. R. Teodoro, A. P. Velosa, C. C. de Oliveira, N. H. Yoshinari and V. L. Capelozzi (2006). "Interstitial and vascular type V collagen morphologic disorganization in usual interstitial pneumonia." The Journal of Histochemistry and Cytochemistry **54**(12): 1315-1325.

Patterson, C. E., W. R. Abrams, N. E. Wolter, J. Rosenbloom and E. C. Davis (2005). "Developmental regulation and coordinate reexpression of FKBP65 with extracellular matrix proteins after lung injury suggest a specialized function for this endoplasmic reticulum immunophilin." Cell Stress Chaperones **10**(4): 285-295.

Philp, C. J., I. Siebeke, D. Clements, S. Miller, A. Habgood, A. E. John, V. Navaratnam, R. B. Hubbard, G. Jenkins and S. R. Johnson (2017). "ECM Crosslinking Enhances Fibroblast Growth and Protects Against Matrix Proteolysis in Lung Fibrosis." Am J Respir Cell Mol Biol.

Pokidysheva, E., K. D. Zientek, Y. Ishikawa, K. Mizuno, J. A. Vranka, N. T. Montgomery, D. R. Keene, T. Kawaguchi, K. Okuyama and H. P. Bächinger (2013). "Posttranslational modifications in type I collagen from different tissues extracted from wild type and prolyl 3-hydroxylase 1 null mice." Journal of Biological Chemistry **288**(34): 24742-24752.

Prockop, D. J. and K. I. Kivirikko (1995). "Collagens: molecular biology, diseases, and potentials for therapy." Annu Rev Biochem **64**: 403-434.

Raghu, G., H. R. Collard, J. J. Egan, F. J. Martinez, J. Behr, K. K. Brown, T. V. Colby, J. F. Cordier, K. R. Flaherty, J. A. Lasky, D. A. Lynch, J. H. Ryu, J. J. Swigris, A. U. Wells, J.

Ancochea, D. Bouros, C. Carvalho, U. Costabel, M. Ebina, D. M. Hansell, T. Johkoh, D. S. Kim, T. E. King, Jr., Y. Kondoh, J. Myers, N. L. Muller, A. G. Nicholson, L. Richeldi, M. Selman, R. F. Dudden, B. S. Griss, S. L. Protzko, H. J. Schunemann and A. E. J. A. C. o. I. P. Fibrosis (2011). "An official ATS/ERS/JRS/ALAT statement: idiopathic pulmonary fibrosis: evidence-based guidelines for diagnosis and management." Am J Respir Crit Care Med **183**(6): 788-824.

Rangarajan, S., A. Kurundkar, D. Kurundkar, K. Bernard, Y. Y. Sanders, Q. Ding, V. B. Antony, J. Zhang, J. Zmijewski and V. J. Thannickal (2015). "Novel Mechanisms for the Anti-Fibrotic Action of Nintedanib." American Journal of Respiratory Cell and Molecular Biology.

Rauch, F. and F. H. Glorieux (2004). "Osteogenesis imperfecta." Lancet **363**(9418): 1377-1385.

Razzaque, M. S., M. A. Hossain, S. Kohno and T. Taguchi (1998). "Bleomycin-induced pulmonary fibrosis in rat is associated with increased expression of collagen-binding heat shock protein (HSP) 47." Virchows Archiv: an international journal of pathology **432**(5): 455-460.

Razzaque, M. S., A. Nazneen and T. Taguchi (1998). "Immunolocalization of collagen and collagen-binding heat shock protein 47 in fibrotic lung diseases." Modern Pathology **11**(12): 1183-1188.

Razzaque, M. S. and T. Taguchi (1997). "Collagen-binding heat shock protein (HSP) 47 expression in anti-thymocyte serum (ATS)-induced glomerulonephritis." J Pathol **183**(1): 24-29.

Reed, C. C. and R. V. Iozzo (2002). "The role of decorin in collagen fibrillogenesis and skin homeostasis." Glycoconj J **19**(4-5): 249-255.

Reiser, K., R. J. McCormick and R. B. Rucker (1992). "Enzymatic and nonenzymatic cross-linking of collagen and elastin." FASEB J **6**(7): 2439-2449.

Renzoni, E., V. Srihari and P. Sestini (2014). "Pathogenesis of idiopathic pulmonary fibrosis: review of recent findings." F1000Prime Rep **6**: 69.

Richeldi, L., R. M. du Bois, G. Raghu, A. Azuma, K. K. Brown, U. Costabel, V. Cottin, K. R. Flaherty, D. M. Hansell, Y. Inoue, D. S. Kim, M. Kolb, A. G. Nicholson, P. W. Noble, M. Selman, H. Taniguchi, M. Brun, F. Le Maulf, M. Girard, S. Stowasser, R. Schlenker-Herceg, B. Disse, H. R. Collard and I. T. Investigators (2014). "Efficacy and safety of

nintedanib in idiopathic pulmonary fibrosis." New England Journal of Medicine **370**(22): 2071-2082.

Riley, D. J., R. A. Berg, R. A. Soltys, J. S. Kerr, H. N. Guss, S. F. Curran and D. L. Laskin (1988). "Neutrophil response following intratracheal instillation of collagen peptides into rat lungs." Exp Lung Res **14**(4): 549-563.

Riley, D. J., J. S. Kerr, R. A. Berg, B. D. Ianni, G. G. Pietra, N. H. Edelman and D. J. Prockop (1982). "beta-Aminopropionitrile prevents bleomycin-induced pulmonary fibrosis in the hamster." Am Rev Respir Dis **125**(1): 67-73.

Robins, S. P. (2007). "Biochemistry and functional significance of collagen cross-linking." Biochem Soc Trans **35**(Pt 5): 849-852.

Rock, J. R., C. E. Barkauskas, M. J. Cronce, Y. Xue, J. R. Harris, J. Liang, P. W. Noble and B. L. Hogan (2011). "Multiple stromal populations contribute to pulmonary fibrosis without evidence for epithelial to mesenchymal transition." Proc Natl Acad Sci U S A **108**(52): E1475-1483.

Rulten, S. L., R. A. Kinloch, H. Tateossian, C. Robinson, L. Gettins and J. E. Kay (2006). "The human FK506-binding proteins: characterization of human FKBP19." Mamm Genome **17**(4): 322-331.

Sardone, F., S. Santi, F. Tagliavini, F. Traina, L. Merlini, S. Squarzoni, M. Cescon, R. Wagener, N. M. Maraldi, P. Bonaldo, C. Faldini and P. Sabatelli (2016). "Collagen VI-NG2 axis in human tendon fibroblasts under conditions mimicking injury response." Matrix Biol **55**: 90-105.

Schaefer, C. J., D. W. Ruhrmund, L. Pan, S. D. Seiwert and K. Kossen (2011). "Antifibrotic activities of pirfenidone in animal models." European Respiratory Review: An Official Journal of the European Respiratory Society **20**(120): 85-97.

Schiller, H. B., I. E. Fernandez, G. Burgstaller, C. Schaab, R. A. Scheltema, T. Schwarzmayr, T. M. Strom, O. Eickelberg and M. Mann (2015). "Time- and compartment-resolved proteome profiling of the extracellular niche in lung injury and repair." Molecular Systems Biology **11**(7): 819.

Schwarze, U., T. Cundy, S. M. Pyott, H. E. Christiansen, M. R. Hegde, R. A. Bank, G. Pals, A. Ankala, K. Conneely, L. Seaver, S. M. Yandow, E. Raney, D. Babovic-Vuksanovic, J. Stoler, Z. Ben-Neriah, R. Segel, S. Lieberman, L. Siderius, A. Al-Aqeel, M. Hannibal, L. Hudgins, E. McPherson, M. Clemens, M. D. Sussman, R. D. Steiner, J. Mahan, R. Smith, K. Anyane-Yeboa, J. Wynn, K. Chong, T. Uster, S. Aftimos, V. R. Sutton, E. C. Davis, L. S.

Kim, M. A. Weis, D. Eyre and P. H. Byers (2013). "Mutations in FKBP10, which result in Bruck syndrome and recessive forms of osteogenesis imperfecta, inhibit the hydroxylation of telopeptide lysines in bone collagen." Hum Mol Genet **22**(1): 1-17.

Scott, I. C., Y. Imamura, W. N. Pappano, J. M. Troedel, A. D. Recklies, P. J. Roughley and D. S. Greenspan (2000). "Bone morphogenetic protein-1 processes probiglycan." J Biol Chem **275**(39): 30504-30511.

Seibold, M. A., A. L. Wise, M. C. Speer, M. P. Steele, K. K. Brown, J. E. Loyd, T. E. Fingerlin, W. Zhang, G. Gudmundsson, S. D. Groshong, C. M. Evans, S. Garantziotis, K. B. Adler, B. F. Dickey, R. M. du Bois, I. V. Yang, A. Herron, D. Kervitsky, J. L. Talbert, C. Markin, J. Park, A. L. Crews, S. H. Slifer, S. Auerbach, M. G. Roy, J. Lin, C. E. Hennessy, M. I. Schwarz and D. A. Schwartz (2011). "A common MUC5B promoter polymorphism and pulmonary fibrosis." N Engl J Med **364**(16): 1503-1512.

Shweke, N., N. Boulos, C. Jouanneau, S. Vandermeersch, G. Melino, J. C. Dussaule, C. Chatziantoniou, P. Ronco and J. J. Boffa (2008). "Tissue transglutaminase contributes to interstitial renal fibrosis by favoring accumulation of fibrillar collagen through TGF-beta activation and cell infiltration." Am J Pathol **173**(3): 631-642.

Smith-Mungo, L. I. and H. M. Kagan (1998). "Lysyl oxidase: properties, regulation and multiple functions in biology." Matrix Biol **16**(7): 387-398.

Song, F., K. Wisithphrom, J. Zhou and L. J. Windsor (2006). "Matrix metalloproteinase dependent and independent collagen degradation." Front Biosci **11**: 3100-3120.

Staab-Weijnitz, C. A., I. E. Fernandez, L. Knüppel, J. Maul, K. Heinzelmann, B. M. Juan-Guardela, E. Hennen, G. Preissler, H. Winter, C. Neurohr, R. Hatz, M. Lindner, J. Behr, N. Kaminski and O. Eickelberg (2015). "FK506-Binding Protein 10, a Potential Novel Drug Target for Idiopathic Pulmonary Fibrosis." Am J Respir Crit Care Med **192**(4): 455-467.

Sunamoto, M., K. Kuze, H. Tsuji, N. Ohishi, K. Yagi, K. Nagata, T. Kita and T. Doi (1998). "Antisense oligonucleotides against collagen-binding stress protein HSP47 suppress collagen accumulation in experimental glomerulonephritis." Lab Invest **78**(8): 967-972.

Taguchi, T. and M. S. Razzaque (2007). "The collagen-specific molecular chaperone HSP47: is there a role in fibrosis?" Trends Mol Med **13**(2): 45-53.

Takaluoma, K., J. Lantto and J. Myllyharju (2007). "Lysyl hydroxylase 2 is a specific telopeptide hydroxylase, while all three isoenzymes hydroxylate collagenous sequences." Matrix Biol **26**(5): 396-403.

Tang, S. S., P. C. Trackman and H. M. Kagan (1983). "Reaction of aortic lysyl oxidase with beta-aminopropionitrile." J Biol Chem **258**(7): 4331-4338.

Tanjore, H., T. S. Blackwell and W. E. Lawson (2012). "Emerging evidence for endoplasmic reticulum stress in the pathogenesis of idiopathic pulmonary fibrosis." Am J Physiol Lung Cell Mol Physiol **302**(8): L721-729.

Tjin, G., E. S. White, A. Faiz, D. Sicard, D. J. Tschumperlin, A. Mahar, E. P. W. Kable and J. K. Burgess (2017). "Lysyl oxidases regulate fibrillar collagen remodelling in idiopathic pulmonary fibrosis." Dis Model Mech **10**(11): 1301-1312.

Uzawa, K., W. J. Grzesik, T. Nishiura, S. A. Kuznetsov, P. G. Robey, D. A. Brenner and M. Yamauchi (1999). "Differential expression of human lysyl hydroxylase genes, lysine hydroxylation, and cross-linking of type I collagen during osteoblastic differentiation in vitro." J Bone Miner Res **14**(8): 1272-1280.

van der Slot, A. J., A. M. Zuurmond, A. F. Bardoel, C. Wijmenga, H. E. Pruijs, D. O. Sillence, J. Brinckmann, D. J. Abraham, C. M. Black, N. Verzijl, J. DeGroot, R. Hanemaaijer, J. M. TeKoppele, T. W. Huizinga and R. A. Bank (2003). "Identification of PLOD2 as telopeptide lysyl hydroxylase, an important enzyme in fibrosis." J Biol Chem **278**(42): 40967-40972.

van der Slot, A. J., A. M. Zuurmond, A. J. van den Bogaerdt, M. M. Ulrich, E. Middelkoop, W. Boers, H. Karel Ronday, J. DeGroot, T. W. Huizinga and R. A. Bank (2004). "Increased formation of pyridinoline cross-links due to higher telopeptide lysyl hydroxylase levels is a general fibrotic phenomenon." Matrix Biol **23**(4): 251-257.

Vater, C. A., E. D. Harris, Jr. and R. C. Siegel (1979). "Native cross-links in collagen fibrils induce resistance to human synovial collagenase." Biochem J **181**(3): 639-645.

Verderio, E. A., T. Johnson and M. Griffin (2004). "Tissue transglutaminase in normal and abnormal wound healing: review article." Amino Acids **26**(4): 387-404.

Verrecchia, F. and A. Mauviel (2007). "Transforming growth factor-beta and fibrosis." World J Gastroenterol **13**(22): 3056-3062.

Vittal, R., E. A. Mickler, A. J. Fisher, C. Zhang, K. Rothhaar, H. Gu, K. M. Brown, A. Emtiazdjoo, J. M. Lott, S. B. Frye, G. N. Smith, G. E. Sandusky, O. W. Cummings and D. S. Wilkes (2013). "Type V collagen induced tolerance suppresses collagen deposition, TGF-beta and associated transcripts in pulmonary fibrosis." PLoS One **8**(10): e76451.

Weathington, N. M., A. H. van Houwelingen, B. D. Noerager, P. L. Jackson, A. D. Kraneveld, F. S. Galin, G. Folkerts, F. P. Nijkamp and J. E. Blalock (2006). "A novel

peptide CXCR ligand derived from extracellular matrix degradation during airway inflammation." Nat Med **12**(3): 317-323.

Weis, M. A., D. M. Hudson, L. Kim, M. Scott, J. J. Wu and D. R. Eyre (2010). "Location of 3-hydroxyproline residues in collagen types I, II, III, and V/XI implies a role in fibril supramolecular assembly." Journal of Biological Chemistry **285**(4): 2580-2590.

Wenstrup, R. J., J. B. Florer, E. W. Brunskill, S. M. Bell, I. Chervoneva and D. E. Birk (2004). "Type V collagen controls the initiation of collagen fibril assembly." J Biol Chem **279**(51): 53331-53337.

Wilson, M. S. and T. A. Wynn (2009). "Pulmonary fibrosis: pathogenesis, etiology and regulation." Mucosal Immunol **2**(2): 103-121.

Wollin, L., I. Maillet, V. Quesniaux, A. Holweg and B. Ryffel (2014). "Antifibrotic and anti-inflammatory activity of the tyrosine kinase inhibitor nintedanib in experimental models of lung fibrosis." Journal of Pharmacology and Experimental Therapeutics **349**(2): 209-220.

Wollin L, S. J., Ostermann A (2015). "The Effect Of Nintedanib Compared To Pirfenidone On Serum-Stimulated Proliferation Of Human Primary Lung Fibroblasts At Clinically Relevant Concentrations." American Journal of Respiratory and Critical Care Medicine **191**.

Wollin, L., E. Wex, A. Pautsch, G. Schnapp, K. E. Hostettler, S. Stowasser and M. Kolb (2015). "Mode of action of nintedanib in the treatment of idiopathic pulmonary fibrosis." European Respiratory Journal **45**(5): 1434-1445.

Wolters, P. J., H. R. Collard and K. D. Jones (2014). "Pathogenesis of idiopathic pulmonary fibrosis." Annual Review of Pathology **9**: 157-179.

Wu, C. S., P. H. Wu, A. H. Fang and C. C. Lan (2012). "FK506 inhibits the enhancing effects of transforming growth factor (TGF)-beta1 on collagen expression and TGF-beta/Smad signalling in keloid fibroblasts: implication for new therapeutic approach." Br J Dermatol **167**(3): 532-541.

Wynn, T. A. (2011). "Integrating mechanisms of pulmonary fibrosis." J Exp Med **208**(7): 1339-1350.

Yamauchi, M. and M. Shiiba (2008). "Lysine hydroxylation and cross-linking of collagen." Methods Mol Biol **446**: 95-108.

Yamauchi, M. and M. Sricholpech (2012). "Lysine post-translational modifications of collagen." Essays in Biochemistry **52**: 113-133.

Zeng, B., J. R. MacDonald, J. G. Bann, K. Beck, J. E. Gambee, B. A. Boswell and H. P. Bächinger (1998). "Chicken FK506-binding protein, FKBP65, a member of the FKBP family of peptidylprolyl cis-trans isomerases, is only partially inhibited by FK506." Biochem J **330 (Pt 1)**: 109-114.

Zhao, X. K., Y. Cheng, M. Liang Cheng, L. Yu, M. Mu, H. Li, Y. Liu, B. Zhang, Y. Yao, H. Guo, R. Wang and Q. Zhang (2016). "Focal Adhesion Kinase Regulates Fibroblast Migration via Integrin beta-1 and Plays a Central Role in Fibrosis." Sci Rep **6**: 19276.

Zhou, P., Y. Liu, F. Lv, M. Nie, Y. Jiang, O. Wang, W. Xia, X. Xing and M. Li (2014). "Novel mutations in FKBP10 and PLOD2 cause rare Bruck syndrome in Chinese patients." PLoS One **9**(9): e107594.

Zuurmond, A. M., A. J. van der Slot-Verhoeven, E. A. van Dura, J. De Groot and R. A. Bank (2005). "Minoxidil exerts different inhibitory effects on gene expression of lysyl hydroxylase 1, 2, and 3: implications for collagen cross-linking and treatment of fibrosis." Matrix Biol **24**(4): 261-270.

Acknowledgements/Danksagung

Mein Dank gilt Prof. Dr. Oliver Eickelberg für die Möglichkeit meine Doktorarbeit in seiner Arbeitsgruppe am CPC auszuführen, als auch für seine Unterstützung und die Ermöglichung zahlreicher Konferenzbesuche während dieser Zeit.

Besonders möchte ich mich bei PD Dr. Claudia Staab-Weijnitz für die erstklassige Betreuung bedanken und dafür, dass sie die beste Mentorin war, die ich mir nur vorstellen konnte. Während meiner Zeit am CPC konnte ich sehr viel von ihr und unseren interessanten Projekten lernen. Ich hatte immer die Chance mich selber durch neue Ideen einzubringen und wurde von ihr unterstützt. Claudia, es hat sehr viel Spaß gemacht mir Dir zusammen zu arbeiten und ich bin traurig, dass sich unsere Wege jetzt trennen.

Darüber hinaus möchte ich mich bei Prof. Dr. Karl-Peter Hopfner für die Betreuung meiner Doktorarbeit als Doktorvater am Department Chemie und Pharmazie und Thesis Committee Member bedanken. Des Weiteren danke ich PD Dr. Dietmar Martin für die Begutachtung meiner Doktorarbeit und die Teilnahme an meiner Verteidigung.

Außerdem danke ich dem gesamten Labor für die gute Zusammenarbeit und Atmosphäre. Besonders möchte ich Elisabeth Hennen für die nette Bench-Nachbarschaft und die schönen Mittagspausen danken.

Ich möchte mich auch bei Prof. Dr. Hans Peter Bächinger für den Aufenthalt in seinem Labor in Portland bedanken, welcher den Grundstein für meine erste Publikation legte. Darüber hinaus bedanke ich mich für seinen wertvollen wissenschaftlichen Input als Thesis Committee Member und auch für die gute Kollaboration mit ihm und Dr. Yoshihiro Ishikawa.

Durch die CPC Research School bekam ich die Möglichkeit an vielen interessanten Kursen teilzunehmen und mein Wissen zu erweitern. Daher möchte ich mich bei Dr. Doreen Franke, PD. Dr. Claudia Staab-Weijnitz und Prof. Dr. Dr. Melanie Königshoff für das tolle Angebot bedanken.

Außerdem danke ich meinen „PhD Buddys“ Flavia Greiffo, Nina Noskovičová, Salome Rehm, Stefanie Weiß und allen anderen die meine Zeit am CPC so schön gemacht haben. Besonders möchte ich Jessica Götzfried für die tolle gemeinsame Zeit von Beginn des

Studiums bis zum Ende der Doktorarbeit bedanken. Es war sehr schön, diesen Abschnitt gemeinsam mit dir zu erleben und ich bin sehr traurig, dass wir uns jetzt nicht mehr jeden Tag sehen werden.

Mein besonderer Dank gilt meinen Eltern, Karin Höh-Knüppel M.A. und Dr. med. Wolfgang Knüppel, meinem Freund Johann Rothkirch sowie meiner ganzen Familie und Felix für ihre Unterstützung.